

# Bulletin of Romanian Chemical Engineering Society

1 2023



ISSN 2360-4697

Edited by SICR and Matrix Rom

The journal is included in the international database  
EBSCO, PROQUEST & INDEX COPERNICUS

ISSN 2360-4697

**Bulletin of Romanian Chemical  
Engineering Society**

---

Volume 10

2023

Number 1

---

## Contents

Laura RENEĂ, Gheorghe MARIA, Cristiana Luminita GIJIU, <i>Optimal operating alternatives of a batch, or a series of batch reactors for mannitol production</i> .....	2
Valeria POP, Mălina PETRESCU-MAG, Crina PETRESCU, Alexandru OZUNU, <i>The risk of microplastic particles seen through the future actions of Romanians</i> .....	27
Tănase DOBRE, Shaalan BDAIWI AHMED, Iuliana Mihaela DELEANU, <i>Heavy metals removal from soil and air – a brief review</i> .....	38
Mustafa HMOUDAH, Cristian POP, Călin BACIU, <i>Estimating methane emissions from urban rivers in South-Eastern Europe - case study: Somes river</i> .....	50
Eliza-Gabriela BRETTFELD, Tănase DOBRE, Cristian Andi NICOLAE, Diana CONSTANTINESCU-ARUXANDEI, Florin OANCEA, <i>Water influence on the thermal properties of deep eutectic solvents: a TGA study</i> .....	59
Cătălin LISA, Silvia CURTEANU, Nicolae HURDUC, Natalia HURDUC, <i>Estimation of Thermal Stability of Some Copolyethers Liquid Crystals Using Artificial Neural Networks</i> .....	67
Tănase DOBRE, Edina RUSEN, Cristian Eugen RADUCANU, Aurel DIACON, Sorin Mircea AXINTE, Alexandra MOCANU, <i>Innovative method for the determination of thermal conductivity of composite materials</i> .....	77
Claudia Ana Maria PATRICHI, Roxana Doinița CIOROIU TIRPAN, Dobre TANASE, <i>Extraction of cellulose from Cladophora Vagabunda</i> .....	89
Ana-Maria Raluca MUȘAT, Cristian Eugen RĂDUCANU, Roxana JIDVEIAN, Doinița-Roxana CIOROIU-TÎRPAN, Gabriel VASILIEVICI, Andreea Luiza MÎRȚ, Tănase DOBRE, Oana Cristina PÂRVULESCU, <i>Lignocellulosic residual biomass as heterogeneous catalyst for transesterification to alkyl ester</i> .....	96

# OPTIMAL OPERATING ALTERNATIVES OF A BATCH, OR A SERIES OF BATCH REACTORS FOR MANNITOL PRODUCTION

Laura RENE<sup>1</sup>, Gheorghe MARIA<sup>1,2,\*</sup>, Cristiana Luminita GIJIU<sup>1</sup>

<sup>1</sup>Chemical and Biochemical Engineering Department, National University of Science and Technology POLITEHNICA Bucharest, 1-7 Gheorghe Polizu Street., 011061 Bucharest, Romania

<sup>2</sup>Romanian Academy, Chemical Sciences section, Calea Victoriei 125, Bucharest 010071, Romania

## **Abstract**

*Multi-enzymatic reactions can successfully replace complex chemical syntheses, using milder reaction conditions, and generating less waste. The model-based analysis of this paper compares performances of several optimally operated Batch Reactors (BR), with those of an optimally operated serial Sequence of BRs (SeqBR). Exemplification was made for the bi-enzymatic reduction of D-fructose to mannitol by using MDH (mannitol dehydrogenase) and NADH cofactor, with the in-situ continuous regeneration of NADH at the expense of formate degradation in the presence of FDH (Formate dehydrogenase). For such coupled systems, the model-based engineering evaluations are difficult tasks, because they must account for interacting reactions, common species initial levels and dynamics, etc. Determination of the optimal operating modes of BR or SeqBR turns into a multi-objective optimization problem with multiple constraints to be solved for every particular system. The study presents multiple elements of novelty, that is: i) the direct comparison of process effectiveness when conducted by using various optimal BRs (a model-, and experimentally-based analysis), or an optimal SeqBR, and ii) the effect of using a multi-objective optimization criteria on the SeqBR performances.*

**Key words:** D-fructose reduction with NADH to D-Mannitol; Sequential batch reactors; Enzymatic reactor optimization; Mannitol dehydrogenase; Formate dehydrogenase for NADH regeneration

## **1. Introduction**

“Remarkable progresses made in the development of new enzymes and in realizing complex coupled enzymatic systems, able to *in-situ* recover the reaction

---

\* Corresponding author: gmaria99m@hotmail.com; [https://en.wikipedia.org/wiki/Gheorghe\\_Maria](https://en.wikipedia.org/wiki/Gheorghe_Maria)

cofactor(s), reported important applications in the industrial biocatalysis, presenting important advantages. Examples include the large number of biosynthesis processes used to produce fine-chemicals, or organic compounds in food, pharma, or detergent industry, such as: the production of monosaccharide derivatives, organic acids, alcohols, amino-acids, etc., by using single- or multi-enzymatic reactors [1, 2]”.

Thus, “multi-enzymatic reactions can successfully replace complex chemical syntheses, using milder reaction conditions, and generating less waste. Multi-enzymatic systems with parallel or sequential reactions are successfully applied for: i) recovering the main reaction co-factor, ii) shift equilibrium of the main reaction, iii) remove the excess of one product, iv) prolongs the life of the main reaction enzyme, by degrading its inhibitor, etc.” [3].

“Even if the multi-enzymatic systems are advantageous, the engineering part for developing and/or optimizing such a process is not an easy task because it must account for the interacting enzymatic reactions, differences in enzymes optimal activity domains, deactivation kinetics (if significant), the presence of multiple and often opposed optimization objectives, technological constraints, and an important degree of uncertainty coming from multiple sources (model/constraints inaccuracies, the presence of disturbances in the control variables), and the highly nonlinear process dynamics.

Classic and simplest technology involves Batch reactors (BR) to efficiently conduct complex (multi-enzymatic) processes. BR are simple, relatively cheap, easy to operate and control, flexible, and adaptable, thus being suitable for the multi-product operation.

Even if an optimal pH and temperature is used, the determination of the optimal operating mode [enzyme(s), substrate(s), cofactor] feeding policy of the BR (or its derivatives) often turns into a difficult multi-objective optimization problem with multiple constraints to be solved for every particular system” [4-8].

Depending on the suspended or immobilized enzyme(s) operation alternatives, the model-based problem to be solved consists in the selection of the most suitable reactor type, and its optimal operation mode for a given (multi-)enzymatic process of the already known kinetic model and enzyme(s) characteristics. “To facilitate the evaluation of the reactor operation alternatives” [5] proposed a computational modular platform, that allows simulating and comparing the optimal operating policies of various enzymatic reactors with respect to certain formulated objectives, thus allowing the best use of the enzyme(s), by screening among various reactor alternatives, that is:

- 1) “Simple Batch Reactor (*BR*) (Figure 1). Substrate(s), biocatalyst, and additives are initially loaded in the recommended amounts (concentrations) [5, 7, 9-11].

2) Sequential Batch-to-batch Reactors (*SeqBR*) (Figure 2) consist in a certain number of (usually identical) BRs operated in series. The content of each BR is transferred to the next BR, with adjusting the reactants and/or biocatalyst(s) amounts (concentrations) at the beginning of each BR from the series to reach optimal levels (in-silico, off-line determined in this paper) [12,13].

3) *BRP*, that is a BR with reactants and/or biocatalyst(s) added during the batch in a Pulse-like addition of equal / uneven solution volumes, with a certain frequency to be in-silico off-line determined (Figure 2), [4-7].

4) Semi-Batch (or Fed-Batch) Reactor (*SBR* or *FBR*), with an optimal feeding policy of enzyme(s)/substrate(s), (Figure 2). In a continuous mode the SBR runs with continuous feeding and evacuation with equal flow rates. Substrates/biomass/enzymes /supplements are added during the batch following a certain (optimal) policy (to be in-silico, off-line determined) [5, 6, 14, 15, 16, 17, 18, 19, 20, 21]. In a *FBR* operation, the feeding policy of biocatalyst/substrate(s) is optimally varied (following a time stepwise policy) to get maximization of the formulated goal. Usually (case dependent), *FBRs* reported better performances compared to other batch operating alternatives [22]. However, *FBRs* are difficult to operate. That is because they need previously prepared stocks of biocatalyst(s), and substrate(s), of different concentrations (a-priori in-silico determined), to be fed for every 'time-arc' (*Ndiv* in total) of the batch (that is a batch-time division in which the feeding composition is constant). It is self-understood that the time-'arcs' feedings usually differ between them. This is 'the price' paid for achieving *FBR* best performances compared to other batch operation modes. [5, 7, 14-25].

5) FiXed-Bed continuous Reactor (*FXBR*) with immobilized enzyme(s) [5, 6, 16].

6) Mechanically Agitated (Semi-)Continuous Reactors (*MA(S)CR*) with immobilized enzyme(s) [6, 16].

As roughly represented in (Figure 2), the simple BR can be operated in various modes: simple (repeated) batch, BRP, FBR, SBR, serial batches (*SeqBR*), cyclic batch, etc. A few number of examples of the above mentioned enzymatic/biological reactor types are given by Maria [14].

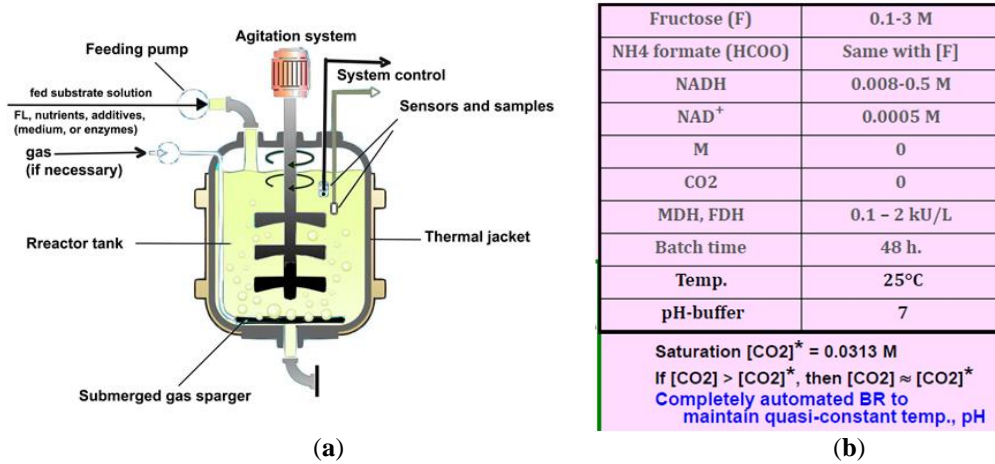


**Fig. 1.** Simplified scheme of a BR or a FBR used to conduct enzymatic or biological processes and reaction conditions: (a) Simplified scheme of a BR or a FBR In the BR operating mode, substrate(s), biocatalyst, and additives are initially loaded in the recommended amounts (concentrations). In the FBR operating mode, the substrate(s)/ biocatalyst(s) and additives (nutrients, pH-control substances) are continuously fed, following a certain (optimal) policy [14]; (b) Nominal reaction conditions of the [26] used for the enzymatic reduction of D-fructose to mannitol using MDH and NADH cofactor in an experimental lab-scale BR, with the in-situ continuous regeneration of the cofactor at the expense of formate degradation in the presence of FDH” [27].

By using an adequate kinetic model from literature, the in-silico analysis of this paper is aiming to evaluate and compare the performances of several optimally operated Batch Reactors (BR), of a single or repeated use, with those of an optimally operated serial Sequence of BRs (SeqBR). Several multi-objective optimization criteria have been used in this regard.

“Exemplification is made for the case of the enzymatic reduction of D-fructose to mannitol by using suspended MDH (mannitol dehydrogenase) and NADH (Nicotinamide adenine dinucleotide) cofactor, with the in-situ continuous regeneration of the cofactor at the expense of formate degradation in the presence of suspended FDH (Formate dehydrogenase).

As an observation, the study presents several elements of novelty, that is: i) the direct comparison of process effectiveness when conducted by using various optimal BRs (a model-, and experimentally based analysis), or an optimal SeqBR, and ii) the effect of using a multi-objective optimization function on the SeqBR performances.

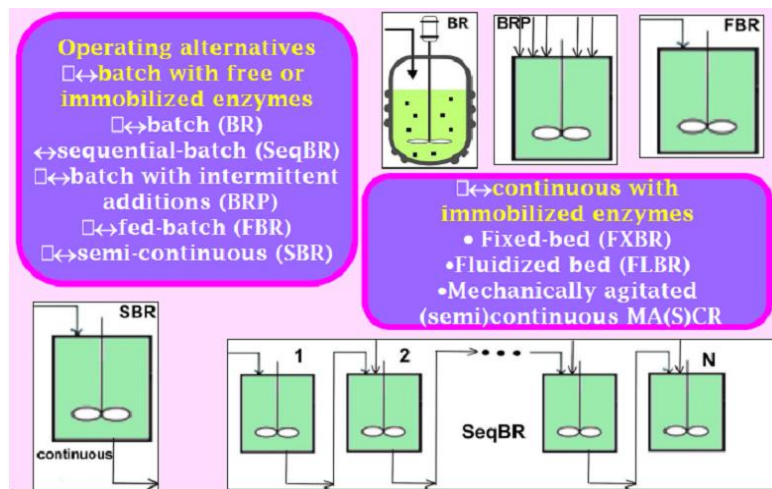


**Fig. 2.** Enzymatic reactors types and operating modes. The usual modelling hypotheses: BR= isothermal, iso-pH, and iso-DO (air sparger, if necessary); perfectly mixed liquid phase. Reactants / biocatalyst(s) / additives added at the beginning of the batch only.

BRP= a BR with reactants and/or biocatalyst(s) added during the batch in a Pulse-like addition of equal / uneven solution volumes, with a certain frequency (to be determined).

FBR= Substrates/biocatalyst(s)/additives are added during the batch following a certain (optimal) policy (to be determined).

SBR= in continuous mode there is a CSTR with continuous feeding and evacuation with equal flow-rates. Substrates/biomass/enzymes /supplements are added during the batch following a certain (optimal) policy (to be determined).

SeqBR= a certain number of (usually identical) BR operated in series. The BR content is transferred from every BR to the next one, with adjusting the reactants and/or biocatalyst(s) amounts (concentrations) at the beginning of each BR, to reach optimal levels (off-line determined, this paper) [14,27] simplified scheme of a BR or a FBR

## 2. Adopted kinetic model of the enzymatic process and batch reactor characteristics

Mannitol “is a natural hexitol with important applications in medicine and food industry due to some other favorable known properties [28], being currently produced via hydrogenation of 50% fructose-50% glucose syrup with a high cost, that is at high pressures and temperatures, by using a Raney nickel catalyst [29]. Over the last decades, several more profitable production alternatives have been developed [28]. The most attractive are: (i) the biological production by fermentation using lactic acid bacteria, yeasts, and fungi, with important advantages: good yields, less by-products, no need of ultra-pure, and expensive raw materials [30], and (ii) the enzymatic production of mannitol. The most promising is that proposed by [26]. A higher productivity was achieved using only D-Fructose as substrate. This method (Figure 3) consists in the enzymatic reduction of D-fructose to D-mannitol in the presence of MDH enzyme and using



NADH as cofactor (proton donor). The advantage of using NADH instead of others is that it is relatively cheap [31], and much more stable than the NADPH [32].

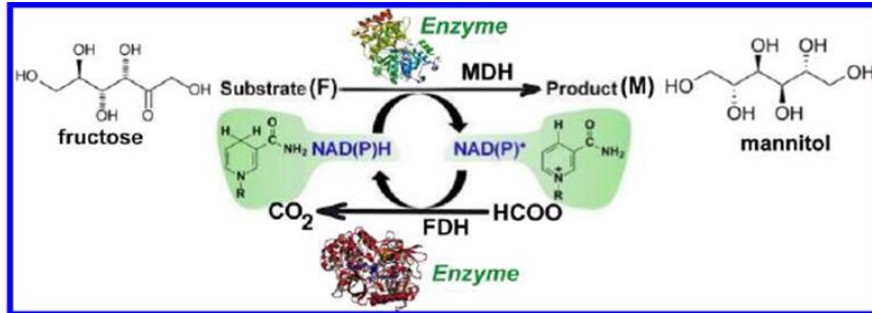


**Fig. 3.** Simplified “reaction scheme of the two coupled enzymatic reactions: (Up) D-fructose (F) reduction to mannitol (M) by using suspended MDH (mannitol dehydrogenase), and the cofactor NADH (Nicotinamide adenine dinucleotide). (Down) NADH cofactor continuous regeneration by the expense of formate (HCOO) degradation in the presence of suspended FDH (Formate dehydrogenase)” [26,27]. The use of NADPH cofactor is not recommended, being much more expensive [31], and very unstable [32].

*Table 1*

**Nominal reaction conditions of the [26] “for the enzymatic reduction of D-fructose to mannitol using MDH and NADH cofactor in an experimental BR, with the in-situ continuous regeneration of the cofactor at the expense of formate degradation in the presence of FDH. The used FDH (EC 1.2.1.2) from *Candida boidinii* has a specific NAD-dependent activity of 2.4 U/mg, measured at 25°C and pH 7.0. The MDH (EC 1.1.1.67) from *Pseudomonas fluorescens* DSM 50106 was over-expressed in *E. coli* JM 109. The NADH-dependent FDH and MDH typical activity in D-fructose reduction varies within the range of 0.5-2 kU/L.**

<i>Parameter</i>	<i>Value [Slatner et al.,1998]</i>
Temperature	25°C
Pressure / pH (buffer solution)	Normal / 7
<i>Molar initial concentrations</i>	
Fructose, [F] <sub>0</sub> (note a)	0.1-1 M (tested by [Slatner et al.,1998] ) 0.1-3 M (this paper)
[NADH] <sub>0</sub>	0.008 M (0.1-0.5 M)(this paper)
[NAD] <sub>0</sub>	0.0005 M
Formate [HCOO] <sub>0</sub>	Identical to [F] <sub>0</sub>
Others: [M] <sub>0</sub> = [CO <sub>2</sub> ] <sub>0</sub> = 0	none
$c_{CO_2}^*$ = CO <sub>2</sub> saturation level at 25°C and pH= 7	0.0313 M [Carroll and Mather (1992); Reid et al. (1987)]
Reaction time	48 h
Initial FDH (referred to the reactor liquid)	0.1-2 kU/L, (to be optimized)
Initial MDH (referred to the reactor liquid)	0.1-2 kU/L, (to be optimized)

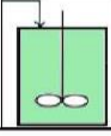
\*Higher initial concentrations of fructose are possible, but have not been checked by [26] due to the side-effects (process inhibition by the products).

By far, the bi-enzymatic alternative of Slatner et al. [26], also approached in this paper, is more advantageous, the process occurring under mild conditions (pH= 7, 25°C) and generating no waste. However, due to the costly enzymes, solving the engineering part (this study) is important. Recent advances try coupling the two reactions, not in the same BR, but in the same genetic modified micro-organism (*Bacillus megaterium*) used as host for both enzymes synthesis, and cofactor regeneration [33].

As mentioned above, the studied bi-enzymatic process involves two concomitant interfering enzymatic reactions (denoted by R1 and R2 in Table 2): The reaction (R1) is the enzymatic reduction of F to M by using suspended MDH and NADH cofactor. This main reaction is supported by the enzymatic reaction (R2) concomitantly taking place in-situ in the same reactor. The reaction (R2) ensures the continuous regeneration of NADH by combining NAD (+) with the ammonium formate in the presence of suspended FDH enzyme (initially added together with the MDH).

Table 2

The kinetic model of Maria [9] referring to the “two coupled enzymatic reactions, that is: (R1) reduction of D-fructose to mannitol using MDH enzyme and NADH cofactor and, (R2) in-situ continuous regeneration of the cofactor NADH at the expense of formate degradation in the presence of FDH (Fig. 3). Rate constants have been estimated under the nominal conditions of Fig. 1 and Table 1 to match the experimental kinetic data of Slatner et al. [26].”

Michaelis-Menten kinetics with non-competitive inhibition of reactants (Maria, 2020 by using Slatner, 1998 experimental data); Reactions occur quantitatively	
Reactions	Rate Expressions
$F + NADH (+H^+) \xrightarrow{MDH} M + NAD^+$	$R1 = \frac{kc1 \cdot C_{MDH} \cdot C_F \cdot C_{NADH}}{KM1 + K_F C_F + K_{NH} C_{NADH}}$
$HCOO^- + NAD^+ \xrightarrow{FDH} CO_2 \uparrow + NADH$	$R2 = \frac{kc2 \cdot C_{FDH} \cdot C_{HCOO^-} \cdot C_{NAD}}{KM2 + K_{HC} C_{HCOO^-} + K_{NAD} C_{NAD}}$
Species rate stoichiometry	
$\frac{dC_F}{dt} = -R1; \frac{dC_{NADH}}{dt} = -R1 + R2; \frac{dC_{NAD}}{dt} = +R1 - R2; \frac{dC_{HCOO^-}}{dt} = -R2$ $\frac{dC_M}{dt} = +R1; \frac{dC_{CO_2}}{dt} = +R2$	
Rate constants	
$kc1 = 2 \times 10^{-3}; kc2 = 8.3259 \times 10^{-3}; 1/h/(U/L)$ $KM1 = 7.2367 \times 10^{-2} M; KM2 = 8.8047 \times 10^{-2} M;$ $K_F = 1; K_{NH} = 1; K_{HC} = 5.0061 \times 10^{-2}; K_{NAD} = 90.181$	
	
Maria, G., Computers & Chem. Eng. 133 (2020) 106628-106635. (kinetic model identification)	
- Slatner et al., Biocatal. Biotransform. 16 (1998) 351-363. (experimental kinetic data)	

To determine the kinetics of this bi-enzymatic process, Slatner et al. [26] conducted a large number of lab-scale batch experiments by using various initial conditions, some of them being displayed in (Figure 4). The main characteristics of this BR are presented briefly in (Fig. 1) and (Table 1). As mentioned by Slatner et al. [26], operation of this BR is subjected to a couple of strong technological constraints, as followings:

A) Because (a) D-mannitol displays a low solubility in water at 25°C (ca. 1.2 M in Table 1), that is much lower than that of D-fructose (ca. 22.2 M), and (b) pure D-fructose is a rather expensive substrate, high substrate conversions (> 90%) are especially important for this process. On the other hand, a high productivity of a BR requires substrate (fructose) high initial concentrations. However, in spite of its extremely high solubility in water (4000 g/L), the work at high fructose concentrations is not considered in the present engineering analysis due to several important drawbacks: (i) a risky extrapolation of the used kinetic model validity; (ii) a high viscosity of the reaction medium raising product separation problems; (iii) a low solubility of mannitol at 25°C (ca. 1.2 M) leading to its crystallization in the bulk liquid phase, with product purification problems, and (iv) a higher substrate inhibition effect (in R1 kinetic expression of Table 2).

B) On the other hand, the experiments of Slatner et al. [26] proved that F-conversion decreases with the growth of the fructose initial concentration, from 98% for  $[F]_o = 0.1$  M to 80% for  $[F]_o = 1$  M. These reasons explain the small range of initial  $[F]_o \in [0.1-1]$  M experimentally investigated by Slatner et al. [26] to determine the process optimal conditions on an exhaustive basis. The product and enzymes recovery do not raise special problems for such a bi-enzymatic process, details being given by Slatner et al. [26].

C) Another technological problem concerns the MDH stability. As experimentally investigated by Slatner et al. [26], a shift in reaction temperature from 25oC to 30oC did not increase D-mannitol productivity significantly. However, because the moderate operational stability of MDH at 30oC and higher temperatures it was not possible to be ensured, then the optimum 25oC was adopted. Because MDH was also found to be sensitive to shear, a 200 rpm of the stirrer was used by Slatner et al. [26] to ensure an efficient mixing of the bulk phase, and a minimal shear inactivation of enzymes. Under these operating conditions, the coenzymes NAD<sup>+</sup> and NADH were proved to be stable. The pH is maintained constant at  $7 \pm 0.1$  (optimum for MDH) by an automatic addition of HCl, due to the shift in pH towards the alkaline region observed when FDH-catalyzes oxidation of the ammonium formate. In fact, this pH is a compromise between the pH-optimum (7.5), and the pH-stability (7.0), according to Slatner et al. [26].

“This is why, Slatner et al. [26] conducted extended experiments at 25°C, and a buffer of pH  $7.0 \pm 0.1$ , under the following ranges of initial conditions:  $[F]_o$

$\in [0.1 - 1] \text{ M}$ ;  $[\text{NADH}]_o \in [0.2 - 1] \text{ M}$ ;  $[\text{HCOO}]_o = [\text{F}]_o$ ;  $[\text{NAD}]_o = 0.0005 \text{ M}$ ;  
 $\{ [\text{MDH}]_o, [\text{FDH}]_o \} \in [0.1 - 2] \text{ kU/L}$ .

The collected kinetic data by Slatner et al. [26] were used by Maria [9] to build-up a kinetic model for this bi-enzymatic process. Based on these quantitative observations, a simple Michaelis-Menten kinetic model of Ping-Pong-Bi-Bi type was proposed for the both involved reaction rates R1 and R2 (Table 2), by analogy with a similar process of pseudo 2-nd order kinetics [34].

The adequacy of the resulted kinetic model was proved to be very good vs. the experimental data [9], roughly illustrated here by the comparative results of (Figure 4), and of (Table 4) for three (experimentally tested) different initial  $[\text{F}]_o$  of 0.1, 0.5, and 1 M. Consequently, this model will further be used for engineering evaluations.

For simplicity, this model includes a non-competitive moderate inhibition with respect to reactants [26], while the mannitol inhibition was neglected. Enzymes MDH and FDH inactivation during the reaction have been neglected due to lack of available data. Concerning interrelationships of the coupled enzyme reactions, formate did not inhibit MDH, and D-fructose had no effect on FDH activity or stability. The pH is maintained constant at  $7 \pm 0.1$  (optimum for MDH, Table 1). Due to its high selectivity, the transformation of fructose (F) in mannitol (M) is quantitative so,  $[\text{M}] = [\text{F}]_o - [\text{F}]$  at any moment” [26].

### 3. Optimization of the BR

The analyzed BR is those of Slatner et al. [26] with the operating conditions range of (Table 1).

“To simulate the BR dynamics, a simple math model of (Table 3) was adopted. This classic ideal model assumes the following hypotheses [35,36]: (i) isothermal, iso-pH; (ii) additives (for the pH-control) are added initially and during the BR operation in an automatic mode to ensure the operating parameters of Table 1; (iii) perfectly mixed liquid phase (with no concentration gradients). The adopted BR model described in (Table 3) includes the differential mass balances of the process key-species, that is: F, M, HCOO, NADH, NAD<sup>+</sup>, CO<sub>2</sub>. The enzymes (MDH, FDH) concentrations are assumed to be constant, due to the neglected inactivation, but maintained at optimal levels to be determined. The initial concentrations of the other compounds (that is,  $[\text{M}]_o$ , and  $[\text{CO}_2]_o$ ) are null, or at values recommended by Slatner et al.[26] (that is  $[\text{NAD}]_o$ , and  $[\text{HCOO}]_o = [\text{F}]_o$ , see Table 1, and Table 5). The liquid volume in the BR is considered constant.

For the analyzed bi-enzymatic process with in-situ cofactor regeneration, a comparative analysis of the optimal BR (with the initial addition of enzymes and substrates), against the BRP with intermittent addition of the key-enzyme MDH following various optimal policies was made by Crisan and Maria [7]. The superiority of BRP is relatively case dependent. Simulations with the present kinetic model revealed that the best operating alternative is the BR, requiring less MDH enzyme to obtain an imposed fructose conversion (99%) over 48 h batch time.

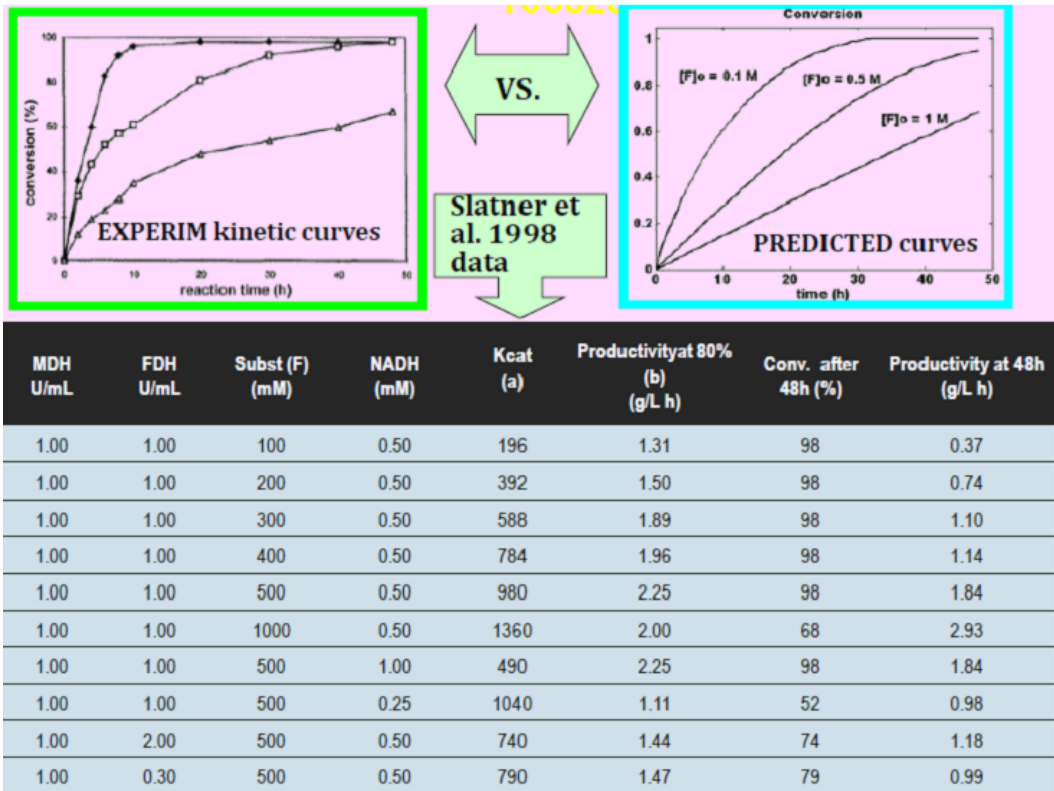


**Fig. 4.** The experimental kinetic data of Slatner et al. [26] obtained in a lab-scale BR with the characteristics of (Table 1). The top figures illustrate the experimental vs. the model-based predicted process kinetics in terms of F-conversion over time, for initial  $[F]_0$  of 0.1, 0.5, and 1 M [9, 27].

Starting from such an approximate result, by using the kinetic model of (Table 2), Maria [9] in-silico analyzed the optimal operation of the **BR** of (Table 1) by using the BR model given in (Table 3). In the present study, the optimal BR operation is determined in a more systematic and complete way, by concomitantly fulfilling several optimization criteria, that is: (1) minimizing the enzymes (MDH and FDH) consumption, with (2) realizing an imposed high fructose conversion (>

0.90-0.95) at the batch end. In short, this optimization problem is formulated in (Fig. 5). The relevant results presented in (Table 5) have been derived for different initial concentrations of fructose  $[F]_o$ , that is 0.1 M, 1 M, and 3 M, respectively with using the same exhaustive algorithm of Maria [9] to solve the multi-objective (1-2) optimization problem. As a general conclusion, in all tested alternatives, the model-based predicted performances of an optimally operated BR are much better in terms of minimum enzymes consumption (2x less for FDH, and 2x-5x less for MDH), compared to the experimental BR randomly (sub-optimal) trials of Slatner et al. [26], to obtain a high F-conversion. The species dynamics for three optimal BR operations are (i.e.  $[F]_o = 0.1$  M, 1 M, and 3 M) are given by Maria [9], and in (Fig. 6). These results lead to several conclusions, as followings:

- i. The optimal BR, for  $[F]_o = 0.1$  M, and for  $[F]_o = 1$  M have been experimentally validated by Slatner et al. [26] (see Table 4).
- ii. “There is a close connection between the coupling reactions, enzyme concentrations, and the quasi-stationary of the NADH/NAD ratio over the batch. For all the optimal conditions of (Fig. 6), the two enzymatic reactions are well coupled. Thus, the high reaction rates R1 and R2 ratio reach a quasi-stationary level, leading to a quasi-constant NADH / NAD ratio much higher than 10, thus maintaining the process efficiency [9].
- iii. The cofactor NADH regeneration is very efficient, formate decomposition being quasi-complete (Fig. 6) and leading to saturation  $[CO_2]^*$  in short time (after ca. 10 h or even earlier), with removal of the  $CO_2$  excess from the system over the rest of the batch-time.”
- iv. As revealed by repeated simulations of Maria [9], and the results of (Table 5, Fig. 6), the BR performances are more sensitive to the initial  $[MDH]_o$  than to the initial  $[FDH]_o$ .

Table 4

**Some BR performances predicted by the kinetic model of Maria [9] compared to the experimental data of Slatner et al. [26]. Initial conditions:  $[HCOO]_o = [F]_o$ ;  $[NADH]_o = 0.008$  M;  $[NAD]_o = 0.0005$  M; Batch =48h; Fig. 4 [9]**

variable	Model validation by [Maria, 2020a]		
	$[F]_o = 0.1, \text{ or } 0.5, \text{ or } 1\text{M}$		
$[F]_o$	0.1 M	0.5 M	1 M
FDH (U/L)	1000	1000	1000
MDH (U/L)	1000	1000	1000
F conv. [Maria,2020a] model	<b>1</b>	<b>0.95</b>	<b>0.68</b>
F conv [Slatner,1998] experimental	<b>0.99</b>	<b>0.95</b>	<b>0.68</b>

Table 3

“The ideal models (species mass balances) for the BR and SeqBR enzymatic reactors. The BR hypotheses [35]: (1) isothermal, iso-pH. (2) Additives for the pH-control are added initially and during the batch in recommended quantities; (3) perfectly mixed liquid phase (with no concentration gradients). Indices: “0” = initial; “f” = final (at the batch time); “i” = reaction; “j” = species; “k” = BR number. NBR = no. of BR in the SeqBR series” [37].

**One simple BR**

$$\frac{dc_j}{dt} = \sum_{i=1}^{n_r} v_{ij}r_i; \quad j = \text{species index (F, M, HCOO, NADH, NAD, CO}_2\text{)}. \text{ Reaction}$$

stoichiometry  $v_{ij}$  is given in **Table 2**.

Initial conditions of  $c_{j,0} = c_j(t=0)$  are given in **Table 1** (nominal). Optimal values should be determined in-silico, off-line.

$$\frac{dc_E}{dt} = 0, \text{ (negligible inactivation of MDH and FDH); } E = \text{enzymes (MDH and FDH);}$$

If  $c_{CO_2} > c_{CO_2}^*$ , then  $c_{CO_2} \approx c_{CO_2}^*$  (the excess being removed from the liquid phase).

**SeqBR, that is a series of ( $k=1, \dots, N_{BR} = 10$ ) simple BR**

$$\frac{dc_j}{dt} = \sum_{i=1}^{n_r} v_{ij}r_i; \quad j = \text{species index (F, M, HCOO, NADH, NAD, CO}_2\text{)}. \text{ Reaction}$$

stoichiometry  $v_{ij}$  is given in (**Table 2**);  $t_f = 40$  h (batch time; this paper).

Initial conditions:

$$[F]_{0,k} \quad k=1, \dots, N_{BR} = \text{to be optimized; } [HCOO]_{0,k} = [F]_{0,k};$$

$$[NADH]_{0,k}; [MDH]_{0,k}; [FDH]_{0,k}, \quad k=1, \dots, N_{BR} = \text{to be optimized}$$

$$[NAD^+]_{0,1} = 0.0005 \text{ M (for the 1-st BR), as recommended in (Table 1).}$$

$$[NAD^+]_{0,k} = [NAD^+]_{f,k-1}; \quad k=2, \dots, N_{BR}$$

$$[CO_2]_{0,1} = 0 \text{ (for the 1-st BR); } [CO_2]_{0,k} = [CO_2]_{f,k-1}; \quad k=2, \dots, N_{BR}$$

$$[M]_{0,1} = 0 \text{ (for the 1-st BR); } [M]_{0,k} = [M]_{f,k-1}; \quad k=2, \dots, N_{BR}$$

$$\frac{dc_E}{dt} = 0, \text{ (negligible inactivation of MDH and FDH); } E = \text{enzymes (MDH and FDH);}$$

If  $c_{CO_2} > c_{CO_2}^*$ , then  $c_{CO_2} \approx c_{CO_2}^*$  (excess being removed from the liquid phase).

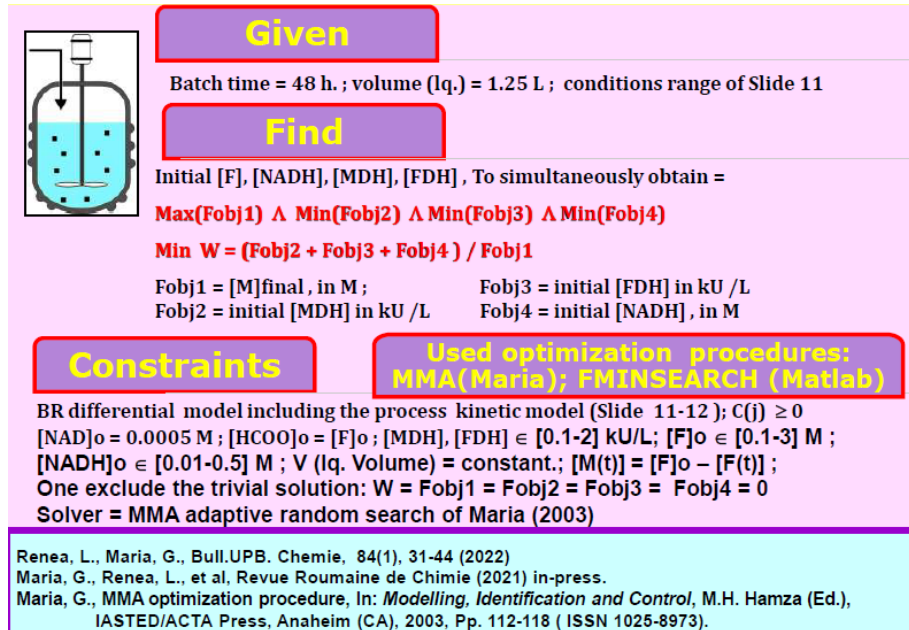


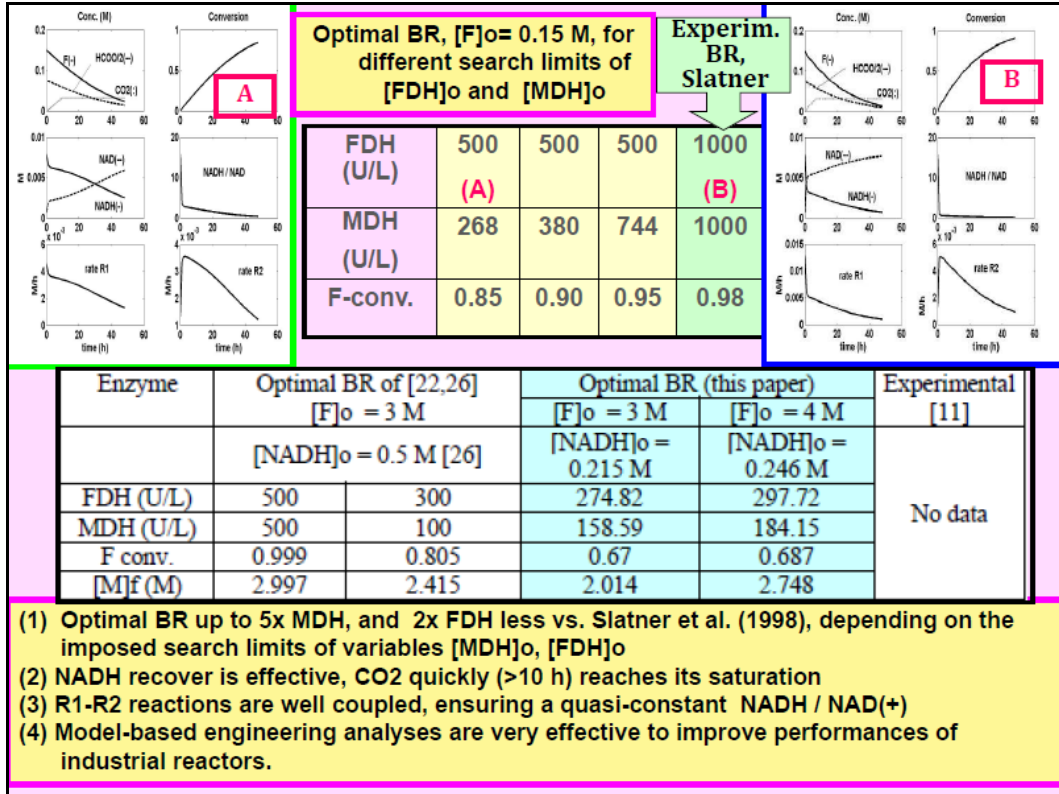
Fig. 5. The BR optimization problem in math terms [27].

Table 5

“Some optimal BRs predicted by the kinetic model of Maria [9] compared to the experimental data of Slatner et al. [26]. Initial conditions: [HCOO]<sub>o</sub> = [F]<sub>o</sub>; [NAD]<sub>o</sub> = 0.0005 M; Batch time = 48 h.”

Enzyme		Optimal BR (this paper)						[Slatner et al.(1998)]
		[F] <sub>o</sub> = 0.1M						Experimental
		[NADH] <sub>o</sub> = 0.008 M						
FDH (U/L)		500		500	500			1000
MDH (U/L)		214		385	879			1000
<b>F conv.</b>		<b>0.89</b>		<b>0.93</b>	<b>0.95</b>			<b>0.98</b>
Enzyme		Optimal BR (this paper)						[Slatner et al.(1998)]
		[F] <sub>o</sub> = 1 M						Experimental
		[NADH] <sub>o</sub> = 0.008 M						
FDH (U/L)		500	1000	500	1000	500	1000	1000
MDH (U/L)		1192	1192	1248	1246	1388	1388	1000
<b>F conv.</b>		<b>0.58</b>	<b>0.76</b>	<b>0.59</b>	<b>0.78</b>	<b>0.61</b>	<b>0.82</b>	<b>0.68</b>
Enzyme		Optimal BR (this paper)					[Slatner et al.(1998)]	
		[F] <sub>o</sub> = 3 M					Experimental	
		[NADH] <sub>o</sub> = 0.5 M;						
FDH (U/L)		500	500	500	300	100	No data	
MDH (U/L)		500	100	50	100	100		
<b>F conv.</b>		<b>1</b>	<b>0.99</b>	<b>0.80</b>	<b>0.87</b>	<b>0.50</b>		





**Fig. 6.** Some optimal BRs predicted by the kinetic model of Maria [9] compared to the experimental data of Slatner et al. [26]. Initial conditions:  $[HCOO]_0 = [F]_0$ ;  $[NAD]_0 = 0.0005$  M; Batch time = 48 h. Species dynamics is presented for the running set-points (A-B). [27] the BR optimization problem in math terms [27].

#### 4. Optimization of the SeqBR

“The high productivity potential of the optimally operated BR, as underlined in chap. 3, raises a legitimate question: (a) is it more profitable to repeatedly use a certain number of BRs of equal volume, by preserving every time the same optimal initial conditions, or, (b) it is more profitable to use a series of batch-to-batch, of a certain number of BRs (denoted by SeqBR), the content at the batch end of each BR being passed to the next BR from the series. However, the initial conditions of each next BR will be in-silico, off-line adjusted to ensure the optimal performance of the whole SeqBR. This section is dedicated to solve this engineering problem roughly formulated in (Fig. 7).

Control variable choice. The SeqBR ideal model approached here is presented in (Table 3). Thus, at the batch end of each BR, its content is transferred

into the next BR of the series. However, the concentrations of the following compounds (control variables) are initially adjusted to match the optimal values (to be determined, see below):  $[F]_o$ ,  $[NADH]_o$ ,  $[MDH]_o$ ,  $[FDH]_o$ . The initial concentrations of the rest of the substances (that is,  $[M]_o$ ,  $[NAD]_o$ ,  $[CO_2]_o$ ) are those from the end of the previous BR.  $[HCOO]_o$  is adjusted to be equal with the  $[F]_o$ .”

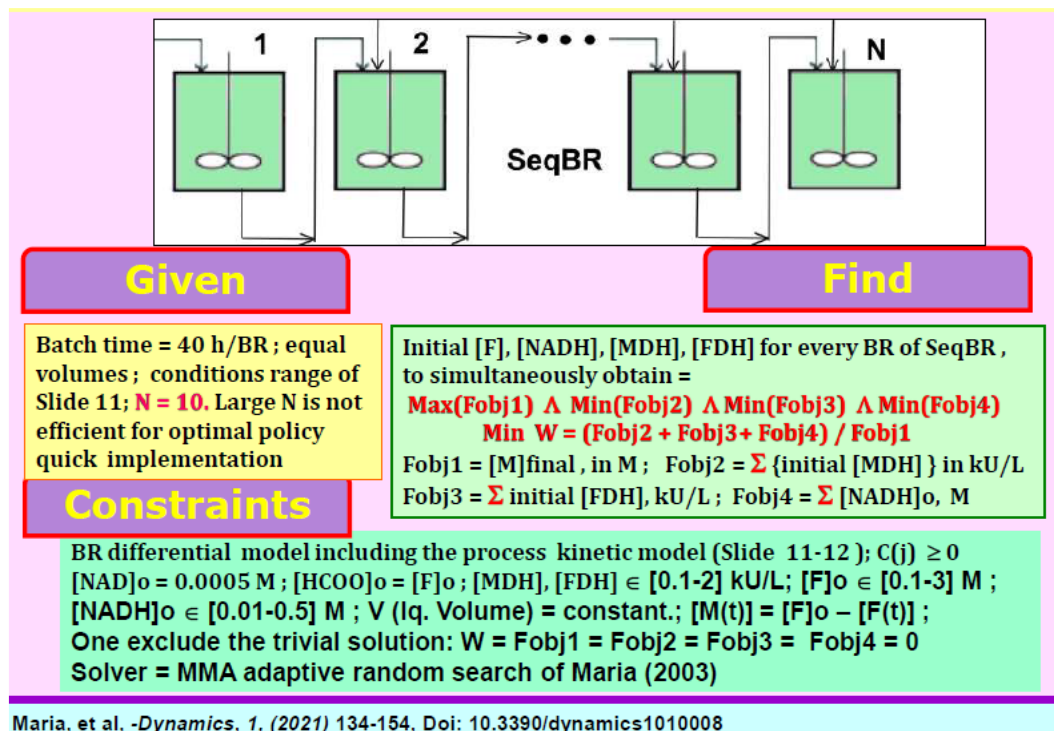


Fig. 7. The SeqBR optimization problem in math terms [27, 37]

The choice of the number of BRs (NBR) in the SeqBR series. A series of a moderately large number  $NBR = 10$  BRs connected in series are considered here with an equal batch time of 40 h for every BR. This will allow a direct comparison of SeqBR performances with those of a FBR with a variable feeding over  $N_{div}$  time-arcs. “It is worth mentioning, by analogy with the time stepwise optimal feeding policies of FBR [14,38], that the use of a SeqBR with a higher number of BRs suffers from a series of disadvantages, that is: (i) as the (NBR) increases, as the number of optimization (control) variables (that is the initial load of substrate(s) / enzyme(s) to be determined for every BR) is higher, thus increasing the computational effort, and the number of local solutions of the SeqBR optimization problem due to its model high non-linearity, thus decreasing the chance to quickly locate the global optimum of the problem; (ii) as the (NBR) increases, the optimal operating policy of SeqBR is more difficult to implement

since the optimal policy requires physical operations to adjust the substrate(s) / enzyme(s) concentrations at the beginning of each BR from the series of BRs; (iii) Besides, SeqBR operation with using a larger number of (NBR) can raise special operating problems when including PAT tools (Process Analytical Technology) [39], and also involves a higher investment and process control cost.

In spite of these difficulties, some trials to operate SeqBR, or cyclic BR, or even parallel BR have been reported in the literature, by using 2-5 biological FBRs [40-42], 14-times cyclic BRs [43], or 48 parallel BRs [44], or even 24 parallel BRs [45]. As expected, optimized FBR reported better performances compared to the simple BR, (even if optimally operated), due to a higher operating flexibility [6,14,24,25]. On the other hand, the chemical reactor theory demonstrated that a series of a large number of CSTRs tends to have the best performances of a plug-flow reactor [46]. Consequently, it is expected that an optimal SeqBR will present better performances than a repeated operation of only a BR with the same initial conditions.”

The SeqBR to be optimized in this paper includes a series of  $NBR = 10$  identical BRs (with the characteristics of Table 1) for the approached bi-enzymatic process described in section 2. The in-silico (model-based), off-line optimization approached here has to solve at least two simultaneously economic objectives:

1).- Determine the optimal initial conditions for every BR from the series to ensure the highest productivity in mannitol at the SeqBR output, that is the output of the last (NBR)-th BR, and

2).- Minimize the costly “enzymes (MDH and FDH) overall consumption, with preserving the best connection of the two enzymatic reactions to ensure a quick regeneration of the cofactor and a high fructose reduction rate.

Other optimization objectives can be formulated as well, depending on the reactor and process type [16,18] but are beyond the scope of this paper.”

From the math point of view, this NLP optimization problem consists in the following formulation eqn. (1):

Find: { [F] <sub>o,k</sub> ; [NADH] <sub>o,k</sub> ; [FDH] <sub>o,k</sub> ; [MDH] <sub>o,k</sub> }, with (k= 1,..., N <sub>BR</sub> ) = = arg Min Ω(c, c <sub>o</sub> , k);	
with the following composite objective function: Ω = (Fobj2 + Fobj3) / Fobj1, where:	
Fobj1 = $\left[ M(t_f)_k \right]_{k=N_{BR}}$ , with [M] in M units;	(1)
Fobj2 = $\sum_{k=1}^{N_{BR}} [MDH]_{0,k}$ , with MDH conc. in kU/L units.	
Fobj3 = $\sum_{k=1}^{N_{BR}} [FDH]_{0,k}$ , with FDH conc. in kU/L units.	

An alternative objective function which gives more weight to the M-production maximization in the detriment of enzymes' consumption is:

Min Ω = Fobj2 + Fobj3 - Fobj1, With the same definition of Fobj1-3, and the same searching variables as those used in eqn.(1).	(2)
--	-----

Both optimization problems eqns. (1-2) are subjected to the following constraints:

(i). $\frac{d_j}{dt} = \sum_{i=1}^n \nu_{ji} r_i$ (dynamic model of the process; <b>Tables 2,3</b> ); J = species index (F, M, HCOO <sup>-</sup> , NADH, NAD <sup>+</sup> , CO <sub>2</sub> , MDH,FDH)	
(ii). Initial conditions of: $[c_{j,0}]_k (t=0)_k = [c_{j,f}]_{k-1} (t=t_f)_{k-1}$ ; k=2,..., N <sub>BR</sub> Except for the "J"-species which are the search variables, that is [F] <sub>o,k</sub> ; [NADH] <sub>o,k</sub> ; [FDH] <sub>o,k</sub> ; [MDH] <sub>o,k</sub> } with (k= 1,..., N <sub>BR</sub> )	
(iii). $c_j(t) \geq 0, \forall t$ (physical significance constraints);	(3)
(iv). Searching ranges suggested by Slatner et al.[26] (experimentally validated), that is: [MDH] <sub>o</sub> ; [FDH] <sub>o</sub> ∈ [0.1-2] kU/L ; 0.1 ≤ [F] <sub>o,k</sub> ≤ 3 M ; 0.01 ≤ [NADH] <sub>o,k</sub> ≤ 0.5 M ;	
(v). $V_1 = V_2 = \dots = V_{N_{BR}}$ , (BR of equal volumes);	
(vi). The main reaction R1 occurs quantitatively, that is	

$[M(t)] = [F]_o - [F(t)]$ , at any moment in each <b>BR</b> .	
(vii). One excludes the trivial solution (infeasible): $\Omega = Fobj2 = Fobj3 = Fobj1 = 0$	
viii). The <b>SeqBR</b> model of (Table 3) imposes that the mannitol [M] produced in each <b>BR</b> is passed (at the batch end) to the next <b>BR</b> of the series, So, it continuously accumulates reaching a maximum concentration in the last <b>BR</b> of the series.	

“Concerning the formulation of the optimization problem eqns.(1-2), some observations are necessary: (a). the chosen units for M, MDH, FDH, allow the direct comparison of Fobj1, Fobj2, Fobj3, and their concomitant use in the  $\square \Omega$  objective function because they present the same order of magnitude; (b) the way by which  $\Omega$  was built, implicitly ensures the simultaneous realization of the following derived objectives: Max(Fobj1), Min(Fobj2), and Min(Fobj3); (c) equal volumes of BRs from the analyzed SeqBR offers the consistency of the summative objectives (Fobj2), and (Fobj3); (d) other formulations of the  $\Omega$  function are also possible, depending on the weight given to each individual sub-objectives (Fobj1, Fobj2, Fobj3)” [18].

## 5. Results and discussions

“The optimization problems eqns. (1,3), or eqns. (2,3) are Nonlinear Programming Problems – NLP [47,48], with 4 NBR = 40 searching variables, and multiple nonlinear implicit and explicit constraints. To avoid local sub-optimal solutions, a very effective multi-modal adaptive random search procedure has successfully been used, that is the MMA of Maria [47-49].

The SeqBR optimization problem eqns.(1,3) was solved in two alternatives, by setting different upper limits of the key substrate(s):

Alternative (a)-  $\text{Max}[F]_{o,k} = 1 \text{ M}$ , and  $\text{Max} [\text{NADH}]_{o,k} = 0.1 \text{ M}$ ,  
 $[\text{MDH}]_o$ ;  $[\text{FDH}]_o \in [0.1-1] \text{ kU/L}$  ;

Alternative (b)-  $\text{Max}[F]_{o,k} = 3 \text{ M}$ , and  $\text{Max} [\text{NADH}]_{o,k} = 0.5 \text{ M}$ ,  
 $[\text{MDH}]_o$  ;  $[\text{FDH}]_o \in [0.1-1] \text{ kU/L}$  ;

The resulted optimal operation policies are plotted in (Figure 7), while systems performances are comparatively summarized in (Table 6).

The analysis of these results reveals several conclusions:

(1) in both tested alternatives, the optimal SeqBR with NBR = 10 identical BRs reported better performances compared to the 10x repeated single optimal BRs. “

More specifically:

- 1a) for the SeqBR optimization problem eqns. (1,3) with the searching variables limits of Alternative (a) the enzyme consumption is roughly 12x higher for 10 individually operated optimal BRs than for an optimal SeqBR with a series of 10 BRs, to obtain a small increase in M-production (Table 6). The 10 individually operated BR-s of Slatner et al. [26] reported a huge (unacceptable) consumption of enzymes to obtain a modest M-production.
- 1b) For searching variables limits of Alternative (b) the enzyme consumption is significantly higher for the 10 individually operated optimal BRs for obtaining ca. 40% increase in M-production compared to the optimal SeqBR with a series of 10 BRs.
- 2) All searching variables ( $[F]_o$ ,  $[NADH]_o$ ,  $[MDH]$ ,  $[FDH]$ ) present a large influence on the objective functions eqns. (1-2).
- 3) “In the SeqBR, passing the content of one BR to the next BR leads to the accumulation of mannitol, but with preserving the non (yet) regenerated NAD(+), while the systematic initial adjustment of the  $[NADH]$  ensures its availability during the whole batches” (Fig. 7).
- 4) The requirement of the SeqBR optimal operating policy to decrease the enzyme content (often both of them concomitantly) for some BR-s of the SeqBR series involves an intermediate physical separation operation, separated enzymes being further re-used. Adjustments of the enzymes levels at the initial state of each BR from the series could be facilitated if immobilized enzymes are used.
- 5) “The direct comparison of the SeqBR with an optimized FBR may be an interesting problem to be studied in a separate numerical analysis.

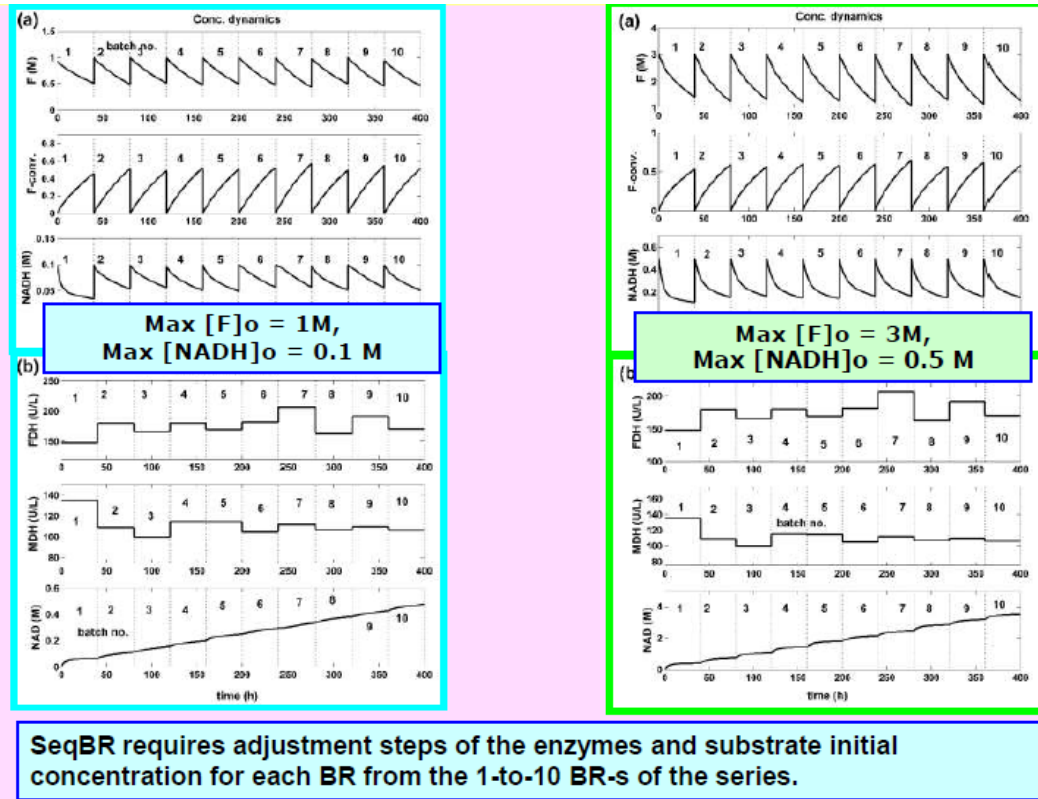


**Fig. 8.** “Species feeds and dynamics for the optimal SeqBR with  $\max[F]_0 = 1 \text{ M}$ ,  $\max[\text{NADH}]_0 = 0.1 \text{ M}$ ,  $[\text{HCOO}]_0 = [F]_0$ ,  $[\text{NAD}](\text{BR}=1) = 5 \times 10^{-4} \text{ M}$ . Solution of the optimization problem eqns.(1,3). Note: transformation of fructose (F) in mannitol (M) is quantitative, so  $[M] = [F]_0 - [F]$  at any moment. [Right] Species feeds and dynamics for the optimal SeqBR with  $\max[F]_0 = 3 \text{ M}$ ,  $\max[\text{NADH}]_0 = 0.5 \text{ M}$ ,  $[\text{HCOO}]_0 = [F]_0$ ,  $[\text{NAD}](\text{BR}=1) = 5 \times 10^{-4} \text{ M}$ . Solution of the optimization problem eqns.(1,3).”

- 6) In all tested alternatives, the optimal SeqBR reports incomparably better performances than the experimentally tested optimal BR of Slatner et al. [26] (Table 5) even if operated in a repetitive manner.
- 7) These results prove the superiority of SeqBR vs. the repeated use of a simple BR with the same initial conditions. Such better performances are due to a greater flexibility in the operation of each BR from the series of BRs.
- 8) Similar positive results with SeqBR have also been reported by” [12, 13, 50].

## 6. Conclusions

“The numerical/engineering analysis of this paper, based on an experimentally validated kinetic model from literature, demonstrates that optimally operated SeqBR can lead to high productivities with a substantially

lower consumption of costly enzymes compared to the repeated use of a simple BR, even if optimally operated.”

“The relatively simple but relevant case study analyzed in this paper proves that for the coupled multi-enzymatic systems, derivation of the optimal operating conditions (minimum enzyme consumption, with maximum reactor productivity) is not a trivial engineering problem even for a simple BR case [8, 9].

Solving this engineering problem by only using an experimental quasi-exhaustive approach, as tried by Slatner et al. [26], may not be the best choice because it involves high costs and a large number of experimental separate tests, while the result it might not be global optimal.

The use of an adequate process model can offer an approximate if not exactly solution to the problem (depending on model quality), with a moderate computational effort. In addition, the paper proves in a simple, yet suggestive way how a lumped but adequately dynamic model can successfully support in silico engineering evaluations aiming to optimize the BR or SeqBR operation, thus saving considerable experimental effort”.

Table 6

**“Performances of the optimal SeqBR policy obtained by solving the optimization problem eqns.(1,3) compared with some optimal BRs of Maria [9], and with the experimental data of Slatner et al.[26]. Initial conditions:  $[HCOO]_o = [F]_o$  ;  $[NAD]_o = 0.0005$  M; Batch time = 48 h for BR, and of 40 h for each of the 10 serial reactors of SeqBR. “**

Initial conditions (maximum amount)	Mannitol production / (total operating time) M/ min	MDH Total consumption (kU/L)	FDH Total consumption (kU/L)
<b>SeqBR</b> (10 BR) max[F] <sub>o</sub> = 1 M max [NADH] <sub>o</sub> = 0.1 M	5.059 / 400	1.112	1.755
10 repeated optimal <b>BR</b> [F] <sub>o</sub> = 1 M max [NADH] <sub>o</sub> = 0.008 M <b>(Table 5)</b>	8.2 / 480	13.88	10
10 repeated experimental <b>BR</b> of [Slatner et al., 1998] [F] <sub>o</sub> = 1 M max [NADH] <sub>o</sub> = 0.008 M <b>(Table 5)</b>	6.8 / 480	10	10
<b>SeqBR</b> (10 BR) max[F] <sub>o</sub> = 3 M max [NADH] <sub>o</sub> = 0.5 M	17.692 / 400	1.112	1,755
10 repeated optimal <b>BR</b> [F] <sub>o</sub> = 3 M max [NADH] <sub>o</sub> = 0.5 M <b>(Table 5)</b>	26.1 / 480	1	3

## Nomenclature



$c_j$	species $j$ concentration
$c_j^*$	species $j$ saturation level
$k_j, K_j$	rate constants
Min / Max	minimum / maximum
$r_j, R_1, R_2$	“species $j$ reaction rate; reaction rates
$t$	time
$t_f$	The batch time
$V$	The BR volume
$x_F$	Fructose conversion
<b>Greek Symbols</b>	
$\varepsilon$	accepted tolerance to achieve the target conversion
$\nu_{ij}$	stoichiometric coefficient of species $j$ in the reaction $i$
$\Omega$	The objective function of the optimization problem
<b>Index</b>	
o	initial
f	final
<b>Abbreviations</b>	
arg	The argument of a function
BR	batch reactor
BRP	BR with intermittent addition of enzyme solution
CSTR	Continuous stirred-tank reactor
DO	Dissolved oxygen
E	enzyme
F	D-Fructose
FDH	Formate dehydrogenase
FXBR	fixed-bed solid-liquid continuous reactor
GFS	fructose/glucose syrup
HCOO <sup>-</sup>	formate
M	Mannitol
MACR/ MASCR	mechanically agitated solid-liquid (semi-)continuous reactor
MDH	Mannitol dehydrogenase
NAD(P)H	nicotinamide adenine dinucleotide (phosphate)
NAD, NAD <sup>+</sup>	Nicotinamide adenine dinucleotide (oxidized form)
NLP	Nonlinear Programming Problem
$N_{BR}$	Number of BR connected in series
$N_{div}$	Number of time-‘arcs’ in which the <b>FBR</b> time was divided (in every time-arc. the feeding composition is constant, but the feeding differs between them).
SeqBR	sequential batch-to-batch reactor
SBR	semi-batch reactor”

[X] Concentration of X

## REFERENCES

- [1] Liese, A.; Seelbach, K.; Wandrey, C., *Industrial biotransformations*, Wiley-VCH, Weinheim, 2006.
- [2] Straathof, A.J.J.; Adlercreutz, P., *Applied biocatalysis*, Harwood Academic Publ., Amsterdam, 2005.
- [3] Xue, R.; Woodley, J.M., *Bioresour. Technol.*, 115 (2012), 183–195. doi: 10.1016/j.biortech.2012.03.033.
- [4] Maria, G., *Comput. & Chem. Eng.*, 31 (2007), 1231-1241. doi:10.1016/j.compchemeng.2006.10.009.
- [5] Maria, G., *Comput. & Chem. Eng.*, 36 (2012), 325–341. DOI: 10.1016/j.compchemeng.2011.06.006.
- [6] Maria, G.; Crisan, M., *Asia-Pac. J. Chem. Eng.*, 10 (2015), 22-44. doi: 10.1002/apj.1825.
- [7] Crisan, M.; Maria, G., *Revista de Chimie* (Bucharest), 68 (2017), 2196-2203.
- [8] Gajardo, P.; Ramirez, H.C.; Rapaport, A.E., *SIAM Journal on Control and Optimization*, 47 (2008), 2827-2856. DOI: 10.1137/070695204
- [9] Maria, G., *Computers & Chemical Engineering*, 133 (2020A), 106628-106635. <https://doi.org/10.1016/j.compchemeng.2019.106628>
- [10] Wang, C.; Quan, H.; Xu, X., *Ind. Eng. Chem. Res.* 35 (1996), 3560-3566. <https://doi.org/10.1021/ie9506633>
- [11] Wang, P., *Appl. Biochem. Biotechnol.* 152 (2009), 343–352. doi: 10.1007/s12010-008-8243-y.
- [12] Martinez, E., *Proc. 2nd Mercosur Congress on Chemical Engineering*, Rio de Janeiro, Costa Verde, Brasil, 2005, paper #20.
- [13] Dewasme, L.; Cote, F.; Filee, P.; Hantson, A.L.; Wouwer, A.V., *Bioengineering* (Basel) 4 (2017), 17. doi:10.3390/bioengineering4010017
- [14] Maria, G., *Molecules*, 25 (2020B), 5648-5674, doi:10.3390/molecules25235648
- [15] DiBiasio, D. Introduction to the control of biological reactors. In: Shuler, M.L. (ed.), *Chemical engineering problems in biotechnology*, American Institute of Chemical Engineers, New York, 1989, pp. 351-391.
- [16] Maria, G.; Crisan, M., *J. Process Control.*, 53 (2017), 95-105 .doi: 10.1016/j.jprocont.2017.02.004
- [17] Smets, I.Y.; Claes, J.E.; November, E.J.; Bastin, G.P.; van Impe, J.F., *J. Process Control.*, 14 (2004), 795-805. doi:10.1016/j.jprocont.2003.12.005
- [18] Scoban, A.G.; Maria, G., *Asia-Pacific J. Chem. Eng.*, 11 (2016), 721-734. <https://doi.org/10.1002/apj.2003>
- [19] Amribt, Z.; Dewasme, L.; Wouwer, A.V.; Bogaerts, P., *Bioprocess Biosyst Eng.*, 37 (2014), 1637–1652, doi 10.1007/s00449-014-1136-2
- [20] Binette, J.C.; Srinivasan, B., *Processes*, 4 (2016), 27. DOI: 10.3390/pr4030027
- [21] Franco-Lara, E.; Weuster-Botz, D., *Bioprocess Biosyst. Eng.*, 28 (2005), 71-77. <https://doi.org/10.1007/s00449-005-0017-0>
- [22] Maria, G.; Renea, L., *Bioengineering-MDPI* 8 (2021), 210-247. <https://doi.org/10.3390/bioengineering8120210>
- [23] Maria, G.; Crisan, M., *Asia-Pacific Journal of Chemical Engineering* 10 (2014), 22-44. doi: 10.1002/apj.1825.

- [24] Maria, G.; Dan, A., *Computers & Chemical Engineering*, 35 (2011), 177-189. Doi: 10.1016/j.compchemeng.2010.05.003
- [25] Avili, M.G.; Fazaelipoor, M.H.; Jafari, S.A.; Ataei, S.A., *Iranian Journal of Biotechnology*, 10 (2012), 263-269.
- [26] Slatner, M.; Nagl, G.; Haltrich, D.; Kulbe, K.D.; Nidetzky, B., *Biotransform.*, 16 (1998), 351-363. <https://doi.org/10.3109/10242429809003628>
- [27] Renea, L., Maria, G., 22-th Romanian International Conference on Chemistry and Chemical Engineering *RICCCE-22*, Sinaia (Romania), 7-9 Sept. 2022.
- [28] Saha, B.C.; Racine, F.M., *Appl Microbiol Biotechnol.*, 89, (2011), 879–891, doi 10.1007/s00253-010-2979-3
- [29] Bhatt, S.M.; Mohan, A.; Srinivastava, S.K., *ISRN Biotechnology*, 2013, Article ID 914187. <https://doi.org/10.5402/2013/914187>
- [30] Von Weymarn, N., Process development for mannitol production by lactic acid bacteria, PhD thesis, TU Helsinki, 2002. <http://lib.tkk.fi/Diss/2002/isbn9512258854/isbn9512258854.pdf>
- [31] Chenault, H.K.; Whitesides, G.M., *Appl. Biochem. Biotechnol.*, 14, (1987), 147-197.
- [32] Maria, G.; Ene, M.D., *Chem. Biochem. Eng. Q.*, 27, (2013), 385–395.
- [33] Bäumchen, C.; Roth, A.H.F.J.; Biedendieck, R.; Malten, M.; Follmann, M.; Sahm, H.; Bringer-Meyer, S.; Jahn, D. D-Mannitol production by resting state whole cell biotransformation of D-fructose by heterologous mannitol and formate dehydrogenase gene expression in *Bacillus megaterium*, *Biotechnol. J.*, 2, (2007), 1408-1416. doi: 10.1002/biot.200700055
- [34] Maria, G.; Ene, M.D.; Jipa, I., *Journal of Molecular Catalysis B: Enzymatic*, 74, (2012), 209-218. DOI: 10.1016/j.molcatb.2011.10.007.
- [35] Moser, A., Bioprocess technology: kinetics and reactors, *Springer-Verlag*, New York, 1988.
- [36] Dutta, R., Fundamentals of biochemical engineering, *Springer verlag*, Berlin, 2008.
- [37] Maria, G., Peptănar, I.M., *Dynamics-MDPI* 1 (2021), 134-154. <https://doi.org/10.3390/dynamics1010008>
- [38] Loeblein, C.; Perkins, J.; Srinivasan, B.; Bonvin, D., *Comput. Chem. Eng.*, 21, (1997), S867-S872.
- [39] Bharat, A., Process analytical technology (PAT), Msc-diss., P.D.V.V.P.F.S. College of pharmacy, Ahmed Nagar (India), 2013. <https://www.slideshare.net/anjalibharat19/process-analytical-technology> (accessed on 28 November 2020).
- [40] Irvine, R.L.; Busch, A.W., *Journal of Water Pollution Control Federation*, 51 (1979), 235-243. <http://www.jstor.org/stable/25039819> (accessed on 02/04/2012)
- [41] Shacham, M., Semicontinuous fed-batch and cyclic-fed batch operation, Proc. Workshop “Modern Problem Solving Techniques in Engineering with POLYMATH, Excel and MATLAB”, Tel-Aviv University, September 23, 2008. pp.1439-1441, Chap. 14.13. <http://www.eng.tau.ac.il/~brauner/Workshop08Participant/Example-7/Prob-14-13.pdf> (accessed on 23 February 2021), <http://www.eng.tau.ac.il/~brauner/> (accessed on 23 February 2021)
- [42] US EPA, Wastewater technology fact sheet: Sequencing Batch Reactors, OWM, Water Permits Division, Municipal Branch, Washington, 2012, Available on-line: [https://www3.epa.gov/npdes/pubs/sbr\\_new.pdf](https://www3.epa.gov/npdes/pubs/sbr_new.pdf) (accessed on 23 February 2021)
- [43] Rätze, K.H.G.; Jokiel, M.; Sundmacher, K., *Proc. ISCRE 25 Symp.*, 20-23 May 2018, Elsevier, Florence(It), 2018.
- [44] Sawatzki, A.; Hans, S.; Narayanan, H.; Haby, B.; Krausch, N.; Sokolov, M.; Glauche, F.; Riedel, S.L.; Neubauer, P.; Bournazou, M.N.C., *Bioengineering*, 5, (2018), 101; doi:10.3390/bioengineering5040101

- [45] Hans, S.; Ulmer, C.; Narayanan, H.; Brautaset, T.; Krausch, N.; Neubauer, P.; Schäffl, I.; Sokolov, M.; Bournazou, M.N.C., *Processes* (MDPI), 8, (2020), 582; doi:10.3390/pr8050582
- [46] Froment, G.F.; Bischoff, K.B., *Chemical Reactor Analysis and Design*, Wiley, New York, 1990.
- [47] Maria, G., Adaptive random search and shortcut techniques for process model identification and monitoring, Pekny, J.F., Blau, G.E., Carnahan, B. (Eds.), *Foundations of Computer Aided Process Operations*, AIChE, New York, 1998; also in: AIChE Symp. Ser., 94 (1998), 351-359.
- [48] Maria, G., *Chemical and Biochemical Engineering Quarterly*, 18, (2004), 195-222. <https://doi.org/10.15255/CABEQ.2014.557>
- [49] Maria, G., ARS combination with an evolutionary algorithm for solving MINLP optimization problems, Hamza, M.H. (Ed.), *Modelling, Identification and Control*, IASTED/ACTA Press, Anaheim (CA), 2003, Pp. 112-118. [https://www.actapress.com/Content\\_of\\_Proceeding.aspx?proceedingID=213](https://www.actapress.com/Content_of_Proceeding.aspx?proceedingID=213) (last accessing March-7, 2021).
- [50] Dewasme, L.; Amribt, Z.; Santos, L.O.; Hantson, A.L.; Bogaerts, P.; Wouwer, A.V., Proc. 12th IFAC symposium on computer applications in biotechnology, Mumbai, India, Dec. 16-18, 2013. *The International Federation of Automatic Control*, 46, (2013), 60-65. doi: 10.3182/20131216-3-IN-2044.00045

## THE RISK OF MICROPLASTIC PARTICLES SEEN THROUGH THE FUTURE ACTIONS OF ROMANIANS

Valeria POP<sup>1</sup>, Mălina PETRESCU-MAG<sup>1</sup>, Crina PETRESCU<sup>1</sup>, Alexandru OZUNU<sup>1,\*</sup>

<sup>1</sup> Department of Environmental Analysis and Engineering, Faculty of Environmental Science and Engineering, University of Babeş-Bolyai, 30 Fantanele Street, RO-400294, Cluj-Napoca Romania

### **Abstract**

*Plastic and microplastic (MP) pollution is known to be widespread across the planet in all types of environments. We are now in the so-called "Plastic" era, which reflects the omnipresence of plastics in our lives. It is already recognized that plastic particles smaller than 5 mm, known as PM, have a tremendous impact on the ecosystem, local economies and human health. Our study is based on a survey (questionnaire) that includes 406 respondents from all over Romania, based on 20 questions. Most of these questions were divided into several points. "Which of the following actions are you planning to do in the near future (within the next 3 months)?" was one of the main questions. Here, the population's perception of this type of risk of microplastic particles was tracked. Respondents answered on a scale from 1 to 7, where: 1= Definitely not... 7= Definitely yes. The actions followed by this type of question were as follows: I will reduce the consumption of plastic items; / I will replace plastic items with eco-friendly products in my purchasing decision whenever possible; / I will recycle my plastic waste (separating it); / I will refuse to buy plastic products even if there is no ecological alternative; / I will reuse plastic items beyond their original use (eg using a plastic water bottle by refilling it; using a plastic cup that is no longer suitable for drinking, such as pots); / I will replace "single-use plastic products" (eg single-use water bottles, plates, straws, cutlery, cotton wool) with environmentally friendly products, to prevent these particles. Over 44% of respondents said they would reduce their plastic consumption in the near future, over 60% said they would recycle and just over 9% agreed to substitute in the purchasing process, products containing plastic with ecological products, whenever needed. A proper perception and attitude of risk related to microplastic particles, by the responders and not least by the government, would reduce this risk related to microplastic particles.*

**Key words:** microplastic, risk perception, pollution, environment

---

\*Corresponding author: Email: alexandru.ozunu@ubbcluj.ro

## 1. Introduction

The production and use of plastics has followed an upward trend in the last two decades and reached a record level with the COVID-19 pandemic [1]. During the COVID-19 pandemic, 1.6 million tons of plastic waste were generated worldwide per day, mainly due to high market demand in the production of single-use personal protective equipment. This means that there was an annual plastic waste generation of 75 kg per capita [2].

The major problem with microplastic particles (MPs) is that they do not biodegrade and once they reach the terrestrial environment they accumulate in the bodies of animals, and in the marine environment they integrate into the bodies of fish and crustaceans, being then consumed by humans as food. MPs have been found in marine, freshwater and terrestrial ecosystems, as well as in food and drinking water. Their continuous release contributes to the permanent pollution of all ecosystems and food chains. In research through laboratory studies, this exposure to that pollutant has been associated with a number of negative ecotoxic and physical effects that act on the health of living organisms [3].

However, plastics are essential raw materials widely used in various fields in our modern society due to their excellent durability and moldability [4]. An increasing number of research on MPs have been reported in the last decade, indicating the importance of this field. A considerable effort and a reduction in plastic production would lead to a decrease in pollution with this occurrence [5].

As a result of environmental and human health concerns, several member states of the European Union have introduced or proposed national bans on the intentional use of MPs in consumer products. Every year, approximately 42,000 tons of MPs end up in the environment from the use of products containing them. It is estimated that around 176,000 tons of unintentionally produced MPs reach the surface waters of the European continent annually as a result of wear and tear from large pieces of plastic [6].

MPs are another symbol of global environmental change and for this reason the perception of individuals is important. Through his study, Pahl [7], helped fill the gap in social research and the "human dimension". Kramm [8], showed that the majority of the German public has a high perception of risk, with a slightly higher concern for environmental risks than for health risks. Although concern was generally high, some differences could be identified.

A decrease in the negative impact of MPs can be successful when there is strong pro-environmental behavior. Kurisu [9] defines pro-environmental behaviors (PEBs) as behaviors that "contribute or are perceived to contribute to environmental conservation," while environmental conservation is described as either reducing negative impacts or increasing positive environmental impacts.

## 2. Experimental

The survey is based on a questionnaire that was drafted in Romanian and carried out on an online platform. The link created for the questionnaire was distributed online on several social platforms (for example, Facebook, Instagram, WhatsApp, mail, Messenger, messages, etc.). According to Cohen [10], the distribution of the link for the survey, followed the method of the Bulgarian snow but the representation according to Amicarelli [11] may suffer distortions. All the discussions were subject to GDPR, being anonymous, not asking the participants for their personal data.

### 2.1. The study area

The study area includes the entire territory of Romania, with respondents from over 30 counties of the country.

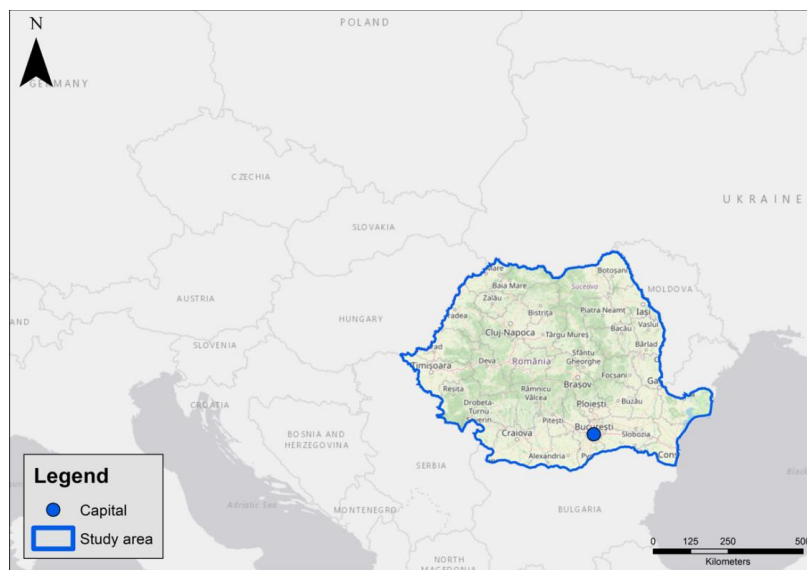


**Fig. 1.** Survey study area

### 2.2. Types of questions in the questionnaire

Establishing the criteria for dividing the questions: introductory questions; closed questions with (given answer options); open questions; content questions that provide most of the information in accordance with the research object (questions with scales); control questions that aim to verify the answer to a previous question; identification questions (age, income, resident).

Each question in the questionnaire corresponds to a specific objective Ex 1. Question number 4 - Which of the following actions do you plan to do in the near future (3 months)? This question results in an answer related to the individual's perception of recycling, reusing, replacing, reducing, refusing to replace plastic items. More precisely, if there is an increasing trend in recycling and consumption of plastic products.

Ex. 2. The identification question, related to the place of residence, is based on obtaining the result that supports another secondary objective proposed in the paper. More precisely we want to see if the place of residence matters, if you are influenced and at the same time if we have a higher rate of growth of the trend for the 4 Rs in certain areas of the country.

The survey used both environmental and social science research methods through a quantitative approach (questionnaire, based on empirical research (the opposite of theoretical research)). A methodology based on a qualitative approach was not carried out because the quantitative process, through the complexity and number of questions, was made through a deeper and more detailed investigation.

The creation of the questionnaire is based on the establishment of the investigated collective, the formulation of the questions, the establishment of the spatial, modal and temporal coordinates. This quantitative research was carried out with the help of data collection and processing and will highlight certain results of the data processing, being extensive and expensive, because a certain amount, a certain volume of data was needed, for the processing and the results to be has relevance. The theoretical documentation necessary and useful for the scientific research undertaken involved the consultation of bibliographic sources regarding the risk of microplastics, both on the territory of Romania and internationally, having as bibliographic sources, books, articles, specialized studies, etc. Current studies in specialized journals show that academic research on the use of qualitative, quantitative and mixed methods in the economic field is in full development and justifies the creation of articles and doctoral theses on this topic. The analysis of classical qualitative and quantitative methods from the perspective of their integration into complex, mixed methodological norms, represents an important and topical research objective [12], [13]. The data were collected from the primary source (questionnaire). Among the sources that could be used: questionnaire, experiment, interview, observations, etc., we chose the questionnaire as a primary source. In this research, an attempt was made to harm the participants by maintaining the confidentiality of the results obtained for this research. SPSS statistical software was used for data analysis.



### 3. Results and discussions

In the study, the perception of Romanians and their attitude related to the present risk of microplastic particles in all four environmental factors was followed: water, air, soil and biodiversity. More than 9% of respondents answered that they will replace plastic with environmentally friendly products in their purchase decisions, whenever possible. Just over 44% answered that they will reduce their consumption of plastic items and 60% said that they will use the process of recycling plastic waste, separating it. All these actions follow a period of 3 months.

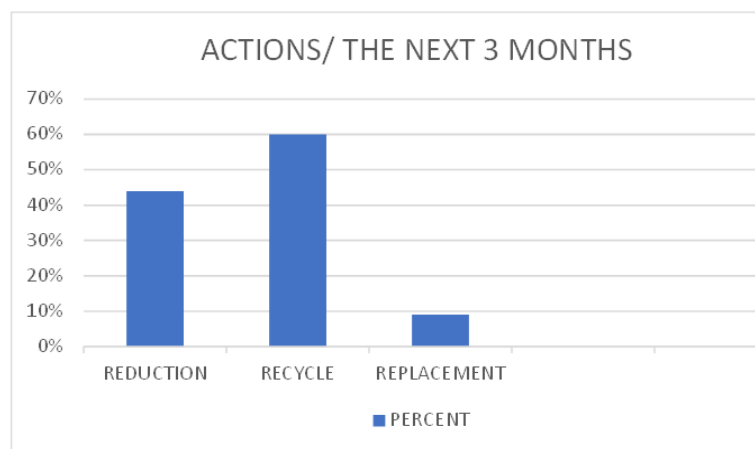


**Fig. 2.** Actions to reduce, recycle and replace plastic for a short period – Romania

#### 3.1. Proposed actions

The actions followed in the study are REDUCTION, REPLACEMENT IN THE BUYING DECISION OF PLASTIC ARTICLES WITH ENVIRONMENTALLY FRIENDLY PRODUCTS, RECYCLING, REFUSAL TO BUY, REUSE AND REPLACEMENT OF SINGLE-USE PRODUCTS.

For each question, a scale from 1 to 7 was used (1 - definitely NO and 7 - definitely YES), I will reduce, replace, etc. my plastic consumption.

##### 3.1.1. Proposed actions

The results obtained have a good impact on the environment, more they reflect pro-environmental actions of the Romanians. Just over 2.97% answered "categorically No" I will reduce my plastic consumption in the next three months, which is a satisfactory result. A little over 16% ticked four which represents "maybe" and a percentage of 44.30% declare that they will reduce their plastic

consumption in the established period, ticking the number 7 "categorically YES", as can be seen from the graph Fig. 3.

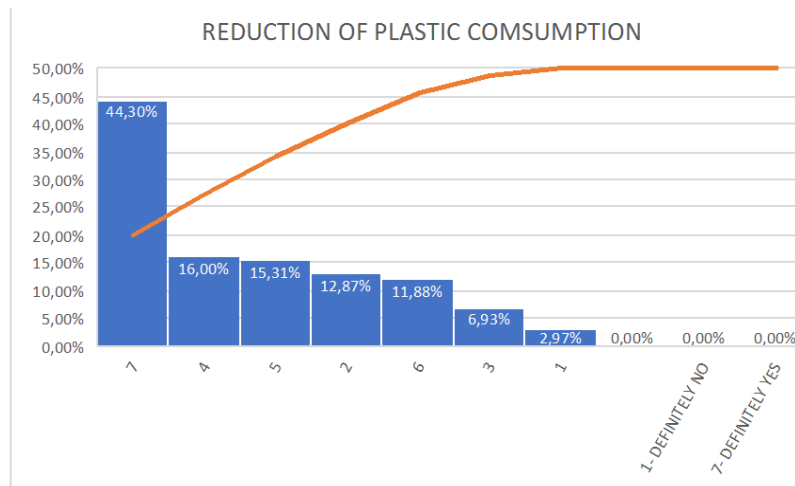


Fig. 3. Reduction of plastic consumption

3.1.2. *Replacing plastic items in purchasing decisions with environmentally friendly products.*

In the process of replacing plastic items in purchasing decisions with environmentally friendly products, the percentages show a lower acceptance rate. A little over 18.81% answered "categorically Yes", 11.88% answered "categorically NO". This 18.88% is not a large percentage, which is not worrying, and 18.56% are still thinking about what decisions they will make related to plastic in the next three months. Table no. 1.

Table 1

**Replacement in purchasing decisions for the next 3 months:  
SUBSTITUTION in purchasing decisions**

Scale from 1-7	Number of prospectuses	Percent %
1 - Definitely NO	48	11.88
2	39	9.65
3	50	12.57
4	75	18.56
5	66	16.33
6	52	12.87
7 - Definitely YES	76	18.81

### 3.1.3. Recycling plastic waste (separating it)

As can be seen in Table 2, related to recycling, the percentages show a high rate of pro-environmental actions. The mass media campaigns, the government through actions and specific legislation and last but not least the supermarkets have left their mark here. Some of them have established plastic waste collection centers in Romania. People's actions are also rewarded, they offer discounts and different offers in return.

Among those questioned, a number of 245 people answered with "sure YES", representing a majority percentage of 60.64%. A small number of people answered with "certainly NO", they very slightly exceed the percentage of 3.46%.

In many countries around the world, the plastic recycling process is on an upward curve. If the plastic material is not disposed of or recycled properly, it can end up in the environment turning into pieces where they remain for centuries. These pieces (< 5mm) are called microplastic particles and are a cause for concern. These are solid particles of plastic material composed of mixtures of functional additives and polymers that may also contain residual impurities.

Table 2

<b>Plastic recycling action in the next 3 months: RECYCLING of plastic</b>		
Scale from 1-7	Number of prospectuses	Percent %
1 - Definitely NO	14	3.46
2	9	2.27
3	16	3.96
4	33	8.16
5	32	7.92
6	57	14.1
7 - Definitely YES	245	60.64

### 3.1.4. Reuse plastic items beyond their original use

Reusing plastic items beyond their original use (for example, use a plastic water bottle by filling it; use a plastic cup that is no longer suitable for drinking as a pot), is a technique that can have a positive long-term impact on the environment. Thus, the packaging does not end up in landfills after a first use, if it is not recycled. The reuse of plastic products, purchased as packaging or in another form, had a good impact in our study. More than 199 people answered "sure YES" to the question above, with a percentage of 49.25% and a little over 9.15% had a "sure NO" answer. Only 6.18% answered "maybe" (Table 3).

Table 3

<b>Reusing plastic items in the next 3 months: REUSING of plastic</b>		
Scale from 1-7	Number of prospectuses	Percent %
1 - Definitely NO	37	9.15
2	13	3.81
3	17	4.2
4	25	6.18
5	43	10.64
6	72	17.82
7 - Definitely YES	199	49.85

*3.1.5. Replacing single-use plastic products, with the aim of preventing pollution with micro and nanoplastic particles*

Currently, plastic production exceeds 350 million tons/year [14]. In 2017, the European Commission took some EU-wide regulatory action on MPs intentionally added to products. An extended solution has been proposed on the intended use of MPs in products placed on the EU market to avoid or reduce the amount released into the environment. The proposal is expected to prevent the release of 500,000 tons of microplastics over 20 years [15].

Among the restrictions among the most important are: banning the intentional addition of microplastics to products such as cosmetics and detergents by 2020; increasing the recycling rate of plastic waste in the EU; the ban in the E.U. of certain single-use plastic products that end up as waste in the seas and for which alternative materials already exist; the ban in the E.U. of light plastic bags. The European Parliament has added oxo-degradable plastics to the list of items to be banned. These are materials that easily break into small pieces due to additives and contribute to ocean pollution with MPs [6].

Starting from September 2, 2021, in Romania, single-use plastic products, products made from oxodegradable plastic materials and fishing equipment containing plastic are regulated by a new simple ordinance (OG 6/2021). Through this Ordinance, certain categories of products will be prohibited from being placed on the market, and consumption reduction targets will be applied for others.

Prohibited products: ear sticks, cutlery, plates, drinking straws, drink stirrers, sticks that attach to balloons, food containers, etc.

The results of our study regarding the process of replacing single-use plastic products, with the aim of purchasing environmentally friendly products, show a percentage of over 50% in the decisions of the interviewed Romanians, who say, with "sure YES". A little over 3.96% answered with "definitely NO", not making any commitments for the next three months, after completing the questionnaire (Table 4).

Table 4

**Replacement single- use plastic products: REPLACEMENT**

Scale from 1-7	Number of prospectuses	Percent %
1 - Definitely NO	16	3.96
2	8	1.98
3	13	3.21
4	39	9.65
5	58	14.35
6	66	19.09
7 - Definitely YES	209	51.73

### 3.1.6. Refusal to purchase plastic items

Even when we have no alternative, we can refuse the purchase of plastic products. A percentage of less than 20% of the respondents used in their answer related to this topic, the number 7, more precisely with "sure YES". Over 11.88% answered categorically No (Table 5).

Table 5

**Refusal to buy plastic products even if there are no environmentally friendly products: REFUSAL**

Scale from 1-7	Number of prospectuses	Percent %
1 - Definitely NO	48	11.88
2	39	9.65
3	50	12.57
4	70	18.56
5	66	16.33
6	52	12.87
7 - Definitely YES	76	18.81

## 4. Conclusions

From the results obtained, we observe a concern of the Romanians for the environment. Government policies implemented through ordinances transposed from European policies, as well as the entire mass media, have left their mark on the area related to the recycling of plastic materials. In this area of recycling, the repetition of this topic in the press, TV, etc., but also online actions brought the percentage to over 60%. There is a need for such actions either by governments or the mass media and on the side of reducing and replacing disposable products with more environmentally friendly products, where the percentages obtained are lower.

Large store chains, through concrete recycling actions, could help to a small extent to increase the percentage on this side. There are very few supermarkets in Romania that have implemented such a system. One of the problems would be the distance from the collection points of the shops, which does not happen in the west.

Our study being carried out online, via the Internet, could be subject to some limitations because according to the I.N.S. 2021, eight out of ten houses in Romania have an internet connection. More than 80% of the Romanian population uses the Internet and the difference between men and women in terms of Internet connection has also decreased. In rural areas, 73.1% of households are connected to the Internet, and in urban areas, 86.3%.



**Fig. 4.** <https://www.dreamstime.com/photos-images/microplastic.html> [16]

## REFERENCES

- [1] Adyel T. M., Accumulation of plastic waste during COVID-19, *Science*, 369, 6509, (2020) 1314–1315, doi: 10.1126/science.abd 9925.
- [2] Prata J. C., Silva A. L. P., Walker T. R., Duarte A. C., Rocha-Santos T., COVID-19 Pandemic Repercussions on the Use and Management of Plastics, *Environ. Sci. Technol.*, 54, 13, (2020), 7760–7765, doi: 10.1021/acs.est.0c02178.
- [3] European Chemicals Agency ECHA, *Microplastics*, (2018). [Online]. Available: <https://echa.europa.eu/ro/hot-topics/microplastics>
- [4] Miri S., Saini R., Davoodi S. M., Pulicharla R., Brar S. K., Magdouli S., Biodegradation of microplastics: Better late than never, *Chemosphere*, 286, (2022), 131670, doi: 10.1016/j.chemosphere.2021.131670.
- [5] Borrelle S. B. *et al.*, Predicted growth in plastic waste exceeds efforts to mitigate plastic pollution, *Science*, 369, 6510, (2020), 1515–1518. doi: 10.1126/science.aba 3656.
- [6] Parlamentul European, Microplastic particles: sources, effects and solutions. (2018). [Online]. Available: <https://www.europarl.europa.eu/news/ro/headlines/society/20181116STO19217/microplasti-cele-surse-efecte-si-solutii>
- [7] Pahl S., Wyles K. J., Thompson R. C., Channelling passion for the ocean towards plastic pollution, *Nat Hum Behav*, 1, 10, (2017), 697–699; doi: 10.1038/s41562-017-0204-4.
- [8] Kramm J., Explaining risk perception of microplastics: Results from a representative survey in Germany, *Global Environmental Change*, (2022), p. 13.
- [9] Kurisu K., *Pro-environmental Behaviors*. Tokyo: Springer Japan, (2015); doi: 10.1007/978-4-431-55834-7.
- [10] Cohen N., Arieli T., Field research in conflict environments: Methodological challenges and snowball sampling, *Journal of Peace Research*, 48, 4, (2011), 423–435, doi: 10.1177/0022343311405698.
- [11] Amicarelli V., Lagioia G., Sampietro S., C. Bux, Has the COVID-19 pandemic changed food waste perception and behavior? Evidence from Italian consumers, *Socio-Economic Planning Sciences*, 82, (2022), 101095, doi: 10.1016/j.seps.2021.101095.
- [12] Dinis M. A. P., Vidal D. G., Dias R. C., Environmental and Health Research Methodologies: Integrating a Transdisciplinary Approach in a Higher Education Cross-Cutting Curricular Unit, in *Sustainable Policies and Practices in Energy, Environment and Health Research*, W. Leal Filho, D. G. Vidal, M. A. P. Dinis, and R. C. Dias, Eds. Cham: Springer International Publishing, (2022), 135–146. doi: 10.1007/978-3-030-86304-3\_8.
- [13] De Almeida, C. D. G. C., Gordin L. C., Dos Santos Almeida A. C., Júnior J. A. S., De Almeida B. G., Provenzano G., Assessing different methodologies for irrigation scheduling in protected environment: a case study of green bell pepper, *Irrig Sci*, (2022), doi: 10.1007/s00271-022-00785-z.
- [14] Plastics Europe Association of Plastics Manufacturers, Plastics – the Facts 2020 An analysis of European plastics production, demand and waste data. (2020). [Online]. Available: [https://plasticseurope.org/wp-content/uploads/2021/09/Plastics\\_the\\_facts-WEB-2020\\_versionJun21\\_final.pdf](https://plasticseurope.org/wp-content/uploads/2021/09/Plastics_the_facts-WEB-2020_versionJun21_final.pdf)
- [15] European Chemicals Agency ECHA, “ECHA proposes to restrict intentionally added microplastics.” (2019). [Online]. Available: <https://echa.europa.eu/ro/-/echa-proposes-to-restrict-intentionally-added-microplastics>
- [16] <https://www.dreamstime.com/photos-images/microplastic.html>

## HEAVY METALS REMOVAL FROM SOIL AND AIR – A BRIEF REVIEW

Tănase DOBRE<sup>1</sup>, Shaalan BDAIWI AHMED<sup>1,2</sup>, Iuliana Mihaela DELEANU<sup>1\*</sup>

<sup>1</sup>Chemical and Biochemical Engineering Dept., Faculty of Chemical Engineering and Biotechnologies, P.O. 35-107, Polizu Str. 1-7, 011061, Bucharest, Romania

<sup>2</sup>Environment and Water Directorate, Ministry of Science and Technology, Baghdad, Iraq

### **Abstract**

*Heavy metals are some of the most harmful pollutants with severe effects on humans, plants, animals, and on the entire environment basically. Today, anywhere in the world, and especially in highly industrialized countries, any analysis of heavy metals in water, soil or air samples will certainly indicate their presence. It is clear that pollution comes from heavy metals compounds, and these compounds rarely result from natural geochemical processes. They are mainly the result of human-related activities, from mining to chemical or non-chemical industrial and agricultural practices. For many decades now, heavy metals pollution has been a major source of worries due to their high level of toxicity, non-biodegradability, persistence and bioaccumulative nature.*

*This review discusses, in brief, conventional and modern technologies for HM removal from soil and air, each with advantages and drawbacks. It is clear that effective removal methods exist already, but new remediation techniques are needed, as will be further detailed.*

**Key words:** Heavy metals; Soil reclamation; Air depollution; Removal methods

### **1. Introduction**

Heavy metals (HMs) results from natural and from anthropogenic sources and accumulate in all environmental components [1].

Lead, cadmium, mercury, arsenic, copper, zinc, and chromium are some of the metals known to be toxic to humans. Cadmium and arsenic are known carcinogens. Copper, lead, and chromium can cause brain and bone damage, while mercury can induce mutations and genetic disorders [2].

---

\* Corresponding author: Email address: iuliana.deleanu@upb.ro



To function properly, the living systems need certain metals like iron, copper, zinc, magnesium, manganese, and others. Therefore, small amounts of these elements are found in nature and are essential to our health, but exposure to excessive levels of any of these elements can have acute or long-term harmful effects [3–5]. Moreover, toxic HMs tend to accumulate in living organisms due to their non-biodegradability and persistence, causing a wide range of diseases and disorders. For example, hemoglobin production and anemia are both determined by the interaction of lead with the enzymes involved in heme biosynthesis [6]. Lead poisoning can cause encephalopathy, convulsions, and mental impairment in humans [7]. Neurobehavioral development is severely harmed by exposure to lead. Thus, industrial wastes containing lead should be thoroughly cleaned before being disposed [8]. Many researchers studied the removal of lead ions by different adsorbents such as natural and industrial materials, granular activated carbon, char, and chitosan [9].

Following the few examples indicated above, it is clear that because of HM's non-degradable properties, the resulting pollution can be defined as irreversible, and consequently it must be carefully monitored and managed. Currently the presence of HM is strictly monitored in soil, outdoor air, surface and ground water, drinking water, in accordance with regulatory mandates, but the human exposure/biological monitoring is rarely achieved [10,11]. While data show continuous decline in heavy metals emissions, improvements in technologies and targeted legislation are needed to reduce the health impact of the pollution [12].

As emphasized before, the pollution with HM exists in different environmental compartments. In air we find particulate matter (PM<sub>10</sub> and smaller) containing HMs resulted from industrial activities, and volatile compounds like tetraethyl lead, tetracarbonyl nickel, etc., resulted from burning fossil fuels. In the soil, HMs accumulate, by their transfer from water (leaching) and from air (re/sedimentation and adsorption). The methods of controlling the effects of HM should refer to drastic and more restrictive environmental rules on HM discharge limits, leading to new highly efficient treatment technologies development and implementation.

## **2. Methods in soil depollution**

According to literature information, the soil pollution with HM is first of all the direct consequence of their increasing use as such, respectively in the form of compounds of industrial interest. In fact, any metal or metal-containing product thrown or abandoned in/on soil becomes a pollution source for longer or shorter time.

In an extensive review on metal contamination of agricultural soils, Huo *et al.* [13] identified sources of pollution with HM(loid)s from surface runoff and irrigation with polluted water sources to aerosols released during industrial activities. So, with respect to high soil pollution, we can say that a larger or smaller area of pollution usually appears around sites where HM were industrially processed. One example, representative for Romania, could emphasize these observations: the case of HM pollution within Bucharest metropolitan area. The most important pollution sources were identified as industrial activities, traffic (cars, railway, and air transportation), power stations and domestic activities [14]. Especially in the area Pantelimon – Brănești, because of the industrial activities 390 ha of land were polluted with lead, 87 ha with copper and 15 ha with zinc. Among others, here, starting with 1978 it was built an industrial site for lead-acid accumulators for all purpose industrial applications (cars, locomotives and wagons, tractors, and trucks, etc.). Due to contamination levels, the entire area has been declared as disaster area since 1998. The lead concentration for instance was, at the time of the study, 230 times higher than the maximum accepted. Population health issues were recorded in the period 1990-2005 [15].

Regarding the problem of HM contaminated soils, there are some solutions for remediations, as shown schematically in Fig. 1. The first category consist in pollutants containment-based techniques (capping/encapsulation), the pollutants removal and extraction express the second category, defined as transport-based techniques, whereas pollutants solidifications and stabilization define the third category of transformation-based techniques for soil decontamination [16].

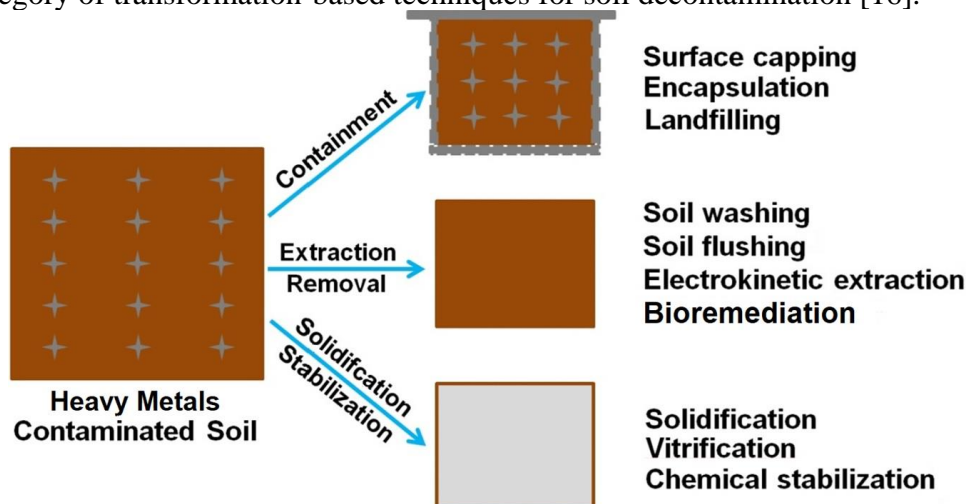


**Fig. 1.** Solutions for soil decontamination in pollution with HM compounds (Adapted with permission from [16])

In the following, more attention is paid to the biotechnological solutions for soil decontamination, included in Fig. 6 as bioremediation.

Bioremediation is defined as the interaction between living organisms (plants or microbial species, native or genetically engineered), and the contaminants (here HMs) resulted in removal or degradation of pollutant through biological activity [13,17]. The organisms must not only be resistant to toxicity, but also to grow and multiply in an environment not normally suitable for living. There are some major advantages of implementing these techniques, considered as natural-based solutions, over the traditional remediation methods: regenerates the soil providing long-term health, low costs, workers safety, smaller life cycle environmental footprints, no secondary pollution [13].

There are three general approaches: microbial remediation, phytoremediation, and multi-techniques joint remediation [18], each divided into different technologies. The methods can be applied *in situ* or *ex situ*, based on the strategies involved [17]. *In situ* is the treatment done on site, where contamination occurs, and *ex situ* involves excavation and moving soil prior and after treatment. Table 1 presents the principle and main mechanisms involved in phytoremediation and microbial remediation.

Phytoremediation can be defined as a plant-based method, performed *in situ*. Starting with the observation of spontaneous colonialization and vegetation of natural plants, defined as natural hyperaccumulators, on highly contaminated mine tailings, the method has quickly been acknowledged as most straightforward, high cost effective and environmentally friendly, allowing the preservation of the physical characteristics of the soil [22,23]. Tolerant plants can be used to extract and remove HMs from soil or to lower bioavailability in soil, using their root systems [24]. The polluted soil is thus reclaimed, and its fertility restored. The main drawbacks of this biological technique are related to slow plant growth. It was observed that these hyperaccumulator plants have a very slow growth rate and low biomass production, especially in highly contaminated soils, so the bioprocess is time-consuming. Therefore, new techniques are currently studied to assist and improve phytoremediation performance on large scale applications: stimulation of plant development using growth regulators and promoters, application of chelating and acidification agents on polluted soils, or improving plant performances through genetic engineering [25,26].

Another sensitive aspect that must be mentioned is the management of resulted biomass, especially when HMs are removed by phytoextraction. In this case, HMs are transferred into above ground plant biomass, so plant residues must be carefully handled and disposed to avoid recontamination [22].

Table 1

## Bioremediation for HM soil decontamination [19–21]

No.	Process	Principle	Mechanisms
<b>Phytoremediation</b>			
1	Phytoextraction	HMs are translocated to accumulate in aboveground parts of the plant.	Absorption by roots, transportation, and storage in the aboveground part of the plant, and elimination by harvesting.
2	Phytostabilization	HMs are in-situ inactivated or immobilized in plants roots.	Accumulation, precipitation, or root surface absorption.
3	Phytotransformation/ phytodegradation	HMs are transformed in or degraded to less-toxic compounds.	Absorption and storage in new plant tissues through lignification. Enzymatic decomposition.
4	Phytovolatilization	HMs are converted in volatile compounds.	Absorption by plant roots, transportation through the xylem, conversion into volatile. Forms, and release into atmosphere through stomata.
<b>Microbial remediation</b>			
5	Biosorption (adsorption/ absorption)	Metal binding on cell surface, intracellular or extracellular parts.	Physical adsorption, Chelation, Complexation, Coordination, Entrapment, Ion Exchange, Micro-Precipitation.
6	Bioprecipitation	Cellular metabolism-independent, due to chemical interaction of microbial cell wall and metal ions.	Immobilization, Chelation, Reduction, Precipitation (as sulfides or phosphates).
7	Bioaccumulation	Influx and accretion of metals within bacterial cells.	Chelation, Adsorption, Precipitation, Complexation, Reduction, Methylation.
8	Bioleaching	Release of metal ions through mineral dissolution.	Sulfide bioleaching, Pyrite leaching, Heterotrophic bacterial leaching.

Like plants, microbial population is either killed or selected by pollutants presence in the environment. The microorganisms capable of developing mechanisms of resistance to HMs toxicity are successfully used for soil microbial remediation. Generally speaking, the microorganisms are changing the ionic state of HMs affecting their solubility and bioavailability [27]. The technology performance is influenced by environment pH, humidity, ambient temperature, soil

type and the presence of additives in the environment (like humic, or other low molecular weight organic acids) [28]. Optimal pH and temperature depend on the microbial species, with direct impact on their growth and multiplication rates. Different techniques are applied to improve performance: bio-stimulation (addition of proper nutrients for indigenous microorganisms), bio-augmentation (addition of pre-adapted microorganisms species or consortia) or even bio-augmentation by genetically improved species [29]. While there are numerous advantages of these methods (simple, environmentally friendly, easy to implement *in situ*, with no residual treatment required and minimal disruption of site) which make the bioremediation a natural process, there are also some drawbacks. Disregarding the conditions, microbial remediation is time-consuming and depends on microorganisms' type and characteristics, but most important, HM remain still in the soil, concentrated or converted to less toxic forms susceptible to future recontamination if hydrological and geochemical conditions are changing [27,29].

Multi-techniques remediation refers to a combination of two or more different remediation methods to increase efficiency and/or to reduce some disadvantages. There could be mentioned: combined physical-chemical-biological remediation, chemical-biological remediation or plant-microbe consortia remediation [18].

New research directions are emerging nowadays, like nano-phytoremediation and microbial-mediated nano-remediation, using nanoparticles to improve properties of hyperaccumulators and indigenous soil microbes. It is however very difficult to estimate further influence of nanoparticles on the environment/ecosystems and this issue needs careful consideration [30].

### **3. Methods in Air Depollution**

In the industrialized zones the most important air pollutants, harmful for human health, are ozone, nitrogen dioxide and particulate matter (PM). Levels of PM in particular have demonstrated influence on respiratory and cardiovascular morbidities [31]. PM, consisting in various chemical and biological components, are classified by the aerodynamic diameter as coarse (PM<sub>10</sub> diameter between 2500 nm and 10000 nm), fine (PM<sub>2.5</sub> with 100 nm and 2500 nm diameter) and ultrafine (PM<sub>0.1</sub> with diameter below 100 nm). With respect to this classification, PM<sub>2.5</sub> are considered as most toxic airborne particles as their number and surface are considerable higher – one third to two thirds of total PM mass [32]. Furthermore, for PM<sub>2.5</sub> it has been stated that “no lower concentration threshold below which exposures can be considered safe at the population level” [33]. Specific to PM<sub>2.5</sub> pollution from various sources, an integrated exposure response curve was developed (Fig. 2).

The basic roots of air pollution come from the explosive development of industry and transport, especially road transportation. Transportation activities, using all sorts of vehicles based on fossil fuels, significantly contributed to air pollution by PM. In urban/industrialized areas, although in last years the values are decreasing in Europe, the traffic remains the second main emission source of fine particles, with almost 20 % share, while the industrial combustion, with a 35 % share of total emissions, represents the leading source [34]. These PM<sub>2.5</sub> are formed of primary particles and secondary particles. Primary particles are those directly emitted because of industrial/combustion processes, minerals, metals salts, pollen, spores resulted from natural or anthropogenic sources. The secondary particles are those resulted from gas to particle conversion in the air, through nucleation [34].

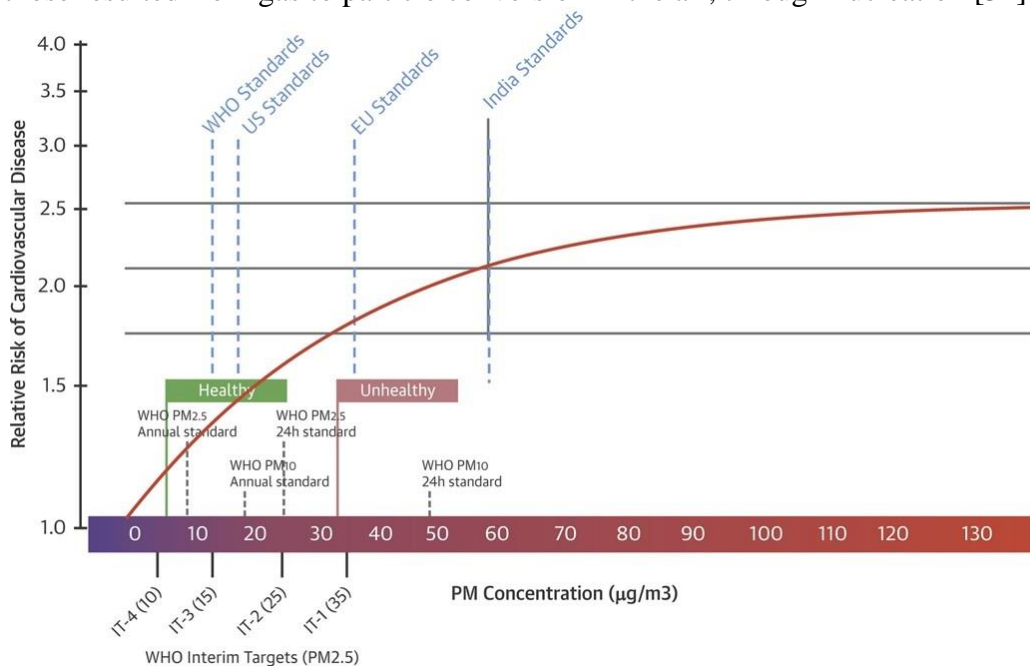


**Fig. 2.** Relative risk of cardiovascular disease associated with long-term exposure to PM<sub>2.5</sub>.

(Adapted with permission from [33])

Toxic heavy metals such as Pb, Cu, Ni, Cr, etc. have a major contribution to aerosols toxicity [35]. Unlike the case of any other contaminants, the pollution with heavy metals is much localized in relation to specific industrial activities location [36].

The dynamic movement from one environmental component to another is especially noticeable for atmospheric HMs, which can enter our bodies directly or can be re-deposited in water, on soil and on plant leaves [37].

When comes to methods for removing HMs from the air, it's clear that their removal is possible only with the removal of PM. And in this sense, there are not many solutions at hand. Most of the measures for cleaner air refer to emissions reduction to minimize air pollutants concentration. Programmes like “Clean Air for Europe” or guidance documents like “Heavy Metals Protocol” of the Convention on Long-range Transboundary Air Pollution recommend research and development of less polluting technologies [38–40]. Specific methods for controlling and preventing HMs emissions are already available: new low-emissions installations, advanced off-gases cleaning technologies, use of low HM content raw materials, better management decisions on every technological aspects from housekeeping to use and disposal of HM containing products [39].

Five major directions to follow for emissions reduction can be enumerated. The first direction can be named *Use green technologies to develop processes*, since there are not many processes that do not produce some powders or aerosols where obviously we will find HMs. The second direction *Energy from the sun, water and wind* urging towards the development and implementation of more and more non-polluting energy solutions, which operate without PM production. The third direction *Use Alternatives to Open Burning* starts from the consideration that the open burning is an important source of PM. The fourth direction having the name *Drive less* considers that the driving of a car is likely a person's single most polluting daily activity. Driving less reduces the amount of vehicles/time on the road which helps to reduce air pollution. The fifth direction having the name *Drive Smart* refers to aspects showing how we can operate our vehicles in order to keep the pollution diminishing.

Referring directly to the methods for PM pollution control, we must mention the air purifiers. These start with the domestic ones and continue with others designed for large urban agglomerations, respectively large industrial platforms. From this last category we can mention innovative projects like the *Smog Free Tower*, which uses positive ionization technology to cleans up to 30,000 m<sup>3</sup>/h air in public spaces. Another example is the project *Green City Without Smog* with two action directions: a) city afforestation with emphasis on the use of vegetal systems that fix the pollutants, including HM; b) large local installations with extremely large air - liquid transfer interphase that remove, locally, pollutants and carbon dioxide.

#### 4. Conclusions

HMs are toxic for the environment and belong to the most important groups of pollutants. The potential harmful effects associated with the accumulation of HM in the environment are too well known. The toxic effects on human populations and potential health hazard of HM requires continuous studies, experimentally and by mathematical modelling, with respect to control of these pollutants' occurrence and to their distribution in all environment compartments. It was noted here that the depollution of HMs contaminated soils using plants or microbes with high capacity for HMs fixing is modern and of interest, especially since it can progress due to genetic intervention on living species; it has been shown that air pollution with HM is a consequence of its pollution with PM and that a major part is related to road transportation based on fossil fuels and specific industries; in HMs pollution control the biosorption and bioaccumulation are recommended as novel, efficient, eco-friendly techniques, with much lower costs than the conventional methods.

#### REFERENCES

1. Pradhan, A.A.; Levine, A.D. Role of Extracellular Components in Microbial Biosorption of Copper and Lead. *Water Sci. Technol.* **1992**, *26*, 2153–2156, doi:10.2166/WST.1992.0684.
2. Wang, J.; Chen, C. Biosorbents for Heavy Metals Removal and Their Future. *Biotechnol. Adv.* **2009**, *27*, 195–226, doi:10.1016/j.biotechadv.2008.11.002.
3. Rengaraj, S.; Moon, S.H. Kinetics of Adsorption of Co(II) Removal from Water and Wastewater by Ion Exchange Resins. *Water Res.* **2002**, *36*, 1783–1793, doi:10.1016/S0043-1354(01)00380-3.
4. Kim, J.S.; Keane, M.A. The Removal of Iron and Cobalt from Aqueous Solutions by Ion Exchange with Na-Y Zeolite: Batch, Semi-Batch and Continuous Operation. *J. Chem. Technol. Biotechnol.* **2002**, *77*, 633–640, doi:10.1002/JCTB.618.
5. Al-Ghouti, M.A.; Khraisheh, M.A.M.; Tutuji, M. Flow Injection Potentiometric Stripping Analysis for Study of Adsorption of Heavy Metal Ions onto Modified Diatomite. *Chem. Eng. J.* **2004**, *104*, 83–91, doi:10.1016/J.CEJ.2004.07.010.
6. Balali-Mood, M.; Naseri, K.; Tahergorabi, Z.; Khazdair, M.R.; Sadeghi, M. Toxic Mechanisms of Five Heavy Metals: Mercury, Lead, Chromium, Cadmium, and Arsenic. *Front. Pharmacol.* **2021**, *12*, 1–19, doi:10.3389/fphar.2021.643972.
7. Schumann, K. Zur Toxikologischen Beurteilung Der Schwermetallgehalte (Cd, Hg, Pb) in Siiuglings-Und Kleinkindnahrung. *Z Ern&hrungswiss* **1990**, *29*, 54–73.
8. Pandey, A.; Shukla, A.; Ray, L. Uptake and Recovery of Lead by Agarose Gel Polymers. *Am.*



- J. Biochem. Biotechnol.* **2009**, *5*, 14–20.
9. Gueu, S.; Yao, B.; Adouby, K.; Ado, G. Kinetics and Thermodynamics Study of Lead Adsorption on to Activated Carbons from Coconut and Seed Hull of the Palm Tree. *Int. J. Environ. Sci. Technol.* **2007**, *4*, 11–17, doi:10.1007/BF03325956.
  10. Jiang, Y.; Cui, S.; Xia, T.; Sun, T.; Tan, H.; Yu, F.; Su, Y.; Wu, S.; Wang, D.; Zhu, N. Real-Time Monitoring of Heavy Metals in Healthcare via Twistable and Washable Smartsensors. *Anal. Chem.* **2020**, *92*, 14536–14541, doi:10.1021/acs.analchem.0c02723.
  11. Technical Working Group on Integrated Monitoring *Draft Report on Actions and Recommendations for Integrated Monitoring of Heavy Metals under the Framework of the European Environment and Health Strategy (COM 2003)338 Final*; 2004;
  12. United Nations Decision 2018/5 Long-Term Strategy for the Convention on Long-Range Transboundary Air Pollution for 2020–2030 and Beyond. **2018**, 1–15.
  13. Hou, D.; O'Connor, D.; Igalavithana, A.D.; Alessi, D.S.; Luo, J.; Tsang, D.C.W.; Sparks, D.L.; Yamauchi, Y.; Rinklebe, J.; Ok, Y.S. Metal Contamination and Bioremediation of Agricultural Soils for Food Safety and Sustainability. *Nat. Rev. Earth Environ.* **2020**, *1*, 366–381, doi:10.1038/s43017-020-0061-y.
  14. Vicol, I. Environmental Quality in Forests from Bucharest Metropolitan Area, Romania. *Environ. Eng. Manag. J.* **2014**, *13*, 2989–2997, doi:10.30638/eemj.2014.337.
  15. C. Ioja *Metode Și Tehnici de Evaluare a Calității Mediului În Aria Metropolitană a Municipiului București*; 2008; ISBN 978-973-737-485-1.
  16. Liu, L.; Li, W.; Song, W.; Guo, M. Remediation Techniques for Heavy Metal-Contaminated Soils: Principles and Applicability. *Sci. Total Environ.* **2018**, *633*, 206–219, doi:10.1016/j.scitotenv.2018.03.161.
  17. Sayqal, A.; Ahmed, O.B. Advances in Heavy Metal Bioremediation: An Overview. *Appl. Bionics Biomech.* **2021**, *2021*, doi:10.1155/2021/1609149.
  18. Jin, T.; Shi, C.; Wang, P.; Liu, J.; Zhan, L. A Review of Bioremediation Techniques for Heavy Metals Pollution in Soil. *IOP Conf. Ser. Earth Environ. Sci.* **2021**, *687*, doi:10.1088/1755-1315/687/1/012012.
  19. Sreedevi, P.R.; Suresh, K.; Jiang, G. Bacterial Bioremediation of Heavy Metals in Wastewater: A Review of Processes and Applications. *J. Water Process Eng.* **2022**, *48*, 102884, doi:10.1016/j.jwpe.2022.102884.
  20. Song, P.; Xu, D.; Yue, J.; Ma, Y.; Dong, S.; Feng, J. Recent Advances in Soil Remediation

- Technology for Heavy Metal Contaminated Sites: A Critical Review. *Sci. Total Environ.* **2022**, 838, 156417, doi:10.1016/j.scitotenv.2022.156417.
21. Verma, S.; Bhatt, P.; Verma, A.; Mudila, H.; Prasher, P.; Rene, E.R. Microbial Technologies for Heavy Metal Remediation: Effect of Process Conditions and Current Practices. *Clean Technol. Environ. Policy* **2021**, 1, 3, doi:10.1007/s10098-021-02029-8.
  22. Bortoloti, G.A.; Baron, D. Phytoremediation of Toxic Heavy Metals by Brassica Plants: A Biochemical and Physiological Approach. *Environ. Adv.* **2022**, 8, 100204, doi:10.1016/j.envadv.2022.100204.
  23. Petelka, J.; Abraham, J.; Bockreis, A.; Deikumah, J.P.; Zerbe, S. Soil Heavy Metal(Loid) Pollution and Phytoremediation Potential of Native Plants on a Former Gold Mine in Ghana. *Water. Air. Soil Pollut.* **2019**, 230, doi:10.1007/s11270-019-4317-4.
  24. Yan, A.; Wang, Y.; Tan, S.N.; Mohd Yusof, M.L.; Ghosh, S.; Chen, Z. Phytoremediation: A Promising Approach for Revegetation of Heavy Metal-Polluted Land. *Front. Plant Sci.* **2020**, 11, 359, doi:10.3389/FPLS.2020.00359/BIBTEX.
  25. Sabreena; Hassan, S.; Bhat, S.A.; Kumar, V.; Ganai, B.A.; Ameen, F. Phytoremediation of Heavy Metals: An Indispensable Contrivance in Green Remediation Technology. *Plants* **2022**, 11, 1–28, doi:10.3390/plants11091255.
  26. Babu, S.M.O.F.; Hossain, M.B.; Rahman, M.S.; Rahman, M.; Ahmed, A.S.S.; Hasan, M.M.; Rakib, A.; Emran, T. Bin; Xiao, J.; Simal-Gandara, J. Phytoremediation of Toxic Metals: A Sustainable Green Solution for Clean Environment. *Appl. Sci.* **2021**, 11, 1–34, doi:10.3390/app112110348.
  27. Pande, V.; Pandey, S.C.; Sati, D.; Bhatt, P.; Samant, M. Microbial Interventions in Bioremediation of Heavy Metal Contaminants in Agroecosystem. *Front. Microbiol.* **2022**, 0, 1417, doi:10.3389/FMICB.2022.824084.
  28. Njoku, K.L.; Akinyede, O.R.; Obidi, O.F. Microbial Remediation of Heavy Metals Contaminated Media by *Bacillus Megaterium* and *Rhizopus Stolonifer*. *Sci. African* **2020**, 10, e00545, doi:10.1016/j.sciaf.2020.e00545.
  29. Raklami, A.; Meddich, A.; Oufdou, K.; Baslam, M. Plants—Microorganisms-Based Bioremediation for Heavy Metal Cleanup: Recent Developments, Phytoremediation Techniques, Regulation Mechanisms, and Molecular Responses. *Int. J. Mol. Sci.* **2022**, 23, doi:10.3390/ijms23095031.
  30. Rajput, V.D.; Minkina, T.; Upadhyay, S.K.; Kumari, A.; Ranjan, A.; Mandzhieva, S.;

- Sushkova, S.; Singh, R.K.; Verma, K.K. Nanotechnology in the Restoration of Polluted Soil. *Nanomaterials* **2022**, *12*, 769, doi:10.3390/nano12050769.
31. Li, T.; Hu, R.; Chen, Z.; Li, Q.; Huang, S.; Zhu, Z.; Zhou, L. Fine Particulate Matter (PM<sub>2.5</sub>): The Culprit for Chronic Lung Diseases in China. *Chronic Dis. Transl. Med.* **2018**, *4*, 176–186, doi:10.1016/J.CDTM.2018.07.002.
32. Moreno-Ríos, A.L.; Tejeda-Benítez, L.P.; Bustillo-Lecompte, C.F. Sources, Characteristics, Toxicity, and Control of Ultrafine Particles: An Overview. *Geosci. Front.* **2022**, *13*, 101147, doi:10.1016/J.GSF.2021.101147.
33. Rajagopalan, S.; Al-Kindi, S.G.; Brook, R.D. Air Pollution and Cardiovascular Disease: JACC State-of-the-Art Review. *J. Am. Coll. Cardiol.* **2018**, *72*, 2054–2070, doi:10.1016/j.jacc.2018.07.099.
34. Torretta, V.; Raboni, M.; Copelli, S.; Rada, E.C.; Ragazzi, M.; Ionescu, G.; Apostol, T.; Badea, A. Application of Strategies for Particulate Matter Reduction in Urban Areas: An Italian Case. *Improv. Urban Environ. Strateg. Heal. More Sustain. Cities* **2016**, *75*, 33–44.
35. Oucher, N.; Kerbachi, R.; Ghezloun, A.; Merabet, H. Magnitude of Air Pollution by Heavy Metals Associated with Aerosols Particles in Algiers. *Energy Procedia* **2015**, *74*, 51–58, doi:10.1016/j.egypro.2015.07.520.
36. Ercilla-Montserrat, M.; Muñoz, P.; Montero, J.I.; Gabarrell, X.; Rieradevall, J. A Study on Air Quality and Heavy Metals Content of Urban Food Produced in a Mediterranean City (Barcelona). *J. Clean. Prod.* **2018**, *195*, 385–395, doi:10.1016/J.JCLEPRO.2018.05.183.
37. Naderizadeh, Z.; Khademi, H.; Ayoubi, S. Biomonitoring of Atmospheric Heavy Metals Pollution Using Dust Deposited on Date Palm Leaves in Southwestern Iran. *Atmosfera* **2016**, *29*, 141–155, doi:10.20937/atm.2016.29.02.04.
38. Schlutow, A.; Schröder, W.; Scheuschner, T. Assessing the Relevance of Atmospheric Heavy Metal Deposition with Regard to Ecosystem Integrity and Human Health in Germany. *Environ. Sci. Eur.* **2021**, *33*, doi:10.1186/s12302-020-00391-w.
39. Economic and Social Council Economic Commission for Europe Guidance Document on Best Available Techniques for Controlling Emissions of Heavy Metals and Their Compounds from the Source Categories Listed in Annex II to the Protocol on Heavy Metals. **2013**, 1–33.
40. European Commission A Clean Air Program for Europe. *COM(2013) 918 Final* **2013**, *918*, 11.

## ESTIMATING METHANE EMISSIONS FROM URBAN RIVERS IN SOUTH-EASTERN EUROPE - CASE STUDY: SOMES RIVER

Mustafa HMOUDAH<sup>1</sup>, Cristian POP<sup>1</sup>, Călin BACIU<sup>1,\*</sup>

<sup>1</sup>Faculty of Environmental Science and Engineering, University of Babeş-Bolyai, 30 Fantanele Street, RO-400294, Cluj-Napoca Romania

### **Abstract**

About 60% of methane emissions in the atmosphere come from anthropogenic activities. Methane is also emitted from wetlands, agricultural activities, energy generation and during the decomposition process of the organic matter. The sources of CH<sub>4</sub> in cities, due to the urbanization, vary from fossil fuel combustion, natural gas network and traffic, wastewater management to industrial activities. The annual emissions of methane from urban water bodies are found to be significantly high. Urban rivers are highly exposed to wide range of environmental and industrial factors that might change their physio-chemical properties. This study is based on measuring CH<sub>4</sub> emissions from urban rivers and lakes. In this study, 50 water samples were collected along Someş river in Cluj-Napoca from different sampling locations, in order to estimate methane concentration in these samples and to include all possible interrupting environmental and urban factors and for appropriately determining the reasons behind these fluxes. The highest values estimated to hit more than 160 ppm which overpasses the device measuring limit, for both of the sampling points LCH 17 and LCH 14. These high CH<sub>4</sub> concentration values were recorded at locations close to industrial activities and wastewater treatment facilities. However, these observations are important indicators towards further sampling and analyzing of methane emissions from urban water bodies, in order to identify their influencing factors whether they are biological organisms, waste water, industrial wastes or any other pollutants, so that they can be introduced into CH<sub>4</sub> mitigation strategies for reducing GHG's emissions. At the same time, this will carry indicators for the quality of air in terms of traffic pollution and CH<sub>4</sub> high concentrations. In addition, it will characterize urban polluting sources.

**Key words:** methane emissions, urban river, wastewater, pollution

---

\* Corresponding author: Email address: calin.baciu@ubbcluj.ro

## 1. Introduction

More than 50% of atmospheric methane are due to human activities [1–3]. Methane emissions mainly come out from rice paddy, wetlands, waste and energy facilities [4], and organic matter decomposition [4, 5]. Emissions from fossil fuel combustion, natural gas network and traffic, wastewater management to industrial activities are the potential sources of CH<sub>4</sub> in the urban area [6]. In the IPPC report [1], it indicates that up to 90% of CH<sub>4</sub> is oxidized by OH in the atmosphere over a period of approximately 10 years which represents the short lifetime of CH<sub>4</sub>. About 4800 Tg(CH<sub>4</sub>) is eliminated during this period in the atmosphere while the microbial activities remove up to 47 Tg(CH<sub>4</sub>). Ito [7] also stated that urbanization and industrial activities are behind the 150% increase in CH<sub>4</sub> emissions in recent decades. Urban rivers were found to have significantly high fluxes. While urban rivers are exposed to different types of pollutants, it is important to receive attention and to estimate their annual participation in the global emissions. In recent studies, the results showed that CH<sub>4</sub> production could occur under aerobic conditions which contradicts previous studies which found out that aerobic conditions promote the oxidation of CH<sub>4</sub> [8]. Other papers [7-9] concluded that temperature, latitude, microbial activities and oxygen concentration are important factors in CH<sub>4</sub> fluxes. However, Cao et al. [10] stated that combining these factors in addition to vegetation cover and organic matter decomposition can determine CH<sub>4</sub> fluxes. As Fernández et al [11] concluded that bacterial activities and plants are important factors in producing and transferring atmospheric CH<sub>4</sub>. Zhao et al. [8] also pointed out that waste water treatment plant has noticeably influenced CH<sub>4</sub> concentration resulting in its high records in river samples close to this treatment plant while it was thought that other sources of CH<sub>4</sub> production, a presence of sediments and algae in-between stony riverbed, might be responsible for high CH<sub>4</sub> concentration. Since the industrial revolution, anthropogenic activities accompanied by population growth increased greenhouse gas (GHG) emissions which stand behind the global warming crisis. However, this crisis would escalate if we do not immediately intervene to stop these emissions [12]. Methane has more than 20 times the warming radiative effects of CO<sub>2</sub> in the atmosphere [13-14]. Fernandez et al. [13] state that despite this negative influence CH<sub>4</sub> has a short life time which is a changing point in dealing with a short-term global warming effect. By better characterizing CH<sub>4</sub> sources, CH<sub>4</sub> emissions can be reduced promoting its oxidation and sinks and declining its fluxes from its identified sources. The presence of high concentration CH<sub>4</sub> in water is a sign of high chemical reactions and/or microbial activity with involved organic matter as part of water contamination [15-16]. The US geological survey in New York [17] found out that natural gas extraction is a significant source of water contamination with CH<sub>4</sub> particularly in extraction locations. This dissolved gas can reach the atmosphere

under high temperature and pressure conditions. In one papers [18] it studied the metals and other pollutants that contaminates the environment in the same urban area our case study. They found out that sediments in Somes river can be used as indicators for contamination detection. Also, they stated that urbanization is the main reason for this river pollution. Nevertheless, they didn't study CH<sub>4</sub> concentration in the river to discover the possibility of another sources of water contamination related to urbanization and to growing anthropogenic activities. Recent studies based on CH<sub>4</sub> fluxes and the implicated factors, microbiology and chemical reactions, such as: . Also, studies of urban CH<sub>4</sub> sources, such as:[3, 11, 13, 21–25].

In our study, we are dealing with CH<sub>4</sub> for particularly have this significance characteristic of short lifetime and for the obvious involvement of the urban area in the recent increase in CH<sub>4</sub> fluxes. The results from CH<sub>4</sub> abatement can be obtained in a short-term similarly for the global warming and polluting effects.

## 2. Experimental

The study of Somes river started from its extension from Gilau in the west to Gherla going through Cold and Warm Somes including lakes and other water bodies along for approximately 75 km which can be observed from Figure 1. Somes has a 100 km length crossing Cluj-Napoca into the Tisa River of the Danube. It is used as an essential source for freshwater in the city and the surrounding communities including important tributaries such as: Someșu Rece, Somes Cald, Feneș, Gârbău, Lujerdiu, Becaș, Borșa, Ocna, Lung, Lonea and Ornan [18]. For measuring CH<sub>4</sub> concentration, water samples were taken for urban rivers and lakes. However, these samples were collected from different sampling locations along Somes river. In this context, CH<sub>4</sub> fluxes were supposed to diversify according to land-use types and to different human activities surrounding these sampling locations, in order to appropriately determining the reasons behind these fluxes. The selection of sampling sites based on the river extension and its morphological varieties with the diversification of surrounding activities.

The 50 samples were collected along the river with respect to the established criteria and to include an important factor of accessibility due to the limitation of resources. The distance between each sample varied from 0.3 – 2 km. Samples were named according to their source either from the stream river SCH or from lakes across its extension distance LCH. These locations were allocated by Google Map and then the samples were collected by tracing these locations

from the same Google Map mobile application. However, the coordinates for each sampling point were registered again in the site for further accuracy. Sampling standard in collecting, transporting and reserving was followed in the sampling stage for obtaining high accuracy in the results in the next stage of conducting sample analysis. A total of 50 water samples were collected from 50 sites. The depth of sampling sites depended on the manually changeable length of the stainless-steel wing sampler of up to 2 m.

Methane can be released from these samples by pumping process and by increasing water temperature [16]. Therefore, sampling collection and pouring were slowly conducted and in an inclination position, in order to avoid bubbles. The samples temperature was increased to the room temperature. Afterwards, each sample was carefully transferred into a gas jar in an inclination position. The jar was closed and shaken for 3 minutes, in order to cause bubbles and to release the resolved CH<sub>4</sub> from the water sample. The extracted data from measurements represent CH<sub>4</sub> concentration (in ppm) in each water sample. The analysis of this data can be summarized by taking the average of CH<sub>4</sub> concentration from the one-minute-measurement. This analysis was prepared by using Microsoft excel with sampling point's code and the average value of CH<sub>4</sub> concentration. The spatial analysis was performed by ArcGIS pro software (Esri, Canada) and symbology categorizing these sampling points was done according to their CH<sub>4</sub> concentration average.

### **3. Results and discussions**

Methane average concentrations from Somes river samples were presented in Figure 1, which illustrates the location of water sampling points and their CH<sub>4</sub> concentrations which were classified into four categories for indicating the high and the low CH<sub>4</sub> concentrations values.

For the first category of values  $\leq 19.33$  ppm 25 sampling points were recorded within this set. Most of these points are located outside the intensive urban area while only 7 points are located within the urban extension. However, only one point is located in the central area which seemed not to be influenced by external factors of traffic, energy consumption or other type of pollution sources.

The second category is for values  $\leq 45.13$  ppm and  $> 19.33$  ppm. This category included 14 sampling points from which 5 sampling points are located within the urban sphere, one to the west and 8 locations to the east outside the city.

The third category includes 9 sampling locations with values  $\leq 107.61$  ppm and  $> 45.13$  ppm which are mostly located in the eastern part of the study area. Only one location is significantly located in the western area outside the urban sphere.

The last two samples are located at points with high CH<sub>4</sub> concentration of more than 160 ppm. Both of these two points are located outside the urban area to the east with the stream direction of Somes river.

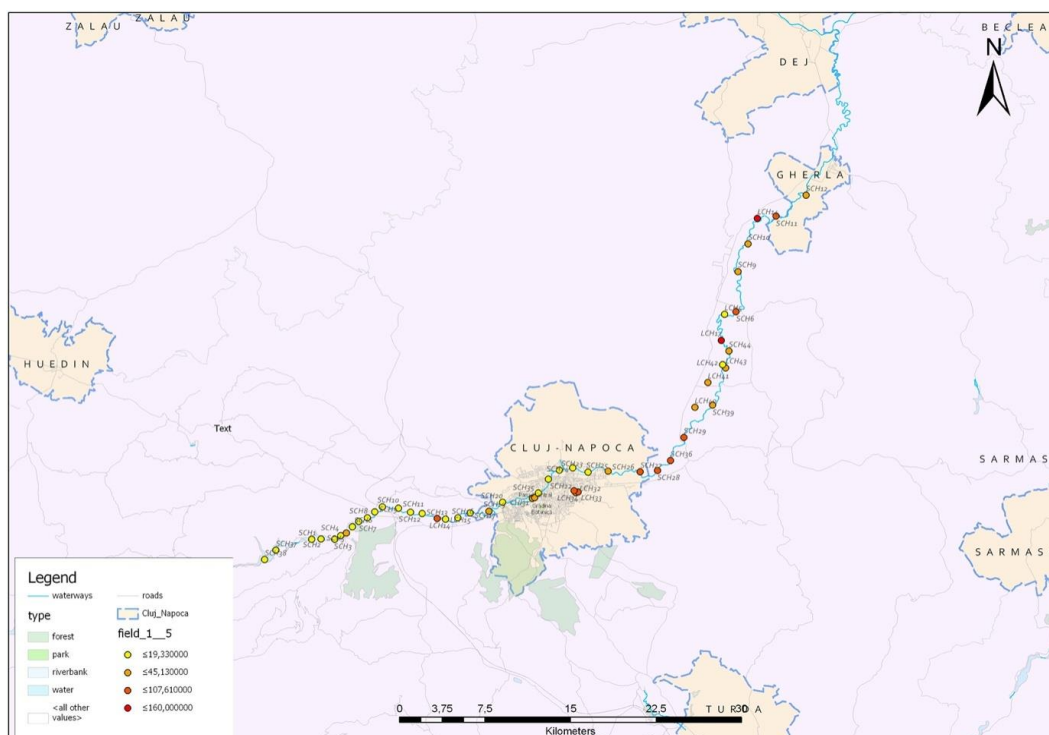


**Fig. 1.** Methane emissions' concentration in Somes

From Figure 2, the minimum CH<sub>4</sub> concentration is 3.89 ppm at the sampling point SCH 2 in the western part of the Somes river, and the maximum value of more than 160 ppm, which overpasses the device measuring capacity, were estimated for the sampling points LCH 17 and LCH 14. Moreover, other maximum values hit 86 ppm and 107.61 ppm at SCH 34 and SCH 27, respectively. However, the mean value of these points is 33.56 ppm. Other points SCH 5, CHI 31, CHI 30, LCH 14, LCH 32, LCH 33 have already recorded high concentration values of CH<sub>4</sub>.



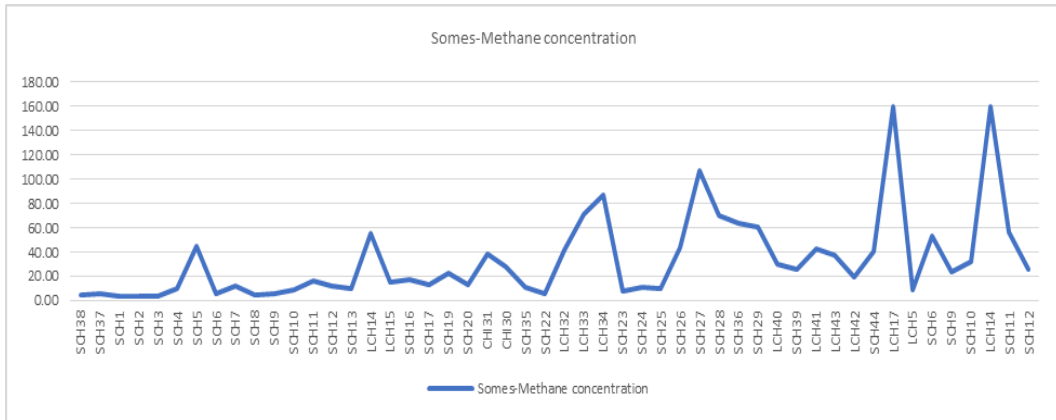


**Fig. 2.** Methane concentration in Somes water body and their estimated average value in ppm

Figure 2 shows that emissions gradually increase as points go with the stream direction crossing the urban area, the airport and wastewater treatment plant.

The first part outside the urban area has only high significant value at LCH 14 of 55.47 ppm. This point was taken from a lake with slow stream flow which indicates to the presence of either microbial activity, a source of pollution or gas leakage. Within the urban sphere average fluxes were obviously high at the lake location. This is another indicator to a presence of an influencing factor that might come from biological activities.

The last part that goes to the east direction with the stream outside the urban area has the most highlighting fluxes that start from SCH 26 with 43.82 ppm until LCH 14 with more than 160 ppm. Methane concentration is significantly high from these samples which were taking from lakes and from points located before and after the airport and the wastewater treatment plant (WTP), but there is not certain information for representing a source of pollution. Nevertheless, points before and after the WTP can be indicators for the need for further investigation. As stated [25] water pollution is considered one of the main reasons that influence CH<sub>4</sub> emissions, particularly from industry and WTP.

The stream direction is west-east which crosses the urban area with its industrial and traffic activities that might represent an influence over the sampling results. However, these lakes can be categorized under wetlands which similarly meet the outcomes of [7, 10, 26, 27] stating that wetlands represent significant source of CH<sub>4</sub> emissions of more than third of the annual methane budget.

Moreover, the speed of the stream might influence CH<sub>4</sub> by creating bubbles and releasing these emissions before they are estimated which is the case with samples taken from lakes with slow stream velocity.

Similar studies based on estimating CH<sub>4</sub> annual fluxes like [14] and [7, 10] rather than estimating their average emissions from water samples, or simply for determining the factors behind these emissions [7, 9, 10, 11]. However, these observations are important indicators toward conducting further sampling and analysis on CH<sub>4</sub> emissions from urban water bodies, in order to identify their influencing factors whether they are biological organisms, waste water, industrial wastes or any other pollutants, so that they can be introduced into CH<sub>4</sub> mitigation strategies for reducing GHG's emissions.

#### **4. Conclusions**

The anthropogenic activities have proven to be the main reasons for the increase in CH<sub>4</sub> fluxes in recent decades. In the urban area, industrial activities, traffic, energy generation and even the urban rivers have a cause in these emission increases.

In combating climate change effects, this study takes an important role in characterizing methane emission sources that participate in increasing CH<sub>4</sub> concentrations in the urban atmosphere. The project employs applicable scientific methods and develops the concept of detecting high methane concentrations in the urban atmosphere, especially the urban rivers and lakes.

High CH<sub>4</sub> fluxes were recorded inside and outside the urban area with mean value 33.56 ppm indicating the presence of microbial activities, waste water from the WTP, traffic pollution or gas leakage.

This study may contribute to enhancing the identification of potential sources for methane emissions, hence, this will by default suggest applying more measurements in climate change mitigation. In other words, this project has the potential for protecting human health and the environment.

However, these observations are important indicators toward conducting further sampling and analysis on CH<sub>4</sub> emissions from urban water bodies, in order to identify their influencing factors whether they are biological organisms, waste water, industrial wastes or any other pollutants, so that they can be introduced into CH<sub>4</sub> mitigation strategies for reducing GHG's emissions.

#### **REFERENCES**

- [1] IPCC, Carbon and Other Biogeochemical Cycles. In: Climate Change 2013: The Physical Science Basis. Contribution of Working Group I to the Fifth Assessment Report of the

- 
- Intergovernmental Panel on Climate Change. Cambridge University Press, Cambridge, United Kingdom and New York, NY, USA, 2013.
- [2] UNEP, Emissions Gap Report 2011: The Heat Is On - A world of climate promises not yet delivered. Nairobi, 2021.
- [3] Zazzeri G., Lowry D., Fisher R. E., France J. L., Lanoisellé M., Nisbet E. G., Plume mapping and isotopic characterization of anthropogenic methane sources, *Atmospheric Environment*, 110, (2015), 151–162, doi:10.1016/j.atmosenv.2015.03.029.
- [4] EPA, Greenhouse Gases, United States Environmental Protection Agency, 2022. <https://www.epa.gov/report-environment/greenhouse-gases>.
- [5] Tate K. R., Soil methane oxidation and land-use change – from process to mitigation, *Soil Biology and Biochemistry*, 80, (2015), 260–272, doi:10.1016/j.soilbio.2014.10.010.
- [6] Maazallahiet H. al., Methane mapping, emission quantification, and attribution in two European cities: Utrecht (NL) and Hamburg (DE), *Atmos. Chem. Phys.*, 20, 23, (2020), 14717–14740, doi:10.5194/acp-20-14717-2020.
- [7] Ito A., Methane emission from pan-Arctic natural wetlands estimated using a process-based model, 1901–2016, *Polar Science*, 21, (2019), 26–36, doi:10.1016/j.polar.2018.12.001.
- [8] Zhao F. et al., Toxic urban rivers as a potential source of atmospheric methane, *Environmental Pollution*, 297, (2022), 118769, doi:10.1016/j.envpol.2021.118769.
- [9] Parker R. J. et al., Evaluating year-to-year anomalies in tropical wetland methane emissions using satellite CH<sub>4</sub> observations, *Remote Sensing of Environment*, 211, (2018), 261–275, doi:10.1016/j.rse.2018.02.011.
- [10] Cao M., Marshal S., K. Gregson, Global carbon and methane emissions from natural wetlands: Application of a process-based model, *Journal for Geophysical Research*, 101, D9, 1996, 14,399-14,414.
- [11] Fernández-Baca C. P. et al., Changes in rhizosphere soil microbial communities across plant developmental stages of high and low methane emitting rice genotypes, *Soil Biology and Biochemistry*, 156, (2021), 108233, doi: 10.1016/j.soilbio.2021.108233.
- [12] IPCC, Agriculture, Forestry and Other Land Use (AFOLU). In: Climate Change 2014: Mitigation of Climate Change. Contribution of Working Group III to the Fifth Assessment Report of the Intergovernmental Panel on Climate Change. Cambridge University Press, Cambridge, United Kingdom and New York, NY, USA, 2014.
- [13] Fernandez J. M. et al., Street-level methane emissions of Bucharest, Romania and the dominance of urban wastewater, *Atmospheric Environment: X*, vol. 13, (2022), 100153, doi: 10.1016/j.aeaoa.2022.100153.
- [14] Xiong J., Sheng X., Wang M., Wu M., Shao X., Comparative study of methane emission in the reclamation-restored wetlands and natural marshes in Hangzhou Bay coastal wetland, *Ecological Engineering*, 175, (2022), 106473, doi: 10.1016/j.ecoleng.2021.106473.
- [15] Kulongoski J. T., McMahon P. B., Land M., Wright M. T., Johnson T. A., Landon M. K., Origin of Methane and Sources of High Concentrations in Los Angeles Groundwater, *J. Geophys. Res. Biogeosci.*, 123, 3, (2018) 818–831, doi: 10.1002/2017JG004026.
- [16] Minnoseta, Methane in Well Water: Well Management Program, Minnoseta, Department of Health -USA, 2022, <https://www.health.state.mn.us/communities/environment/water/wells/waterquality/methane.html#removal>
- [17] U.S.G.S., Dissolved Methane in New York Groundwater. 2012. [https://pubs.usgs.gov/of/2012/1162/pdf/ofr2012-1162\\_508\\_09072012.pdf](https://pubs.usgs.gov/of/2012/1162/pdf/ofr2012-1162_508_09072012.pdf)
- [18] Barhoumiet B. et al., Occurrence, distribution and ecological risk of trace metals and organic pollutants in surface sediments from a Southeastern European river (Someşu Mic

- River, Romania), *Science of The Total Environment*, 660, (2019), 660–676, doi: 10.1016/j.scitotenv.2018.12.428.
- [19] Tate K. R. et al., Methane uptake in soils from *Pinus radiata* plantations, a reverting shrub land and adjacent pastures: Effects of land-use change, and soil texture, water and mineral nitrogen, *Soil Biology and Biochemistry*, 39, 7, (2007), 1437–1449, doi: 10.1016/j.soilbio.2007.01.005.
- [20] Bradley R. L., Chroňáková A., Elhottová D., Šimek M., Interactions between land-use history and earthworms control gross rates of soil methane production in an overwintering pasture, *Soil Biology and Biochemistry*, 53, (2012) 64–71, doi: 10.1016/j.soilbio.2012.04.025.
- [21] Chamberlain S. D., Ingraffea A. R., Sparks J. P., Sourcing methane and carbon dioxide emissions from a small city: Influence of natural gas leakage and combustion, *Environmental Pollution*, 218, (2016), 102–110, doi: 10.1016/j.envpol.2016.08.036.
- [22] Lowry D. et al., Environmental baseline monitoring for shale gas development in the UK: Identification and geochemical characterisation of local source emissions of methane to atmosphere, *Science of The Total Environment*, 708, (2020), 134600, doi: 10.1016/j.scitotenv.2019.134600.
- [23] Takano T., Ueyama M., Spatial variations in daytime methane and carbon dioxide emissions in two urban landscapes, Sakai, Japan, *Urban Climate*, 36, (2021), 100798, doi: 10.1016/j.uclim.2021.100798.
- [24] Ueyama M., Ando T., Diurnal, weekly, seasonal, and spatial variabilities in carbon dioxide flux in different urban landscapes in Sakai, Japan, *Atmos. Chem. Phys.*, 16, 22, (2016), 14727–14740, doi:10.5194/acp-16-14727-2016.
- [25] Yang S.S., Chen I.C., Ching-Pao L., Liu L.Y., Chang C.H., Carbon dioxide and methane emissions from Tanswei River in Northern Taiwan, *Atmospheric Pollution Research*, 6, 1, (2015), 52–61, doi: 10.5094/APR.2015.007.
- [26] Potter C. S., An ecosystem simulation model for methane production and emission from wetlands, *Global Biological Cycle*, 11, 4, (1997), 495–506.
- [27] Walter B. P., Heimann M., A process-based, climate-sensitive model to derive methane emissions from natural wetlands: Application to five wetland sites, sensitivity to model parameters, and climate, *Global Biogeochem Cycles*, 14, 3, (2000), 745–765, doi: 10.1029/1999GB001204

## WATER INFLUENCE ON THE THERMAL PROPERTIES OF DEEP EUTECTIC SOLVENTS: A TGA STUDY

Eliza-Gabriela BRETTFELD<sup>1,2</sup>, Tănase DOBRE<sup>2</sup>, Cristian Andi NICOLAE<sup>1</sup>,  
Diana CONSTANTINESCU-ARUXANDEI<sup>1</sup>, Florin OANCEA<sup>1,3\*</sup>

<sup>1</sup> INCDCP-ICECHIM Bucharest, 202 Spl. Independentei, 6<sup>th</sup> District, Romania

<sup>2</sup> University Politehnica Bucharest, Faculty of Chemical Engineering and  
Biotechnology, Romania

<sup>3</sup> University of Agronomic Sciences and Veterinary Medicine of Bucharest,  
Faculty of Biotechnologies, Romania

### **Abstract**

*This TGA study investigates the impact of water on ethaline and reline deep eutectic solvents. The results reveal significant variations in the decomposition behavior due to the presence of water, characterized by distinct temperature minima and changing weight loss patterns. For choline chloride and urea eutectic solvents, water content induces notable alterations in thermal degradation, including lower temperature maxima and variable weight loss profiles. These findings underscore the eutectic nature of these solvents and emphasize the critical role of water in their thermal properties. This research advances our understanding of eutectic solvents and their potential applications.*

**Key words:** thermal stability, reline, ethaline, decomposition

### **1. Introduction**

Deep eutectic solvents (DES) have gained substantial recognition as a sustainable class of green solvents, offering a promising avenue in the field of green chemistry [1-3]. These remarkable solvents are characterized by their unique composition, typically formed through the establishment of hydrogen bonds between two or more compounds. The resultant deep eutectic solvents, which are composed of common and readily available ingredients, possess exceptional attributes that render them appealing as environmentally friendly alternatives to traditional organic solvents [4-8].

---

\*Corresponding author: Email address: florin.oancea@icechim.ro

Choline chloride (ChCl) stands out as an important component in the creation of DES, because of its cost-effectiveness and low toxicity [5]. In this study, we focus is on two specific deep eutectic solvents: ethaline (ChCl and ethylene glycol, EG, in a molar ratio of 1:2) and reline (ChCl and urea, U, in a molar ratio of 1:2) [9, 10]. These DESs demonstrate a unique blend of chemical and physical characteristics, offering versatile properties that make them highly intriguing for various applications in fields such as catalysis, separation processes, and energy storage.

A fundamental aspect of deep eutectic solvents is their thermal behavior, which plays a critical role in determining their utility in different processes. The presence of water, a ubiquitous component, can significantly affect the thermal properties of these DESs. Investigating how varying water content influences the thermal stability and decomposition patterns of these deep eutectic solvents is essential for tailoring their properties to specific applications.

The primary objective of this study was to unveil the role of water in modulating the thermal properties of ethaline and reline through comprehensive thermogravimetric analysis (TGA) [11, 12]. TGA is a powerful technique for scrutinizing the thermal characteristics of materials by monitoring changes in weight as a function of temperature or time. The present analysis will yield valuable insights into the decomposition pathways, temperature profiles, and weight loss patterns of these deep eutectic solvents under different water content conditions [2, 13].

By elucidating how water content influences these systems, we aim to contribute to the broader understanding of deep eutectic solvents and their potential for sustainable applications in the realm of green chemistry. In addition, this research underscores the critical role of water content as a pivotal variable in the design and use of DES.

## 2. Experimental

### *Reagents*

The reagents chosen for this study were of the highest quality, ensuring the reliability of the experiments. Choline chloride from Alfa Aesar Thermo Scientific had a purity of over 98%, while ethylene glycol from Merck and urea from Scharlau both exceeded 99% purity. The water source was prepared in-house using an Elga Micra Veolia system.

### *Deep eutectic solvent preparation*

The preparation of the two deep eutectic solvents (DES) involved precise measurements to four decimal places using a Mettler Toledo ML104T analytical balance. The required quantities of choline chloride (ChCl), urea, and ethylene

glycol (EG) were accurately weighed to maintain the 1:2 molar ratio (ChCl:component) [14, 15]. The synthesis occurred in a well-equipped system, featuring a glass-bottomed vessel with an attached vertical condenser to minimize gas loss, an oil bath for ensuring uniform heating, an electric hotplate with a magnetic stirrer and magnetic bar, and a thermometer. The reaction temperature was maintained at 40°C with continuous stirring at 600 rpm for 2 h. Upon completion of the reaction, clear, viscous solutions were obtained, which were perfectly homogeneous and presented a subtle yellowish tint.

#### *TGA Analysis*

The thermogravimetric analyzer TGA Q5000IR from TA Instruments (USA) measures the quantity and rate of weight change in a material, either with respect to temperature increase or isothermally with respect to time, in a controlled atmosphere. It can be used to characterize any material exhibiting changes in weight and detect phase changes resulting from decomposition, oxidation, or dehydration.

Samples with water contents of 0, 5, 10, 20, 30, 40, 50, and 60% were examined and designated as E0, E5, E10, E20, E30, E40, E50, and E60 for ethaline and R0, R5, R10, R20, R30, R40, R50, and R60 for reline, respectively. The working method employed involved placing 20-25 mg of each sample on a platinum tray with a 99.999% nitrogen gas flow at a rate of 50 ml/min. The temperature was ramped at 10°C per minute, reaching 450°C.

### **3. Results and Discussion**

#### *Ethaline*

The thermogram reveals four distinct mass loss steps, each characterized by an increasingly steep slope, concurrent with rising water content (Fig. 1). The initial step, occurring at approximately 100°C, is associated with the removal of water from the sample. Subsequently, intermediate acids such as formic, glycolic, and/or oxalic acids are formed in the second and third steps [16, 17], and in the final stage, choline chloride degradation is observed. This signifies the intermediate thermal stability of the solvent composed of ethylene glycol and choline chloride, confirming the eutectic point theory [18].

In alignment with Fig. 1, the thermogram of ChCl:EG 1:2 with various water percentages is complemented by Table 1, which calculates the mass loss percentages for diluted ethaline samples. Notably, the first step, spanning from room temperature (RT) to 105°C, revealed an increase in mass loss with increasing water content. This loss encompasses not only the water content but also negligible losses of ethylene glycol (in pure form, over a quarter of the mass is lost) [19] and substantially fewer, almost negligible, losses of ChCl (0.11%).

In the subsequent temperature range of 105-210°C, mass losses are primarily attributed to EG, which, in its pure form, fully vaporizes at 134.9°C [20]. In the case of DES, specifically E0 (ethaline with no water), the loss is only 27.57%, thereby reinforcing the definition and properties of eutectic solvents and enhancing their chemical and physical stability compared to individual components. Mass losses in eutectic solvents with water content do not exceed those of E0, falling between 15% and 27%. All eight samples exhibit decomposition temperatures within the 125-140°C range, with higher temperatures observed for samples with lower water content (E5-E20).

Moving to the subsequent temperature range of 210-270°C, mass losses originate from both ethylene glycol (in trace amounts) and choline chloride. The percentages start at 6% for E60, the sample with the highest water content, and increase to 17.45% for E0, the anhydrous sample. The maximum temperature at which decomposition occurs varies between 253-260°C, decreasing to 237°C, inversely proportional to the initial water content in the samples.

Starting from 270°C up to 450°C, choline chloride decomposition occurs in the E0–E60 samples at lower temperatures than in pure choline chloride, which evaporates at 318.9°C. These decompositions occur alongside slight decreases in the water content of the samples. The residual mass losses after 450°C do not exceed 0.26%, with ethaline undergoing virtually complete decomposition.

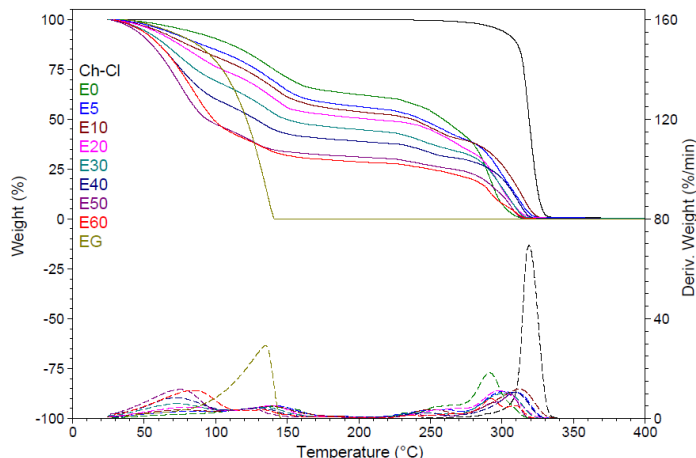


**Fig. 1.** Thermogram of ChCl:EG 1:2 with different water concentrations

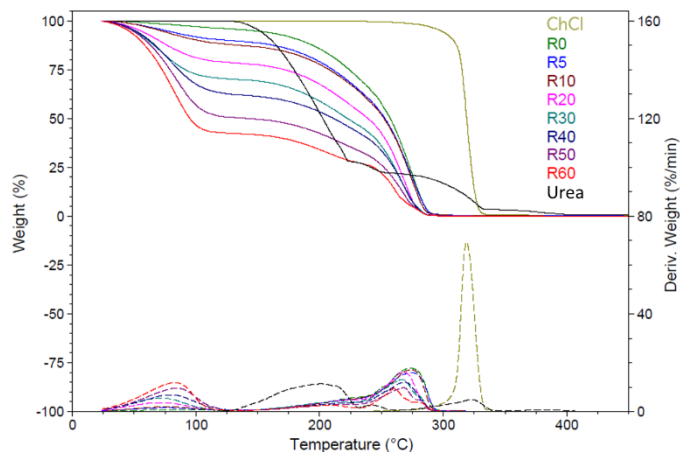


**Fig. 2.** Thermogram of ChCl:U 1:2 with different water concentrations



Table 1

Weight loss by temperature steps for ethaline

	RT - 105°C		105 - 210°C		210 - 270°C		270 - 350°C		350 - 450°C		Residue 450°C
	Wt. loss	Tmax	Wt. loss	Tmax	Wt. loss	Tmax	Wt. loss	Tmax	Wt. loss	Tmax	
	%	°C	°C	°C	%	°C	%	°C	%	°C	
<b>E0</b>	10,9 0	0,0	27,5 7	137, 5	17,4 5	253, 3	43,9 2	291,2	0,0 6		0,09
<b>E5</b>	16,6 0	80,7	27,8 7	140, 9	14,4 5	259, 0	40,4 9	303,3	0,3 3		0,26
<b>E10</b>	20,0 7	75,6	26,9 0	139, 9	12,8 6	249, 9	39,8 4	312,1	0,1 7		0,16
<b>E20</b>	25,2 8	75,3	24,8 7	139, 7	12,7 8	252, 8	36,6 2	297,7	0,2 7		0,19
<b>E30</b>	32,5 1	73,3	23,3 1	134, 1	10,5 4	243, 3	33,2 5	302,3	0,2 3		0,16
<b>E40</b>	41,6 0	72,2	19,9 8	130, 0	8,10	246, 5	30,1 2	309,5	0,0 6		0,14
<b>E50</b>	54,0 1	75,1	15,2 9	125, 6	6,22	241, 1	24,3 3	306,0	0,0 9		0,06
<b>E60</b>	54,1 9	84,3	17,5 7	132, 8	6,50	237, 5	21,5 9	292.3/30 9	0,0 4		0,12
<b>ChCl</b>	0,11		0,03		0,96		98,2 5	318,9	0,3 2		0,33
<b>EG</b>	25,4 6		74,4 7	134, 9	0,01		0,01		0,0 0		0,05
	Water + EG		EG		EG + ChCl		ChCl				

### Reline

The subsequent set of samples, reline (R0-R60), was investigated using the same methodology, as illustrated in Figure 2 and detailed in Table 2. Similar to ethaline, mass loss in reline sample starts within the RT-105°C range. These mass losses do not significantly exceed the actual water content in the samples because of the enhanced stability of urea compared with EG [18].

In the following temperature range of 135-230°C, urea decomposition exceeding 75% occurs individually [21]. In the eutectic mixture with ChCl, mass losses reach a maximum of 23.99% for E0 and decrease with increasing water content, reaching a minimum of 14.67% for E60. The vaporization temperature is inversely proportional to the water content, ranging between 208-223°C.

Continuing to the 230-350°C temperature range, the quantity of the sample diminishes primarily due to the loss of ChCl (99% at 318.9°C) from the system, as well as urea (17.72% at 241 and 308°C). Notably, the mixture exhibits a lower temperature compared with individual compounds, ranging from 260 to 274°C. This temperature decrease is inversely proportional to the water content.

Urea undergoes a final decomposition step at 376.5°C, accounting for 6.28% of the mass loss. It is worth noting that the ChCl and urea mixture has lost more weight (maximum residue of 0.18%) than each individual compound and has achieved lower maximum temperatures than the individual compounds. This once again demonstrates the eutectic nature of the reline.

Table 2

	Weight loss by temperature steps for reline								
	RT - 135°C		135 - 230°C		230 - 350°C		350 - 450°C		Residue
	Wt. loss %	Tmax °C	Wt. loss %	Tmax °C	Wt. loss %	Tmax °C	Wt. loss %	Tmax °C	450°C %
<b>R0</b>	4,38	97,1	23,99	220,5	71,42	273,3	0,06		0,15
<b>R5</b>	10,36	76,9	23,98	222,9	65,44	274,3	0,04		0,18
<b>R10</b>	12,44	76,6	22,66	213,0	64,71	274,3	0,02		0,17
<b>R20</b>	21,66	71,4	23,76	214,3	54,43	267,9	0,04		0,11
<b>R30</b>	30,00	71,7	22,88	217,4	46,99	266,6	0,03		0,10
<b>R40</b>	37,84	79,6	18,75	210,5	43,32	269,2	0,01		0,08
<b>R50</b>	49,65	84,2	16,27	217,3	33,91	267,9	0,02		0,15
<b>R60</b>	57,74	83,0	14,67	208,0	27,49	260,2	0,03		0,07
<b>ChCl</b>	0,11		0,11		99,13	318,9	0,32		0,33
<b>Urea</b>	0,09		75,75	181,3	17,72	241.6/308.5	6,28	376,50	0,17
	Water		Urea		ChCl + urea				

#### 4. Conclusions

In conclusion, this study sheds light on the intriguing thermal properties of deep eutectic solvents (DES) comprising choline chloride (ChCl) and ethylene glycol (EG) in a 1:2 molar ratio, known as ethaline, as well as choline chloride and urea (U) in a 1:2 molar ratio, termed reline. The investigation focused on the influence of water content on the thermal behavior of these DESs, offering valuable insights into their stability and decomposition characteristics.

Thermal analysis, conducted using a thermogravimetric analyzer (TGA), revealed the distinctive mass loss patterns associated with the varying water concentrations in both ethaline and reline. As the water content increased, the DES demonstrated progressively higher mass losses, highlighting the intricate interplay between water and the DES components. Notably, the thermal stability of the DES, particularly in the presence of water, was affirmed, showcasing their potential as robust green solvents for various applications.

Ethaline, composed of ChCl and EG, displayed distinct thermal profiles, with each component contributing differently to the overall mass loss behavior. The eutectic nature of ethaline was confirmed, as evidenced by the lower decomposition temperatures and increased mass losses in the presence of water.

Similarly, reline, composed of ChCl and urea, exhibited remarkable thermal stability, with urea proving to be more robust than EG in terms of mass loss. The eutectic behavior was reaffirmed, with the reline showcasing lower decomposition temperatures and increased mass losses in the presence of water, further highlighting its potential as a green solvent.

Overall, this research contributes to the understanding of the thermal characteristics of these DESs and their response to varying water content, making them promising candidates in the realm of green chemistry and sustainable solvent systems.

**Acknowledgments:** The research leading to these results received funding from the European Regional Development Fund (ERDF), the Competitiveness Operational Program (POC), Axis 1, project POC-A1-A1.2.3-G-2015-P\_40\_352, My\_SMIS 105684, “Sequential processes of closing the side streams from bioeconomy and innovative (bio)products resulting from it – SECVENT”, subsidiary projects 617/2022 – DiaCer and 2147/2020 – NeXT-CAR.

## REFERENCES

- [1] B. B. Hansen *et al.*, Deep Eutectic Solvents: A Review of Fundamentals and Applications, *Chemical Reviews*, 121, 3, (2021), 1232-1285.
- [2] Y. Marcus, The Variety of Deep Eutectic Solvents, *Springer International Publishing*, (2019), 13-44.
- [3] Y. Liu, J. B. Friesen, J. B. McAlpine, D. C. Lankin, S.-N. Chen, and G. F. Pauli, Natural Deep Eutectic Solvents: Properties, Applications, and Perspectives, *Journal of Natural Products*, 81, 3, (2018), 679-690.
- [4] Q. Zaib, Z. Masoumi, N. Aich, and D. Kyung, Review of the synthesis and applications of deep eutectic solvent-functionalized adsorbents for water treatment, *Journal of Environmental Chemical Engineering*, 11, 3, (2023), 110214.
- [5] Y. Zhang, X. Ji, and X. Lu, Choline-based deep eutectic solvents for CO<sub>2</sub> separation: Review and thermodynamic analysis, *Ren. and Sus. En. Rev.*, 97, (2018) 436-455.
- [6] I. Adeyemi, M. R. M. Abu-Zahra, and I. Alnashef, Novel Green Solvents for CO<sub>2</sub> Capture, *Energy Procedia*, 114, (2017), 2552-2560.
- [7] Q. Zhang, K. De Oliveira Vigier, S. Royer, and F. Jérôme, Deep eutectic solvents: syntheses, properties and applications, *Chem. Soc. Reviews*, 41, 21, (2012), 7108-7146.
- [8] A. P. Abbott, G. Capper, and S. Gray, Design of Improved Deep Eutectic Solvents Using Hole Theory, *ChemPhysChem*, 7, 4, (2006), 803-806.
- [9] A. Malik, H. S. Dhatarwal, and H. K. Kashyap, Distinct Solvation Structures of CO<sub>2</sub> and SO<sub>2</sub> in Reline and Ethaline Deep Eutectic Solvents Revealed by AIMD Simulations, *The Journal of Physical Chemistry B*, 125, 7, (2021), 1852-1860.

- [10] M. B. Haider, D. Jha, B. Marriyappan Sivagnanam, and R. Kumar, Modelling and simulation of CO<sub>2</sub> removal from shale gas using deep eutectic solvents, *Journal of Environmental Chemical Engineering*, 7, 1, (2019), 102747.
- [11] N. Delgado-Mellado *et al.*, Thermal stability of choline chloride deep eutectic solvents by TGA/FTIR-ATR analysis, *Journal of Molecular Liquids*, 260, (2018), 37-43.
- [12] Z. X. U. E. J. W. J. J. X. Z. T. M. U. Wenjun Chen, Investigation on the Thermal Stability of Deep Eutectic Solvents, *Acta Physico-Chimica Sinica*, 34, 8, (2018), 904-911.
- [13] N. López-Salas *et al.*, Looking at the "Water-in-Deep-Eutectic-Solvent" System: A Dilution Range for High Performance Eutectics, *ACS Sustainable Chemistry & Engineering*, 7, 21, (2019), 17565-17573.
- [14] S. Sarmad, Y. Xie, J.-P. Mikkola, and X. Ji, Screening of deep eutectic solvents (DESs) as green CO<sub>2</sub> sorbents: from solubility to viscosity, *New Journal of Chemistry*, 41, 1, (2017), 290-301.
- [15] J. Naser, F. Mjalli, B. Jibril, S. Al-Hatmi, and Z. Sani Gano, Potassium Carbonate as a Salt for Deep Eutectic Solvents, *IJCEA*, 4, (2013), 114-118.
- [16] S. H. Kim *et al.*, Effect of deep eutectic solvent mixtures on lipase activity and stability, *Journal of Molecular Catalysis B: Enzymatic*, 128, (2016), 65-72.
- [17] K. Jafari, M. H. Fatemi, and L. Lugo, An experimental study of novel nanofluids based on deep eutectic solvents (DESs) by Choline chloride and ethylene glycol, *Journal of Molecular Liquids*, 360, (2022), 119521.
- [18] C. R. Ashworth, R. P. Matthews, T. Welton, and P. A. Hunt, Doubly ionic hydrogen bond interactions within the choline chloride–urea deep eutectic solvent, *Physical Chemistry Chemical Physics*, 18, 27, (2016), 18145-18160.
- [19] Y.-C. Guo, Observation of conformational changes in ethylene glycol–water complexes by FTIR–ATR spectroscopy and computational studies, *AIP Advances*, 8,(2018), 055308.
- [20] R. K. Ibrahim, M. Hayyan, M. A. AlSaadi, S. Ibrahim, A. Hayyan, and M. A. Hashim, Physical properties of ethylene glycol-based deep eutectic solvents, *Journal of Molecular Liquids*, 276, (2019), 794-800.
- [21] X. Li, M. Hou, B. Han, X. Wang, and L. Zou, Solubility of CO<sub>2</sub> in a Choline Chloride +Urea Eutectic Mixture, *Journal of Chemical & Engineering Data*, 53, 2, (2008), 548-550.

## ESTIMATION OF THERMAL STABILITY OF SOME COPOLYETHERS LIQUID CRYSTALS USING ARTIFICIAL NEURAL NETWORKS

Cătălin LISA<sup>1,\*</sup>, Silvia CURTEANU<sup>1</sup>, Nicolae HURDUC<sup>1</sup>, Natalia HURDUC<sup>2</sup>

<sup>1</sup>Gheorghe Asachi Technical University of Iasi, “Cristofor Simionescu” Chemical Engineering and Environmental Protection Faculty, B-dul D. Mangeron, no. 71, 700050 Iasi, Romania

<sup>2</sup>Al. I. Cuza University of Iasi, Faculty of Chemistry, B-dul Carol I, no. 11, 700506 Iasi

### **Abstract**

*Liquid crystalline polymers represent an interesting research field, especially in the last few years, taking into consideration their potential applications in micro-electronics, such as display technology and optical memory materials. In order to be used for different applications, the first requirement of these materials is the good thermal stability that is why it is easy to understand the important role that thermal stability plays for liquid crystals. One of the most important properties of the so-called feed-forward neural networks is their ability to work as universal approximator of functions determined by a set of values of independent and dependent variables. First of all, a series of experimental data is obtained applying thermal analysis methods under dynamic heating conditions. Neural networks were used to predict the thermostability (appreciated by the temperature when the degradation process starts and the temperature corresponding to the maximal degradation rate) as function of some characteristics of the studied compounds (molecular weight, and a series of structural characteristics estimated by mechanical molecular simulation).*

**Key words:** Thermal stability, Feed-forward neural networks, Liquid crystals

### **1. Introduction**

Since the discovery of liquid crystals and especially their important applications in LCD (liquid crystals display), these materials received a great attention in the last years. Thermotropic liquid crystals are materials in which

---

\* Corresponding author: Email address: [clisa@ch.tuiasi.ro](mailto:clisa@ch.tuiasi.ro)

ordering in liquid crystalline structures takes place to a certain temperature range and implies increasing of material's temperature [1]. In order to be used for different applications, the first requirements of these materials are the good thermal stability, that is why it is easy to understand the important role that thermal stability plays for liquid crystals. For example, in the case of liquid crystals with the clearing point above the decomposition temperature, a study of thermal degradation process is mandatory [2].

An artificial neural network is a "black box" model obtained by training with input/output pairs, which have to be related by transformation which is being modeled.

The most common neural network architecture is the multi-layer feed-forward neural network (often called multi-layer perceptron, MLP). One of the most important properties of the so-called feed-forward neural networks is their ability to work as universal approximator of functions determined by a set of values of independent and dependent variables [3].

Artificial neural networks are becoming a promising alternative tool for classical processes modeling techniques [4-6]. Obtaining phenomenological models, when there is not enough information available, for different chemical processes is difficult to achieve [7]. In these reasons, neural networks could overcome the modeling difficulties, having a few advantages: the possibility to apply it on complex non-linear processes, the ease in obtaining and using neural models, the possibility to substitute experiments with predictions.

This paper presents a new methodology to study the thermal stability of some copolyether derivatives with liquid crystals properties and to analyze the influence of some structural factors on their thermal stability. Prediction and optimization of thermal stability of liquid crystals properties is a complex and highly non-linear problem with no easy method to predict polymeric liquid crystals properties directly and accurately. The neural network model is used to learn, then generalize, the thermal stability based on the structure of the compounds, quantified by a series of molecular descriptors. This procedure may substitute experiments, which are time and material consuming.

The goal of this paper is to predict the thermal stability of certain copolyethers with liquid crystal characteristics using neural networks. It is important to emphasize that is a new approach to use neural networks for estimation the thermal behavior of some complex compounds. Another significant issue addressed in this paper refers to the choice of the variables which could influence the thermal stability and the thermal stability criteria. The parameters considered as inputs of the neural model were molecular weight, copolymer composition and structural characteristics. The output variables of the neural model were the temperature when the degradation process starts and the first temperature corresponding to the maximal degradation rate.

## 2. Experimental

### *Methodology*

Multilayer feed-forward neural networks, trained with a back-propagation learning algorithm, are the most popular neural networks. They are applied to a wide variety of chemically related problems. The basic feed-forward network performs a nonlinear transformation of the input data in order to approximate the output data. In general, a neural network consists of processing neurons and information flow channels between neurons, usually called „interconnections”. Processing neurons have the role of evaluating the weighted sum of the interconnected signals from the previous layers and generating an output [8]. The adjustment of the neural network function to experimental data (learning process or training) is based on a non-linear regression procedure. Training is done by assigning, at the beginning, random weights to each neuron, evaluating the output of the network and calculating the error between the output of the network and the known results by means of an error or objective function [9]. After that, the back-propagation rules are used to adjust the values of these weights. The purpose of developing a neural model is to devise a network (set of formulae) that captures the essential relationships in the data. Once these relationships between input and output data are established, they can be applied to new inputs in the validation stage [8]. Since a neural network is a nonlinear optimization process made up of a learning phase and a testing phase, the initial data set must be split into two subsets: one for training and one for testing. The neural model obtained generalizes well the relationship between inputs and outputs if good results are obtained in the validation stage when new input data, not used in the training stage (“unseen data”), are used [8].

### *Materials and methods*

The copolyethers were synthesized by the phase transfer catalysis technique in a liquid/liquid system starting from various bisphenols and  $\alpha,\omega$ -dihalogenated hydrocarbon compounds. Details concerning the synthesis and characterization procedures were previously reported [10-13].

A typical polymerization reaction, the bisphenols chemical structures and abbreviations are presented in Figure 1.

## Estimation of Thermal Stability of Some Copolyethers Liquid Crystals Using Artificial Neural Networks

---

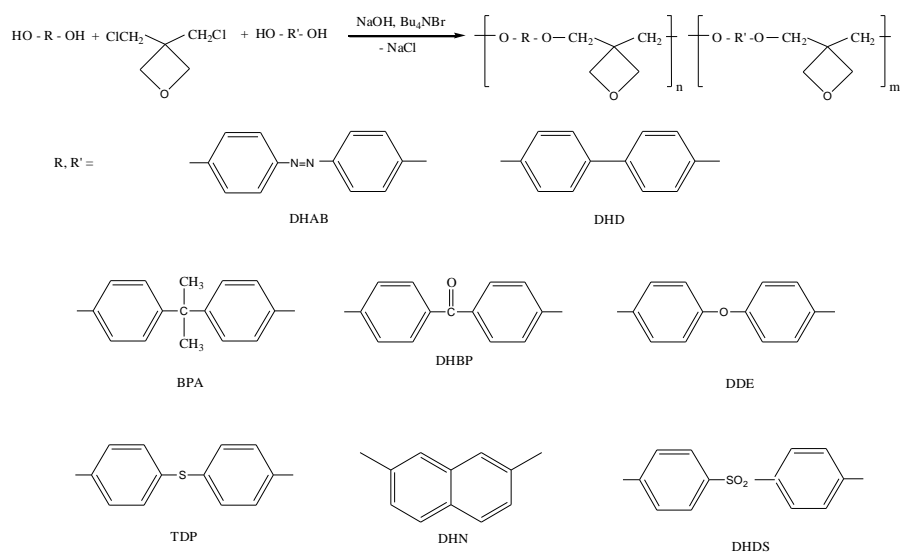


**Fig. 1.** Reaction scheme for copolyether synthesis; DHAB - 4,4' – dihydroxyazobenzene; DHD - 4,4'–dihydroxydiphenyl; BPA - bisphenol A; DHBP - 4,4'–dihydroxybenzophenone; DDE - 4,4' – dihydroxydiphenylether; TDP - 4 – hydroxydiphenyl – sulfide; DHN - 2,7- dihydroxynaphthalene; DHDS - 4,4'–dihydroxydiphenylsulfone.

The thermal behavior was investigated on a MOM-Budapest derivatograph [14-18]. The recordings were effectuated in static air atmosphere, at heating rate of 10 K/min. Thermostability was determined by applying as thermal stability criteria  $T_i$  – the temperature when the degradation process starts and  $T_{max}$  – first temperature corresponding to the maximal degradation rate.

The establishment of the numerical inputs for machine learning models (molecular descriptors) is a critical and difficult problem. This is due to the fact that the molecular descriptors must represent the molecular structural features related to the properties of interest as distinctly as possible. The accurate prediction of the learning methods depends heavily on the amount of correction between the molecular descriptors and the structural features.

The molecular simulations were performed with a HYPERCHEM force-field program. The initial macromolecular conformation of the simulated copolyethers was optimized and the value of the potential energy of the single chain was obtained. In order to search the real value for minimum energy (not a local minimum), the conformation obtained was followed by a molecular dynamic cycle and re-minimized. The criterion of energy convergence is to obtain a residual root-mean-square force in the simulated polymeric system that is less than 0.12 kJ/mol·Å. Minimization was performed using a conjugate – gradient algorithm described by Fletcher and Reeves [19]. The spacer length parameters were estimated by mechanical molecular simulation using Hyperchem program.



### Case study

In finding new properties, thermal stability of the compounds is one of the most important requirements [20]. Because liquid crystals are materials in which mesomorphic properties appear to a certain temperature domain, it is easy to understand the important role played by thermal stability for such compounds. In this paper we used a copolyethers database (27 in all), which includes a wide variety of compounds (Figure 1). The bisphenol can be 4,4'-dihydroxydiphenyl (DHD), bisphenol A (BPA), 4,4'-dihydroxybenzophenone (DHBP), 4,4' - dihydroxydiphenylether (DDE), 4 - hydroxydiphenyl-sulfide (TDP), 2,7-dihydroxynaphthalene (DHN), 4,4'-dihydroxydiphenylsulfone (DHDS) or 4,4' - dihydroxyazobenzene (DHAB). The thermal stability of the copolyethers which have liquid crystal characteristics is made using neural networks.

### 3. Results and discussions

Neural networks were used to predict the thermostability as a function of some characteristics of the studied compounds. The thermostability is characterized by the temperature when the degradation process starts (noted  $T_i$ ) and the ratio  $T_{max}/T_i$  (noted  $L$ ), these representing the outputs of the network. The parameters considered as inputs of the neural model were molecular weight ( $M$ ), copolymer composition ( $R_c$ ) and a structural characteristics - the length of the spacer ( $L_s$ ). The output variables of the neural model are  $T_i$  and  $L$ .

The neural networks employed here are the simple feed-forward networks trained with the back-propagation algorithm. One major problem in the construction of neural networks is determining the network architecture, that is the number of hidden layers and the number of neurons in each hidden layer. The initial data were split into training (2/3) and validation sets (1/3). The topology of the network is developed by a trial-and-error method, following a balance between complexity and performance. It is the most used technique for developing the architecture of the neural model [21, 22]. Table 1 contains different feed-forward topologies tested with selected training data and the main performances for these networks: MSE (Mean Squared Error),  $r$  (correlation between experimental and simulation data) and  $E_p$  (percent error). These performances were registered for the training phase.

The structure of a network of MLP type (multilayer perceptron) is given by the number of neurons in the input layer, corresponding to the three input variables, then the number of hidden neurons (in one or two intermediate layers) and, finally, the number of neurons in output layer for the output variables.

Table 1

**Different topologies tested for the feed-forward neural networks**

No.	Network topology	MSE	r	E <sub>p</sub> (%)
1.	MLP(3:4:2)	0.00075	0.989	1.243
2.	MLP(3:8:2)	0.00001	0.9999	0.025
3.	MLP(3:12:2)	0.000015	0.9999	0.023
4.	MLP(3:16:2)	0.00001	0.9999	0.003
6.	MLP(3:24:2)	0.00002	0.9999	0.0001
7.	MLP(3:30:2)	0.00001	0.9999	0.0001
8.	MLP(3:35:2)	0.00001	0.9999	0.0001
9.	MLP(3:3:9:2)	0.00002	0.9999	0.0003
10.	MLP(3:12:4:2)	0.00001	0.9999	0.0001

The networks with the best performances were MLP (3:8:2) and MLP(3:12:4:2), having one or two hidden layers.

Good predictions are obtained with these neural models on training data. Table 2 presents an example for the MLP(3:8:2). The code C in Table 2 identifies the two components in pairs: 1-DHAB, 2-DHD, 3-BPA, 4-DDE, 5-DHDS, 6-DHBP, 7-TDP, 8-DHN (for instance, 6/8 represent DHABP/DHN). The last four columns which appear in Table 2 contain experimental data (T<sub>i</sub> exp and L exp) and the predictions of the network (T<sub>i</sub> net and L net).

Table 2.

**Prediction of MLP(3:8:2) on training data**

C	R <sub>c</sub>	M	L <sub>s</sub>	T <sub>i</sub> exp	L exp	T <sub>i</sub> net	L net
6/8	1	4100	6.4	350	1.20	350	1.20
2/3	2.54	3800	2.5	302	1.30	302	1.29
2/7	0.91	3600	2.5	370	1.08	370	1.08
1/2	3.7	3000	0	274	1.19	274	1.19
1/2	1.5	2900	0	277	1.16	277	1.16
1/5	0.01	3850	6.4	320	1.13	320	1.14
1/7	0.322	3700	2.5	320	1.25	320	1.25
2/4	0.91	3550	0	450	1.01	450	1.01
2/4	0.312	3700	0	390	1.22	390	1.22
6/8	0.344	4000	6.4	400	1.05	400	1.05

C	R <sub>c</sub>	M	L <sub>s</sub>	T <sub>i</sub> exp	L exp	T <sub>i</sub> net	L net
2/3	0.4	4000	2.5	302	1.33	302	1.33
1/3	0.588	2500	8.9	285	1.18	285	1.18
1/2	0.833	2300	6.4	277	1.23	277	1.23
3/4	3.5	3600	2.5	400	1.13	400	1.13
1/3	2.7	3100	10.2	284	1.14	284	1.14
3/4	2	3450	2.5	405	1.14	405	1.14
1/3	1.1	3000	0	286	1.18	286	1.18
1/4	1.1	3500	0	320	1.30	320	1.30
1/7	2.9	3800	2.5	335	1.25	335	1.25
2/7	2.8	3700	2.5	360	1.17	360	1.17

The selected neural models have learned very well the behavior of the system, but the real test for them will be the validation phase - the answer of the network to data not included in the training set [23].

An important feature related to the neural network topology is the generalization capability, which means how well the network predicts unseen (validation) data. Compared to the training phase, the validation *MSE* were higher and *r* were smaller. For instance, MLP(3:12:4:2) had *MSE* = 0.0025 and *r* = 0.890.

The predictions of the two selected networks on validation data are given in Tables 3 and 4.

Table 3.

Prediction of MLP(3:8:2) on validation data							
C	R <sub>c</sub>	M	L <sub>s</sub>	T <sub>i</sub> exp	L exp	T <sub>i</sub> net	L net
2/3	1	3900	2.5	339	1.19	302	1.28
6/8	2.8	4200	6.4	340	1.06	308	1.14
3/4	0.5	3500	2.5	470	1.02	443	1.05
1/7	0.833	3750	2.5	330	1.15	321	1.25
1/4	0.5	3450	0	340	1.26	315	1.32
1/5	2.1	4100	6.4	320	1.09	290	1.14
2/7	0.333	3550	2.5	340	1.18	360	1.09

Table 4.

**Prediction of MLP(3:12:4:2) on validation data**

C	R <sub>c</sub>	M	L <sub>s</sub>	T <sub>i</sub> exp	L exp	T <sub>i</sub> net	L net
2/3	1	3900	2.5	339	1.19	319	1.27
6/8	2.8	4200	6.4	340	1.06	331	1.11
3/4	0.5	3500	2.5	470	1.02	442	1.01
1/7	0.833	3750	2.5	330	1.15	310	1.21
1/4	0.5	3450	0	340	1.26	344	1.27
1/5	2.1	4100	6.4	320	1.09	299	1.2
2/7	0.333	3550	2.5	340	1.18	334	1.09

Predictions of the neural models on validation data have small relative errors as can be seen in Table 5. These errors were calculated with the following formula:

$$E_r = \frac{P_{exp} - P_{net}}{P_{exp}} \cdot 100 \quad (1)$$

where  $p$  is  $T_i$  or  $L$  and indices  $exp$  and  $net$  denote experimental and neural network values. The last two rows in Table 5 contain average relative errors and maximum relative errors for the two predicted parameters.

Table 5.

**Relative errors of the neural networks on validation data**

C	MLP(3:8:2)		MLP(3:12:4:2)	
	Relative error for T <sub>i</sub> (%)	Relative error for L (%)	Relative error for T <sub>i</sub> (%)	Relative error for L (%)
2/3	10.9145	7.5630	5.8997	6.7227
6/8	9.4118	7.5472	2.6471	4.7170
3/4	5.7447	2.9412	5.9574	0.9804
1/7	2.7273	8.6957	6.0606	5.2174
1/4	7.3529	4.7619	1.2735	0.7937
1/5	9.3750	4.5872	6.5625	10.0917
2/7	5.8824	7.6271	1.7647	7.6271
avg	7.3441	6.2462	4.3094	5.1643
max	10.9145	8.6957	6.5625	10.0917

Generally, good results are obtained in validation phase, with average relative error below 7 %. Consequently, the developed neural networks can be used to make predictions for different compounds (different structures and properties), substituting the experiments that are time and material consuming.

## 6. Conclusions

This paper proposes a neural network-based procedure for estimation the thermal behavior of some copolyethers which are important compounds because their liquid crystalline proprieties.

Simple architecture neural networks and simple methods of establishing the networks' structure are proposed for process modeling: feed-forward networks with one or two hidden layers, developed by trial-and-error method and trained with back-propagation algorithm. Good predictions for the temperature when the degradation process starts and the temperature corresponding to the maximal degradation rate were obtained. Consequently, this neural network modeling methodology gives a very good representation for the material thermostability analysis.

A future work will deal with a complex analysis of the thermal stability of the compounds in our data base. More input parameters will be taken into account and their importance will be estimated within a genetic algorithm-based procedure. A direct neural network modeling that means prediction of proprieties as function of structural parameters will be completed with an inverse modeling procedure in order to appreciate the structures that lead to imposed characteristics.

**Acknowledgement:** This research occurred in the framework of the Project PN II ID\_600/ no.64/1.10.2007 and ID\_592 no.59/1.10.2007, for which the authors acknowledge financing authority.

## REFERENCES

- [1] Imrie C. T., Loubser C., Engelbrecht P., McClelland C. W., Zheng Y.F., The synthesis and liquid crystal behaviour of monosubstituted ferrocenomesogens, *Journal of Organometallic Chemistry*, 665, 1-2, (2003), 48-64.
- [2] Apreutesei D., Lisa G., Hurduc N., Scutaru D., Thermal behavior of some cholesteric esters, *Journal of Thermal Analysis and Calorimetry*, 83, 2, (2006), 335-340.
- [3] Zupan J., Gasteiger J., *Neural Networks in Chemistry and Drug Design*, 2<sup>nd</sup> Edition, Wiley-VCH, Weinheim, 1999.
- [4] Zhilong L., Zhiwei L., Shuo Z., Yiwen S., Jinying Y., Changshui Z., Machine-learning exploration of polymer compatibility, *Cell Reports Physical Science*, 3, 6, (2022), 100931.
- [5] Zhilong L., Zhenzhi T., Ruixin H., Wanli O., Jinying Y., Changshui Z., Automatically Predict Material Properties with Microscopic Image: Example Polymer Miscibility, *Journal of Chemical Information and Modeling*, 63, 19, (2023), 5971–5980.
- [6] Baroiu N., Costin G. A., Teodor V. G., Nedelcu D., Tăbăcaru V., Prediction of Surface Roughness in Drilling of Polymers using a Geometrical Model and Artificial Neural Networks, *Materiale Plastice*, 57, (2020) 160-173.
- [7] Piuleac C. G., Rodrigo M. A., Canizares P., Curteanu S., Saez C., Ten steps modeling of electrolysis processes by using neural networks, *Environmental Modelling and Software*, 25, 1 (2010) 74-81.

- [8] Piuleac C., Curteanu S., Ţelipan G., Cazacu M., Neural network based modeling of NO<sub>x</sub> detection with a sensor – polymer system, *Scientific Study & Research*, IX, 1, (2008), 35-48.
- [9] Curteanu S., Popa A. M., Applications of neural networks in polymerization reaction engineering, *Revue Roumaine de Chimie*, 49, 1, (2004), 3-23.
- [10] Alazaroaie S., Catanescu O., Toader V., Taran E., Pavel V., Hurduc N., Scutaru D., Simionescu C. I., Thermal behavior of some aromatic copolyethers containing a propylenic spacer, *High Performance Polymers*, 17, (2005), 149-160.
- [11] Alazaroaie S., Toader V., Carlescu I., Kazmierski K., Scutaru D., Hurduc N., Simionescu C. I., Liquid crystalline polymers. 14. Synthesis and thermal behaviour of some polyethers containing azo- and bis-(azobenzenic) mesogens, *European Polymer Journal*, 39, (2003), 1333-1339.
- [12] Catanescu O., Hurduc N., Scutaru D., Toader V., Stoleru A., Simionescu C. I., Liquid Crystalline Polymers. 9. Synthesis and Thermal Properties of Some Oligomers Containing a Diethyletheric Spacer, *Die Angewandte Makromolekulare Chemie*, 273, 1, (1999), 91-95.
- [13] Hurduc N., Daoudi A., Buisine J. M., Barboiu V., Simionescu C. I., Liquid crystalline polymers—VI. A study of the thermal behavior of some ternary copolyethers, containing 4,4'-dihydroxyazobenzene, bisphenol a and 1,1-bis(4-hydroxyphenyl)ethane, *European Polymer Journal*, 34, 1, (1998), 123-125.
- [14] Hurduc N., Creanga A., Pavel D., Hurduc N., Thermal properties and molecular simulation of some polyethers and copolyethers with semi-rigid chains, *Polymer Degradation and Stability* 70, 2, (2000), 277-282.
- [15] Foia C., Toader V., Hurduc N., Hurduc N., Phase transfer catalysis in polycondensation processes (XIX): Thermal behaviour of some polyesters containing oxetanic rings in the main chain with potential nlo properties, *Iranian Polymer Journal*, 8, 1, (1999), 9-15.
- [16] Hurduc N., Ionescu D., Hurduc N., Bordianu A., Liquid-crystalline polymers. II. Thermal analysis of some copolyethers based on bisphenol A, 4, 4'-dihydroxyazobenzene, 4, 4'-dihydroxydiphenyl and 3, 3'-bis (chloromethyl) oxetane, *Iranian Journal of Polymer Science and Technology* 4, 2, (1995), 104-109.
- [17] Hurduc N., Dragoi N., Ghirvu C., Hurduc N., Phase Transfer Catalysis in Polycondensation Processes: XVIII. Thermal properties and molecular simulation of some polyethers containing oxetane rings in the main chain, *Journal of Thermal Analysis and Calorimetry*, 58, 3, (1999), 525-532.
- [18] Damian C., Hurduc N., Hurduc N., Shanks, R., Yarovsky I., Pavel D., Thermal behavior and molecular simulation of liquid crystalline polymers containing a pentamethylene spacer, *Computational Materials Science* 27, 4, (2003), 393-402.
- [19] Fletcher R., Reeves C. M., Function minimization by conjugate gradient, *Computer Journal*, 7, (1964), 149-154.
- [20] Apreutesei D., Lisa G., Hurduc N., Scutaru D., Synthesis and un-isotherm kinetic study of some ferrocene acids, *Central European Journal of Chemistry*, 2, 4, (2004), 553-562.
- [21] Leon F., Curteanu S., Lisa C., Hurduc N., Machine learning methods used to predict the liquid-crystalline behavior of some copolyethers, *Molecular Crystals and Liquid Crystals*, 469, 1, (2007), 1-22.
- [22] Curteanu S., Cazacu M., Neural networks and genetic algorithms used for modeling and optimization of the siloxane-siloxane copolymers synthesis, *Journal of Macromolecular Science, Part A: Pure and Applied Chemistry*, 45, 1, (2007), 23-26.
- [23] Luketina J., Berglund M., Greff K., Raiko T., Scalable Gradient-Based Tuning of Continuous Regularization Hyperparameters, Proceedings of the 33<sup>rd</sup> International Conference on Machine Learning, New York, NY, USA, JMLR: W&CP, 48, (2016), 2952-2960.

## INNOVATIVE METHOD FOR DETERMINATION OF THERMAL CONDUCTIVITY OF COMPOSITE MATERIALS

Tănase DOBRE<sup>1</sup>, Edina RUSEN<sup>1</sup>, Cristian Eugen Răducanu<sup>1</sup>, Aurel DIACON<sup>1,2</sup>, Sorin Mircea AXINTE<sup>3</sup>, Alexandra MOCANU<sup>1,4\*</sup>

<sup>1</sup>Faculty of Chemical Engineering and Biotechnologies, University Politehnica Bucharest, Gh. Polizu Street, 011061 Bucharest, Romania,

<sup>2</sup>Military Technical Academy “Ferdinand I”, 39-49 George Coșbuc Boulevard, Bucharest, 050141, Romania,

<sup>3</sup>S.C. Daily Sourcing & Research SRL, 95-97 Calea Griviței, 010705, Bucharest, Romania,

<sup>4</sup>National Institute for Research and Development in Microtechnologies—IMT Bucharest, 126A Erou Iancu Nicolae Street, 077190 Bucharest, Romania

### **Abstract**

*The paper includes a brief review of the methods for determining the thermal conductivity of materials, including thermal insulation composites. Among the methods for rapid determination of the thermal conductivity, the method of measuring the dynamics of the temperature on the surface of the flat plate composite is chosen and an innovative method is developed. This method imposes a constant temperature on the opposite surface to the measurement. The dynamic measurements of the surface temperatures were carried out keeping the temperature of the warm face of the sample not higher than 90 °C, for 8 samples of plate-type composites. The use of these composites to insulate the walls of houses can be of great interest since the registered thermal conductivities were below 0.1 W/(m K).*

**Key words:** composite material, thermal conductivity, plate-type composite

### **1. Introduction**

The development of composite materials for the thermal isolation of buildings still represents an interesting subject in the world of research scientists, industrial producers and small consumers.

---

\*Corresponding author: Email address: alexandra.mocanu@imt.ro

Only in 2023, more than 1300 papers as indexed by sciencedirect.com were dedicated to the subject of composite materials based on the most diverse components for the achievement of a thermo-efficient structures [1]. One of the most important requirements in the field of these materials is related with the value of thermal conductivity ( $\lambda$ ) which must be less than 0.2 W/(m·K) [2, 3].

Most of the times the fulfillment of this request is done by developing composites as porous structures, because air (dry air) has the lowest thermal conductivity (0.023 W/(m·K) [4, 5]. Designing porous composites can be challenging since it is quite difficult to manufacture from the beginning composites with an imposed thermal conductivity. Thus, several methods have been developed to measure this property.

The first category is that of the methods based on the measurement of the constant heat flow under steady-state conditions in the case of a thin plate. This is assigned as Dr. Bock's method, and La Mort method respectively [6].

The steady state technique is used to conduct a measurement when the material under study is in perfect equilibrium. Signal analysis is made easier because a steady condition implies constant signals. The disadvantage is usually that it takes some time to reach the required balance.

Depending on the type of material, several techniques are applied to measure thermal conductivity such as guarded hot plate, hot wire, modified hot wire, and laser flash diffusivity [7, 8]. Among all these four methods, the most suitable for porous materials is the hot wire method which involves the insertion of a heated wire into the material. The temperature changes are recorded while the heat flows out the sample [8]. Consequently, the thermal conductivity can be determined by plotting the registered temperature of the wire versus logarithm of time if the density and capacity are well known parameters [8].

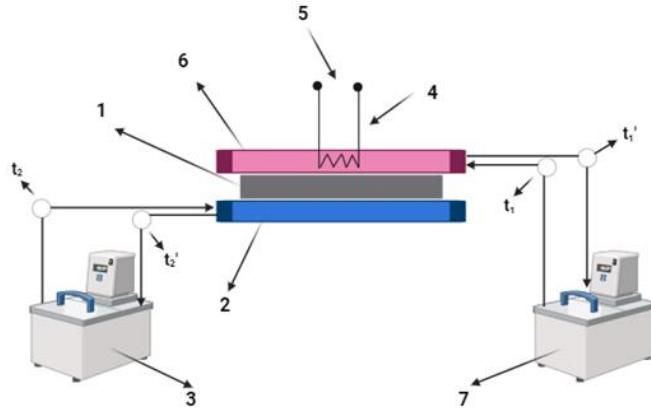
Dr. Bock's apparatus [6] is manufactured by two smooth flat plates designed for measuring thermal conductivity for solid materials. The upper plate which is electrically heated and is embedded in a compensation plate that is kept at temperature  $t_1$ , while the bottom or the cooling plate is kept at temperature  $t_2$ .

In **Scheme 1**, *Dr. Bock's* method is exemplified for the measurement of the thermal conductivity of a thin plate while keeping constant temperatures  $t_1$ , respectively  $t_2$  on both sides of the sample. Both temperatures  $t_1$ , respectively  $t_2$  are kept constant by a thermostat connected to each plate, while the heat flow that comes from is measured [6]. The sample has a cylindrical or rectangular shape with one side ranging from 160 to 250 mm.

The changes in temperature of the hot, respectively cold plate are recorded and the thermal conductivity is determined based on Equation 1:

$$\lambda = \frac{q \cdot \delta}{\tau \cdot S \cdot (t_1 - t_2)} \quad (1)$$

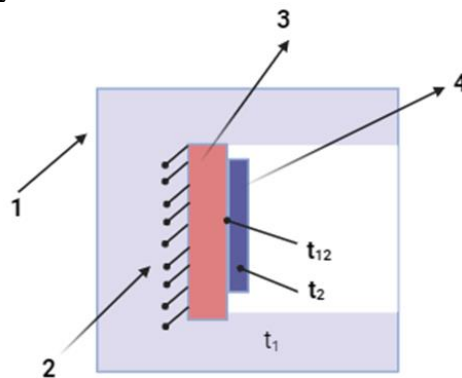




**Scheme 1.** Device for the determination of thermal conductivity based on *Dr. Bock's* method (1 – the tested sample; 2 – bottom device plate kept at temperature  $t_2$ ; 3- thermostat for bottom plate; 4 – electrical resistance for heating; 5 – controller system for electrical resistance; 6 – upper plate maintained at  $t_1$  temperature; 7 – thermostat for upper device plate) (*adaptation after* [6])

In Equation 1,  $Q$  is the amount of heat of the hot plate (W),  $\delta$  is the mean thickness of the sample (m),  $\tau$  is the time (s), and  $S$  is the area of the sample (m),  $t_1$  and  $t_2$  are the measured temperatures of the hot, respectively cooling plate.

*La Mort* method uses comparison with a standard sample (sample of known thermal conductivity) to establish the thermal conductivity of the designed specimen [7]. As it follows from **Scheme 2**, the measurement is based on the differences between the constant thermal flow that passes through the standard and the sample while the thermal regime is stationary.



**Scheme 2.** Schematic representation for thermal conductivity measurement using *La Mort* method (1 – oven insulating; 2 – electrical heating; 3 – sample to be tested; 4 – standard sample)

When temperature  $t_1$ ,  $t_{12}$ , respectively  $t_2$  are constant, the heat flow that passes through the sample is equal to the one passing through the standard sample. Thus, the determination of thermal conductivity is based on Equation 2:

$$\lambda_1 = \lambda_2 \left( \frac{\delta_1}{\delta_2} \right) \cdot \left( \frac{t_{12} - t_2}{t_1 - t_{12}} \right) \quad (2)$$

Where  $\lambda_1$  – the thermal conductivity of the tested sample,  $\lambda_2$  – the thermal conductivity of the standard sample,  $\delta_1$  – the thickness of the tested sample,  $\delta_2$  – the thickness of the standard sample,  $t_1$  – the temperature ensured by the insulating oven,  $t_2$  – the temperature of the standard sample,  $t_{12}$  – the temperature at the contact of the standard and tested sample. In the case of *La Mort* method, the thickness of both tested and standard sample must be measured with high precision. Additionally, two other conditions have to be taken into account, one related with the thickness of the standard sample that has to be smaller compared with the one of the tested samples, and the other related with the measuring precision of the thermocouples that should not introduce a non-negligible thermal resistance in the measurement area.

The use of thermal conductivity determination methods based on unsteady state conductive heat transfer in a solid sample is frequently used, developing more or less standardized devices in this sense. These methods are preferred for measuring the thermal conductivity of all materials and especially wet materials. They are fast, as data are obtained in minutes or tens of minutes, as opposed to hours for a steady-state measurement [9]. Fitch method [10] uses a flat plate type plate partially embedded in an insulated copper block (the contact surface between the sample and the flat type plate is not isolated). The temperature of the copper block is brought to  $t_0$  which represents the beginning of the measurement, while the temperature of the contact surface is kept constant at  $t_b$ .

Measuring the temperature drop of the copper block, considered to have a constant temperature in its mass due to its extremely high thermal conductivity, allows to write, if it is accepted that the sample does not accumulate heat, the differential thermal balance from relation (3). Thus, the thermal conductivity of the sample ( $\lambda$ ) will be in accordance with relation (4), where  $A$  is the copper transfer surface between the copper block, sample, and the area kept at constant temperature,  $\delta$  is the thickness of the sample (m),  $m_{Cu}$  is the mass of the copper plate (kg),  $c_{Cu}$  (J/kg·K) is the specific heat of the copper plate, and  $t$  is the registered temperature at a certain moment in time ( $\tau$ ) expressed as minutes.

$$m_{Cu} c_{Cu} d(t - t_b) = \frac{\lambda}{\delta} A (t - t_b) d\tau \quad (3)$$

$$\ln \left( \frac{t - t_b}{t_0 - t_b} \right) = \frac{\lambda A}{\delta m_{Cu} c_{Cu}} \tau \quad (4)$$

Most dynamic methods for measuring thermal conductivity, based on the recording of the temperature field inside the sample of the tested material, use the analytical [11] or numerical solution of a heat transfer model, coupled with an optimization mathematical approach [12 -15].

Thus, a distinct situation in the class of these methods is the case developed in this work. The aim of our study is based on a fast unsteady state thermal conduction in the flat plate coupled with establishing the exact thermal flow that leaves by natural convection from the plate to the adjacent environment.

## 2. Experimental

### *Mathematical model for fast determination of thermal conductivity*

**Figure 1** presents the thermal transfer scheme associated with the proposed method for the determination of thermal conductivity of a sample that can be included in the thermal isolation materials category. If on a flat horizontal thermally isolated surface, the sample is placed in a specific area and the plate is heated with a constant temperature  $t_b$  the sample will reach a certain temperature called initial temperature,  $t_0$ . The heat will be lost through the surface exposed to the exterior medium for which the temperature will be considered  $t_a$ .

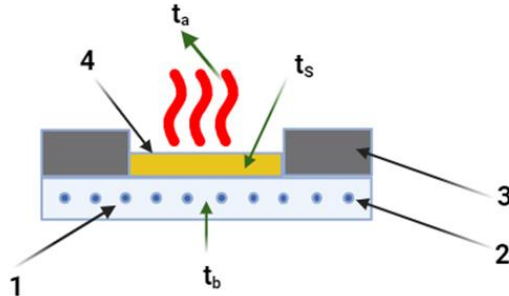


**Fig 1.** Scheme of fast method for thermal conductivity determination (1 – heated plate; 2 – electrical heater with thermosetting control; 3 – thermal insulation; 4 – sample)

The mathematical model associated with the case of thermal transfer through the flat plate contains the equation of the temperature flux, the initial conditions. The heat flow goes through the heated plate through the sample imposing that the limit conditions are  $z = 0$ , respectively  $z = \delta$  (thickness of the sample) in which  $z$  represents the distance of the heat flow from the contact surface between the sample and the heated plate to the top of the sample. Thus, the mathematical model is based on equations 5-8.

$$\frac{\partial t}{\partial \tau} = a(\lambda) \frac{\partial^2 t}{\partial z^2} \quad (5)$$

$$\tau = 0, 0 \leq z \leq \delta, t = t_0 \quad (6)$$

$$\tau > 0, z = 0, t = t_b \quad (7)$$

$$\tau > 0, z = \delta, -\lambda \frac{dt}{dz} = \alpha_s(t)(t - t_a) \quad (8)$$

If the temperature dynamics is measured at the surface of the sample ( $t_s$ ) as a function of time ( $\tau$ ), then the analytical or numerical solution of the model can serve as a building point for equation/function (9) which gives the mean square deviation between the  $N$  large experimental measurements of the surface temperature and the  $N$  values calculated according to the model. Minimizing this function will yield the sought value for the thermal conductivity of the sample. The condition is that the dependence of the thermal transfer coefficient from the plate to the medium  $\alpha_s(t_s, t_a)$  is known and very precise. For instance, it is shown that for  $\alpha_s(t_s, t_a)$  relation (10), where  $A$  has the value 1.45,  $m$  is equal to 0.25 and the characteristic length is represented by the geometric mean between the length and the width of the plate. This expression for  $\alpha_s(t_s, t_a)$  is verified by an extremely large number of transfer data from horizontal surface to the adjacent air [16].

$$F(\lambda) = \sum_{i=0}^N (t_{s \text{ exp}}(\tau_i) - t_s(\lambda, \tau_i))^2 \quad (9)$$

$$\alpha_s(t_s, t_a) = A \left( \frac{t_s - t_a}{l_c} \right)^m \quad (10)$$

$$t_s(\lambda) := \begin{array}{l} \text{for } i \in 0..M \\ \quad t_{0,i} \leftarrow t_{\text{inf}} \\ \quad z \leftarrow i \cdot \Delta z \\ \quad \text{for } j \in 1..N \\ \quad \quad t_{j,0} \leftarrow 88 \\ \quad \quad \tau \leftarrow j \cdot \Delta \tau \\ \quad \quad \text{for } i \in 1..(M-1) \\ \quad \quad \quad t_{j,i} \leftarrow \begin{cases} t_{j-1,i} + \frac{a(\lambda) \cdot \Delta \tau}{(\Delta z)^2} \cdot (t_{j-1,i+1} + t_{j-1,i-1} - 2t_{j-1,i}) & \text{if } t_{j-1,i} + \frac{a(\lambda) \cdot \Delta \tau}{(\Delta z)^2} \cdot (t_{j-1,i+1} + t_{j-1,i-1} - 2t_{j-1,i}) \geq t_{j-1,i} \\ t_{j-1,i} & \text{otherwise} \end{cases} \\ \quad \quad t_{j,M} \leftarrow 88 \\ \quad \quad t_{j,0} \leftarrow \frac{\frac{\lambda}{\Delta z} \cdot t_{j,1} + \alpha(t_{j,1}, t_{\text{inf}}) \cdot t_{\text{inf}}}{\frac{\lambda}{\Delta z} + \alpha(t_{j,1}, t_{\text{inf}})} \\ \quad \quad t_m \leftarrow t_{j,0} \\ \quad \quad q_{e,j} \leftarrow \frac{(t_{j,M-1} - t_{j,M})}{\Delta z} \cdot \lambda \\ \quad t_m \end{array} \quad (11)$$

There are cases where the density and specific heat of the sample, part of the thermal diffusivity, are not sufficiently well known. In this case, one can use, as

a start, for  $t_s(\lambda, \tau_i)$  the numerical variant in which in (11) it considers the numerical expression Schmidt [17] with a convenient chosen time step.

One can then come back with an estimate for the density and specific heat of the sample and proceed to a more precise numerical integration. An estimation of the thermal conductivity of the sample can be made considering the state of thermal equilibrium that is established when the temperature of the sample surface does not change over time, for example  $t_{s\ exp}(\tau_{\infty}) = t_{s\ \infty} = \text{constant}$ . The relation (12) proves this fact.

$$\lambda = \frac{\alpha_s(t_{s\ \infty}, t_a)(t_{s\ \infty} - t_a)\delta}{[t_b - t_{s\ \infty}]} \quad (12)$$

Then it is specified that the minimum of relation (10) can be obtained running through the search domain identified with relation (12). Also, this minimum can be identified numerically by solving equation (13), both for the case that the numerical expression of the model is given by relation (11) or in a complete form, with the thermal diffusivity calculated for the samples based on densities from **Table 1** and a caloric capacity of 1800 J/(kg·K).

$$\frac{d}{d\lambda} F(\lambda) = 0 \quad (13)$$

### *Experimental and measured results*

The experimental installation, as shown in **Figure 1**, was made of an electric stove with precision thermostat, thermal insulator made of glass fiber cut according to the shape of the samples, precision thermocouple coupled with acquisition system, thermal data logger for data acquisition and computer for reading the temperature data logger.

*Table 1*

**The dimension, density and aspect of the investigated samples**

Proba	Lenght (mm)	Witdh (mm)	Thickness (mm)	Density (kg/m3)	t <sub>b</sub> , °C	t <sub>a</sub> , °C	Aspect
P1	45	35	10	205	88	21.8	Porous, soft plastic
P2	67	55	10	205	88	21.8	Porous, soft plastic
P3	67	55	10	215	88	21.8	Porous, soft plastic
P4	67	58	10	205	88	22.2	Porous, soft plastic
P5	43	42	10	202	88	21.2	Porous, soft plastic
P6	65	54	10	205	88	23.5	Porous, soft plastic
P7	66	55	10	205	88	23.1	Porous, soft plastic
P8	69	57	10	198	88	23.5	Porous, soft plastic

**Table 2** shows an example of the measured temperature dynamics at the sample surface for most of the samples reported in **Table 1**.

**Table 2.** Example of temperature dynamics at the sample surface

	0	1
0	0	22.1
1	1	32.3
2	2	38.5
3	3	42.2
4	4	42.6
5	5	42.8
6	6	43.4
7	7	44.2
8	8	43.7
9	9	44.5
10	10	44.2
11	11	45.4
12	12	44.8
13	13	44.7
14	14	44.5
15	15	...

P1 =

	0	1
0	0	21.8
1	2	29.6
2	4	36.3
3	6	39.7
4	8	39.9
5	10	40
6	12	40.7
7	14	41.2
8	16	41.4
9	18	41.8
10	20	41.8
11	22	42.1
12	24	42.3
13	26	42.7

P3 =

	0	1
0	0	22.2
1	1	31.5
2	2	40.1
3	3	43.4
4	4	44
5	5	44.2
6	6	44.5
7	7	44.6
8	8	44.7
9	9	45
10	10	45.1
11	11	45.2
12	12	45.2
13	13	44.6

P4 =

	0	1
0	0	21.2
1	1	30.3
2	2	36.6
3	3	39.6
4	4	41.7
5	5	42.5
6	6	43.4
7	7	42.8
8	8	43.3
9	9	43.7
10	10	44.1
11	11	43.4
12	12	43
13	13	42.6
14	14	42.2

P5 =

	0	1
0	0	23.5
1	1	23.5
2	2	33.8
3	3	40.1
4	4	42.4
5	5	43.9
6	6	44
7	7	43.7
8	8	43.8
9	9	44.4
10	10	44.5
11	11	44.8
12	12	44.7
13	13	44.6
14	14	44.5

P6 =

	0	1
0	0	23.2
1	1	23.1
2	2	26.3
3	3	35.6
4	4	40.9
5	5	42.1
6	6	41.7
7	7	41
8	8	40.8
9	9	41.6
10	10	42.5
11	11	42.7
12	12	43.6
13	13	42.8
14	14	43.4

P7 =

	0	1
3	3	40.9
4	4	42
5	5	42.8
6	6	43.1
7	7	42.8
8	8	43.2
9	9	43.1
10	10	42.8
11	11	42.3
12	12	42.9
13	13	42.8
14	14	42.6
15	15	42
16	16	41.5
17	17	41.1

P8 =

### 3. Results and discussions

From **Table 2**, it is worth mentioning that, depending on the sample, there are differences in the surface temperature dynamics. It is also observable that these dynamics are still sufficiently similar so that it is not expected to obtain more differences between the thermal conductivities of the samples.

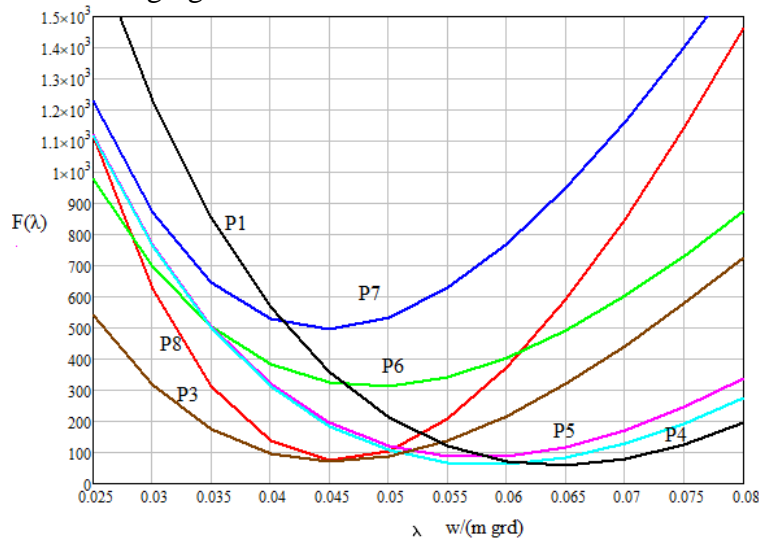
**Table 3** shows the thermal conductivity identifications of each sample, namely: i) initial identification with relation (12), ii) identification according to relation (13) using the numerical model in the form (11) and iii) identification according to relation (13) considering the full numerical model.

Table 3

Identified values for thermal conductivity for samples P1-P8			
Proba	$\lambda$ (W/m·K) Equation (12)	$\lambda$ (W/m·K) Equation (13) – numerical model (11)	$\lambda$ (W/m·K) Equation (13) – full numerical model
P1	0.064	0.064	0.095
P2	0.057	0.052	-
P3	0.051	0.045	0.071
P4	0.058	0.058	0.087
P5	0.055	0.057	0.083
P6	0.057	0.049	0.073
P7	0.052	0.045	0.061
P8	0.047	0.045	0.058

From **Table 3** it can be noticed that the values of the thermal conductivity are quite similar for all samples in the cases in which equation (12), respectively equations of the numerical model (11) were applied. However, taking into account the full numerical model according to equation (13), the values of thermal conductivity are increased with 22 up to 33% in all cases. Nevertheless, regardless of the used method for the determination of the thermal conductivity the values of this parameters were lower compared to the thermal conductivity of air (less than 0.1 W/m·K) showing an excellent insulating characteristic of the plastic porous samples.

**Figures 2 and 3** show the location of the minimum of the function  $F(\lambda)$  when  $\lambda$  is in the belonging domain.



**Fig.2.** Localization according to the simplified numerical model (11) of the minimum average quadratic deviation  $F(\lambda)$  for samples P1-P8

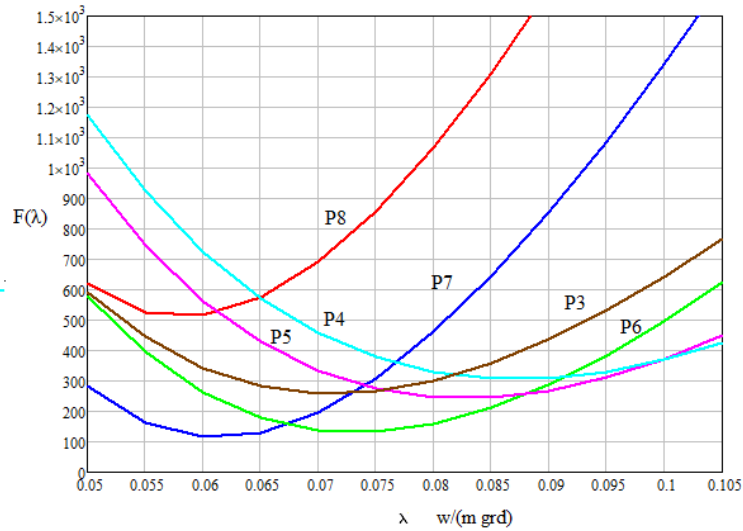


**Fig.3.** Localization according to the unsimplified numerical model of the minimum of the average quadratic deviation  $F(\lambda)$  for samples P1-P8

**Figures 2 and 3** revealed quite similar behavior of the samples in terms of the shape of the curves, all showing plots with clear minimum values regardless of the applied model.

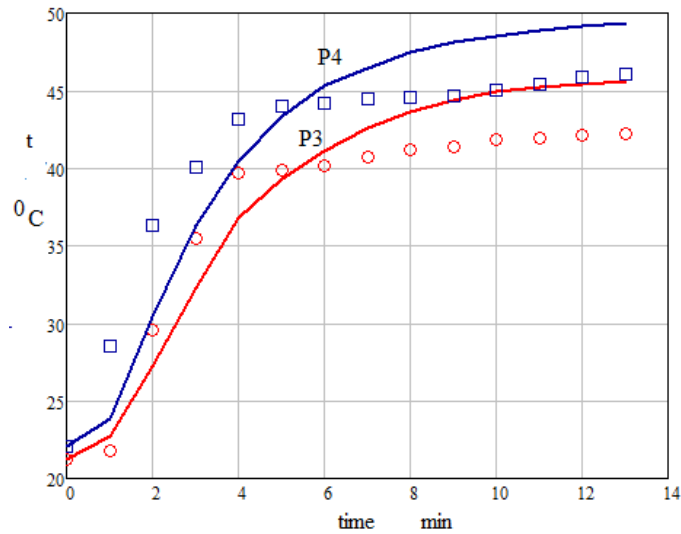


**Fig.4.** Surface temperature dynamics for P3 and P4 samples (red circles and blue squares - experimental data; red and blue line – results obtained from the unsimplified model)

**Figure 4** shows some temperature surface dynamic curves measured experimentally and accordingly to model established in Equations (5) - (8) for a



better comparison between experimental and theoretical data. The red and blue curves represent the results obtained from the use of the unsimplified numerical mathematical model, while the red circles and blue squares represent the experimental data.

#### 4. Conclusions

A fast method for the determination of thermal conductivity was determined for plate-type composite porous materials based on the registration of the temperature dynamics on the surface of the samples keeping the other face of the sample at a constant temperature. The method was successfully tested for 8 composite samples designed for thermal insulation of civil constructions. The method based on the unsimplified mathematical model requires the density and specific heat of the tested material to be known. In all cases, regardless of the applied model, the values for the thermal conductivities were less than 0.1 W/m·K (thermal conductivity of air) making the samples good candidates for insulating materials to be used in constructions due also to their low densities.

#### Acknowledgement

The authors acknowledge the financial support received from the Competitiveness Operational Program 2014–2020 Priority axis: Research, technological development, and innovation (RDI) in support of economic competitiveness and business development Operation: Stimulating the demand of enterprises for innovation through RDI projects carried out by enterprises individually or in partnership with R&D institutes and universities, in order to innovate processes and products in economic sectors that have growth potential Project title: “Greenol-Biopolyols obtained through an unconventional technology of vegetal waste recovery” Project code: 122990. This work was partially granted by the Ministry of National Education (by UEFISCDI) through the national research projects PN-III-P2-2.1-PTE-2021-0514-ctr.80PTE/2022.

#### REFERENCES

- [1] Wang Y. Xu, X., Hao Q., *A mini review on thermally conductive polymers and polymer based composites*, Compos. Commun. 24 (2021).
- [2] Kausar A., *Polyurethane Composite Foams in High-Performance Applications: A Review*, Polymer-Plastics Technology and Engineering, 57, 4, (2018), 346-369.
- [3] Calderón V., Gutiérrez-González S., Gadea J., Rodríguez Á., Junco C., Chapter 10 - *Construction Applications of Polyurethane Foam Wastes*. In Recycling of Polyurethane Foams, Eds. William Andrew Publishing 2018.
- [4] Saha M. C., Kabir M. E., Jeelani S., *Enhancement in thermal and mechanical properties of polyurethane foam infused with nanoparticles*. Materials Science and Engineering A., 479, 1, (2008), 213-222.

- [5] Mort R., Vorst K., Curtzwiler G., Jiang S., *Biobased foams for thermal insulation: material selection, processing, modelling, and performance*, RSC Advances, 11, 8, (2021), 4375-4394.
- [6] Bratu Em. A., *Operații Unitare în Ingineria Chimică*, Vol 2, Editura Tehnica, București, 1983.
- [7] Michal P., Ondřej N., *Measurement and Numerical Modeling of Mechanical Properties of Polyurethane Foams*. In Aspects of Polyurethanes, Ed. IntechOpen, Rijeka, 2017.
- [8] Uram K., Prociak A., Vevere L., Pomilovskis R., Cabulis U., Kirpluks M., *Natural Oil-Based Rigid Polyurethane Foam Thermal Insulation Applicable at Cryogenic Temperatures*, Polymers, 13, 24, (2021), 4276-4289.
- [9] Tache F. *Manufacturing Processes and Properties Modelling of a New Composite Material*, PhD Thesis, University Politehnica of Bucharest, 2010.
- [10] Mohsenin N. N., *Thermal Properties of Foods and Agricultural Materials*, Gordon and Breach Science Publishers, New York 1980.
- [11] Dobre T., Sanchez J.M., *Chemical Engineering Modelling Simulation and Similitude*, Wiley VCH 2007.
- [12] Gustafsson S., *Transient Hot Strip Techniques for Measuring Thermal Conductivity and Thermal Diffusivity*, The Rigaku Journal, 4, 1/2, (1987), 16-29.
- [13] Krishpersad M., David W. Y., James R. B., *Measurement of Apparent Thermal Conductivity by the Thermal Probe Method*, Journal of Testing and Evaluation, 5, 3, (2000), 349-352.
- [14] Bezjack M., *Dynamic Method for Thermal Conductivity Measurement, XVIII IMEKO WORLD CONGRESS, Metrology for a Sustainable Development*, September, 17-22, Rio de Janeiro, Brazil, 2006.
- [15] Osako M., *Simultaneous Thermal Diffusivity and Thermal Conductivity Measurements of Mantle Materials up to 10GPa*, Technical Report of ISEI, Ser. A., No.67, September 1997.
- [16] Leca A., Pop M. G., Prisecaru I., Neaga C., Zidaru Gh., Musatescu V., Isbasoiu E. C., *Îndrumar. Tabele, nomograme și formule termotehnice*, vol. II, p. 71, Editura Tehnică, București 1987.
- [17] Crank J., *The Mathematics of Diffusion*, Clarendon Press, 1957.

## **CLADOPHORA VAGABUNDA MARINE GREEN ALGAE AS A SUSTAINABLE SOURCE OF NEW CELLULOSE NANOFIBERS**

Claudia Ana Maria PATRICHI<sup>1</sup>, Doinita-Roxana CIOROIU TIRPAN<sup>2,\*</sup>, Dobre TANASE<sup>1</sup>

<sup>1</sup>University “Politehnica” of Bucharest, Chemical and Biochemical Engineering Department, 1-7 Gheorghe Polizu Str., Bucharest, 011061, Romania

<sup>2</sup>Ovidius University of Constanta, Chemical and Chemical Engineering Department, 124 Mamaia Blvd., Constanta, 900527, Romania

### **Abstract**

*Cladophora vagabunda* specie is a green alga found along the Romanian Black Sea Coast which offers a rich source of a natural product such as cellulose. This natural biopolymer is biodegradable and can play a particularly important role in solving environmental problems raised by the use of polymeric materials. In this work, seaweed was freshly harvested, dried at 45 °C for 2 days and grounded into a fine powder. Cellulose extraction from *Cladophora vagabunda* specie was performed in a Soxhlet apparatus with ethanol followed by several chemical treatments. The extracted cellulose content from algae was 17.42% in dry matter (DM) thus opening wide possibilities for different industrial applications.

**Key words:** *Cladophora Vagabunda* specie, ethanol, cellulose

### **1. Introduction**

Biodegradable polymers such as polysaccharides (cellulose, starch) can be obtained through different chemical syntheses from green algae found along the Romanian Black Sea Coast. Biodegradable biopolymers represent a large current field of research with important implications in the chemical, food, cosmetic, pharmaceutical and agronomy industries [1]. Scientists’ concern for the consequences on the environment increased when products made of non-biodegradable materials (packaging) end up in the landfill. Polysaccharides, which are found in *Cladophora vagabunda* species, have gained much attention due to their presence of bioactive constituents [2].

Also, an increasing interest is given to algal biomass for different reasons. It is mainly characterized by a high growth rate, high carbon dioxide fixation coupled with the facility of cultivation outdoor in aquatic media such as

---

\* Corresponding author: Email address: tirpanroxana@gmail.com

photobioreactors or open basins. Additionally, the use of algae doesn't affect any human food sources. Macrophytes are classified in green, red and brown algae.

Green macroalgae are considered as opportunistic organisms because they proliferate in biotic or abiotic conditions. They live principally on coastal rocks and shallow seas. Green macroalgae are poorly exploited due to their special composition. According to the study carried out by the Grigore Antipa Institute [3], for *Cladophora vagabunda* species, the biochemical composition of the algal powder is the following: carbohydrates - 48.45%, proteins - 15.43%, lipids - 3.85%, total volatile solids - 67.73% and azote -2.45%. Comparatively, following other experimental studies, polysaccharides in *Cladophora vagabunda* algae depends on the season of harvesting and climatic factors of the area: solar radiation, location of the region, sea-dry ratio, existence of sea currents and existence of air currents [4]. The main polysaccharides in green algae species are ulvans, sulfuric acid polysaccharides, xylan and sulfated galactans [5]. Polysaccharides are found mainly in the cell wall with a role in structural reinforcement of the algae; cellulose is insoluble and can be separated from the other polysaccharides.

Exploiting green macroalgae will have a considerable interest in the environmental and biotechnological fields. This abundant resource represents an interesting substrate for bio refinery or for the production of highly added-value molecules. However few studies have focused on the parietal cell-wall polysaccharides like cellulose.

For the extraction of various substances with solvents (liquid media) from algae, they are finely ground to achieve the conditions for reducing the resistance that this phase opposes to the transport and transfer of the species being extracted.

## 2. Experimental

Fresh *Cladophora vagabunda* algae was harvested from the north of the Romanian Black Sea Coast (Latitude: 44°18'14.9"N; Longitude: 28°55'24.0"E) in June 2022. The seaweeds were washed with sea water, distilled water and cleaned of impurities. Then were placed for 2 days in a dehydrator with 5 overlapping trays, where they dehydrate evenly. The temperature of the warm air flow circulating horizontally has been set at 50°C in order not to destroy the bioactive substances in algae [6]. Subsequently, the dried algae were finely ground by mortaring.

For cellulose extraction from algae were used ethyl alcohol of different concentrations and sodium hydroxide purchased from Merck Romania SRL; ammonium oxalate and acetic acid were purchased from "S.C. Chemical Company S.A.", Romania; hydrochloric acid was provided from Inter Star S.A.

To extract cellulose from algae species *Cladophora vagabunda*, 10 g of

algae were introduced into a solution of ethyl alcohol. The extraction was performed in a Soxhlet extractor (Figure 1a).



**Fig. 1.** a) Soxhlet extractor; b) Chemical treatment with ammonium oxalate; c) Algae bleaching

The lipids were then extracted by adding 100 mL ammonium oxalate (0.05%) to the skimmed algae. The mixture was then heated for one hour between 90 and 100°C while stirring (Figure 1b). Successive washing with hot water were carried out to remove the residues of the hydrophilic fraction. To allow the pigments (chlorophyll) to be removed the algae were bleached at 60°C in a mixture of 200 mL acetic acid (5%) and 100 mL NaClO (5%) (Figure 1c). According to literature and experimental research conducted, many extraction methods have been reported regarding conventional and unconventional chlorophyll separation procedures, which can be intensified when is used heating and/or stirring during extraction [7]. The algae thus obtained was washed (Figure 2a) with distilled water and dried at 105°C. In the final extraction step, algae were treated with 100 mL NaOH (0,5 M) overnight at 60°C under constant stirring. The insoluble fraction extracted was washed to neutrality and dried. The powder

obtained was mixed with 200 mL hydrochloric acid (5%), the prepared mixture was heated to boiling, after which the solution was kept under continuous stirring at 30°C for 12 hours. The extracted cellulose was washed to neutral pH and dried at 105°C (Figure 2b). Thus, a yield of 17.42 % wt cellulose per DM was obtained proving that *Cladophora vagabunda* species is a viable alternative resource in cellulose production.



**Fig. 2.** a) Cellulose washing; b) Dry cellulose from *Cladophora Vagabunda* sp.

### 3. Results and discussions

The dried algae (Figure 3) and the dry cellulose extracted from algae (Figure 4) were subjected to observation by transmission under the SEM TM4000 Tabletop SEM microscope (Hitachi, Japan).

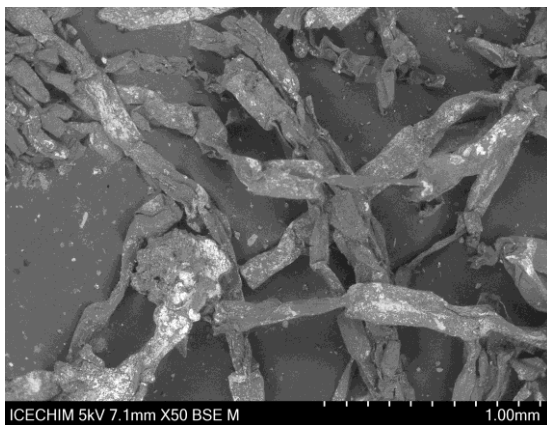


**Fig. 3.** SEM image of dry *Cladophora vagabunda* sp.



**Fig. 4.** SEM image of dry cellulose from *Cladophora vagabunda* sp.

In Figure 3 it can be observed that the algal powder contains certain cellulose structures and in Figure 4 it can be observed clearly microfibers and cellulose structures.

In order to highlight the functional groups of species in the *Cladophora vagabunda* algae sample, the equipment for FTIR -Tensor 37 Bruker analyses (Woodstock, NY, USA) were used.

The FTIR spectra in the region 4000-400  $\text{cm}^{-1}$  for *Cladophora vagabunda* species powder is shown in Figure 5. The big width of the band at 3283.06  $\text{cm}^{-1}$  indicates the presence of functional group -OH. A broad band in 1800-1500  $\text{cm}^{-1}$  range with a wavelength of 1640.67  $\text{cm}^{-1}$  can include proteins and amides I from the protein structure. Also, the wavelength 1539.24 indicates the presence of amides II in the protein structure. The peak at 1236.64  $\text{cm}^{-1}$  is showing carboxylic group  $\text{COO}^-$  ( $\nu_{\text{COO}^-} = 1250-1200 \text{ cm}^{-1}$ ) and the characteristic band for phosphate  $\text{P=O}$  -esters. The presence of carboxylic acid and -OH group is an indication of polysaccharides presence (especially cellulose), which is also confirmed by the peak at 1042.72  $\text{cm}^{-1}$  ( $\nu_{\text{polysaccharides}} = 1200-900 \text{ cm}^{-1}$ ).

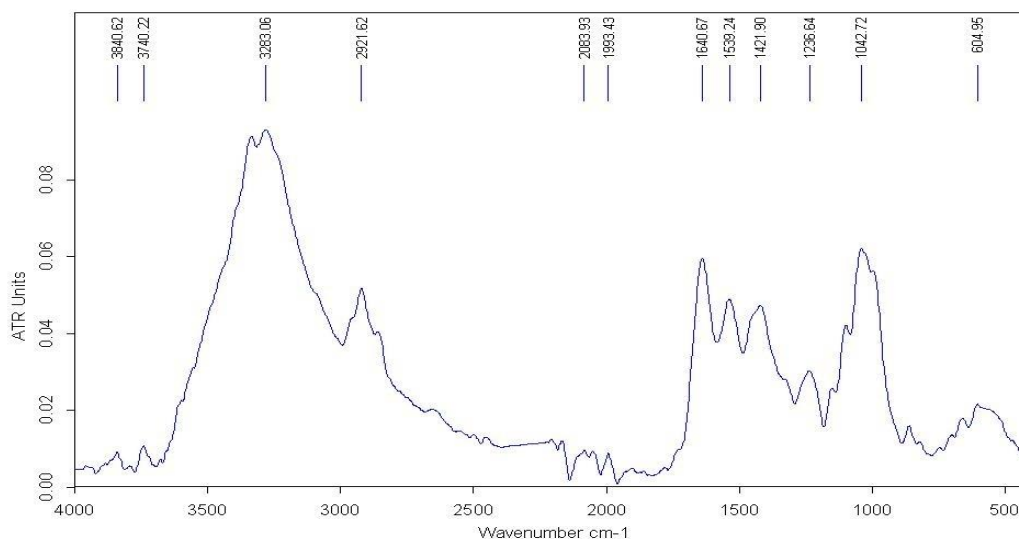


**Fig. 5.** FT-IR spectrum of algal powder from *Cladophora vagabunda* sp. before the extraction

The spectral analysis of the cellulose extracted from *Cladophora vagabunda* species is presented in Figure 6. FTIR analysis shows the characteristic bands of the oscillation vibrations of the -OH group (3342.66  $\text{cm}^{-1}$ ). A broad band in 1800-1500  $\text{cm}^{-1}$  range with a wavelength of 1643.45  $\text{cm}^{-1}$  can include proteins and amides I from the protein structure. The peak at 1204.19  $\text{cm}^{-1}$  is showing carboxylic group  $\text{COO}^-$  presence ( $\nu_{\text{COO}^-} = 1250-1200 \text{ cm}^{-1}$ ).

Characteristic bands for polysaccharides (especially cellulose) are confirmed by peaks at 1108.09 and 1047.59  $\text{cm}^{-1}$ .

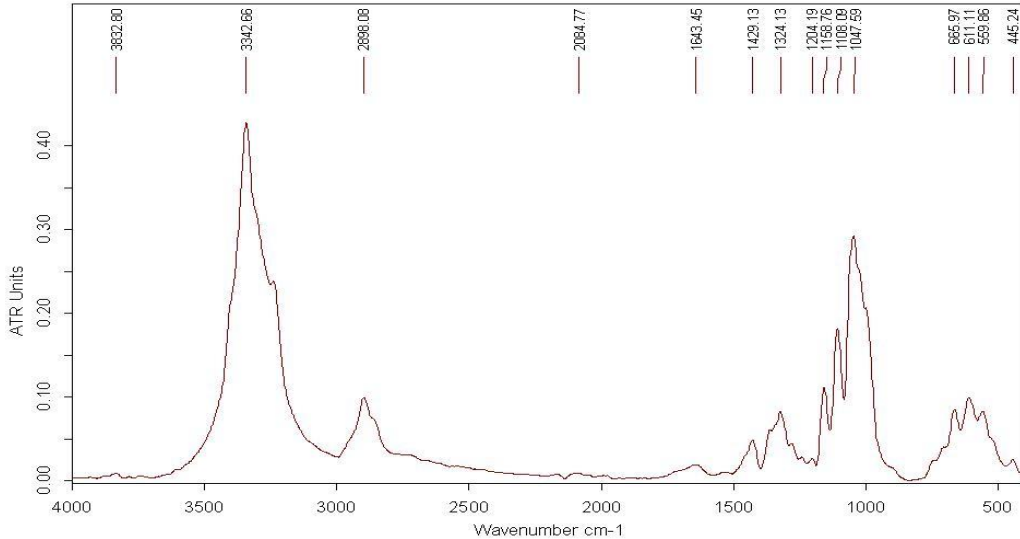


**Fig. 6.** FT-IR analysis of cellulose extracted from *Cladophora vagabunda* sp.

## 6. Conclusions

In this study, a physicochemical characterization of *Cladophora vagabunda* species in Black Sea was performed: dry matter content, optical microscopy and chemical structure by functional group identification with a FT-IR spectrometer. Then, the extraction of cellulose was performed in a separation scheme including the removal of lipids, pigments, ulvans, and hemicellulose. The scheme includes operations for the removal of undesirable substances but don't affect the cellulose which is obtained as a white powder. A yield of 17.42 % cellulose per dry matter was obtained proving that *Cladophora vagabunda* species is a viable alternative resource in cellulose production.

## Acknowledgments

This work has been funded by the European Social Fund from the Sectoral Operational Program Human Capital 2014-2020, through the Financial Agreement with the title "Training of PhD students and postdoctoral researchers in order to acquire applied research skills - SMART", Contract no. 13530/16.06.2022 - SMIS code: 153734"



## REFERENCES

- [1]. Cioroiu Tirpan D.R., Raducanu C.E., Chis T.V., Dobre T., *Extraction of polysaccharides from Ceramium Rubrum*, Bulletin of Romanian Chemical Engineering Society, Vol 9, No 1, pp.94-102, 2022.
- [2]. Cioroiu D.R., *Integrated chemical and biochemical processes with the processing of plant products and residues: macrophyte algae*, PhD Thesis, University Politehnica of Bucharest, 2017.
- [3]. Institute Grigore Antipa, *Research report No. 3*, Project MACROEVAL, 2010, <http://www.rmri.ro/WebPages/MACROEVAL/32-144%20Etapa3.pdf>
- [4]. Kidgell J.T., Magnusson M., de Nys R., Glasson Ch.R.K., *Ulvan: A systematic review of extraction, composition and function*, Algal Research 39, 101422, 2019. <https://doi.org/10.1016/j.algal.2019.101422>
- [5]. Özçimen D., İnan B., Morkoç O. and Efe A., *A Review on Algal Biopolymers*, Journal of Chemical Engineering Research Updates, Vol 4, pp. 7-14, 2017.
- [6]. Cioroiu Tirpan D.R., Koncsag C.I., Dobre T., *Cellulose fibers extraction from Ulva lactuca from the Black Sea*, Ovidius University Annals of Chemistry, Volume 31, Number 2, pp. 158 - 162, 2020.
- [7]. Buliga D.I., Popa I., Diacon A., Boscornea C.A., *Optimization of Ultrasound-Assisted Extraction of Chlorophyll Using Design of Experiments and Stability Improvement via Encapsulation*, UPB Scientific Bulletin, Series B, 84(4), 59-72, ISSN:1454-2331, WOS:000897670000005, 2022

## LIGNOCELLULOSIC RESIDUAL BIOMASS AS HETEROGENEOUS CATALYST FOR TRANSESTERIFICATION TO ALKYL ESTERS

Ana-Maria Raluca MUȘAT<sup>1</sup>, Cristian Eugen RĂDUCANU<sup>1,\*</sup>, Roxana JIDVEIAN<sup>1</sup>, Doinița-Roxana CIOROIU-TÎRPAN<sup>2</sup>, Gabriel VASILIEVICI<sup>3</sup>, Andreea Luiza MÎRȚ<sup>3</sup>, Tănase DOBRE<sup>1,4</sup>, Oana Cristina PÂRVULESCU<sup>1</sup>

<sup>1</sup>Chemical and Biochemical Engineering Department, National University of Science and Technology POLITEHNICA Bucharest, 1-7 Gheorghe Polizu St., 011061 Bucharest, Romania,

<sup>2</sup>Ovidius University of Constanta, 124 Mamaia Blvd., 900527 Constanta, Romania,

<sup>3</sup>National Institute for Research Development for Chemistry and Petrochemistry-ICECHIM, 202 Spl. Independentei, S6, 060021, Bucharest, Romania; <sup>4</sup>Technical Sciences Academy of Romania, 26 Dacia Blvd., 030167 Bucharest, Romania.

**Abstract.** *In this experimental investigation a heterogeneous catalyst from lignocellulosic residual biomass was developed and tested while catalyzing transesterification of waste cooking oils to alkyl esters. A fixed-bed catalyst reactor carried out a methanol oil transesterification reaction. For two hours operating time, at 70 °C process temperature, and yields values in the range of 88.97-95.01% were obtained. The performance study of the processes carried out highlighted the importance of the height of the catalytic layer and the concentration of the catalyst, the interaction between them and the correlation with the feed rate of the reactants.*

**Key words:** catalytic bed reactor, heterogeneous catalyst, lignocellulosic residual biomass, alkyl esters

### 1. Introduction

The increasing popularity of alternatives to fossil fuels leads us, day by day, to research and discover new solutions and methods of *environmentally friendly* fuels. Whether it is the use of biofuels, hybrid cars or fully electric cars, this topic has become of interest to most countries in recent years.

Automobiles are a major source of carbon dioxide, the main man-made greenhouse gas believed to be one of the main causes of global warming. If the cars were to use biofuels, then the plants grown for this purpose could absorb a large part of the carbon dioxide that the cars would release through the exhaust gases. This would maintain a balance between the amount of carbon dioxide produced by cars and the amount of carbon dioxide absorbed by plants. Currently,

---

\* Corresponding author: cristianrdcn1@yahoo.com

by extracting oil we bring to the surface large amounts of carbon, released then into the atmosphere and thus contributing to global warming.

Petro diesel is obtained from oil which is characterized today by a series of factors such as majority availability in areas of permanent conflict, financial instability in specific markets, huge extractive or refining installations, whose costs execution or maintenance and especially security today are added to the prospective ones, thus becoming true barriers for some and allowing only certain actors to play in this field. On the other hand, biodiesel, which is a synthetic chemical compound but with properties similar to petro diesel, is characterized by factors located at the opposite side: it can be obtained currently in lower quantity not requiring necessarily huge installations, the production capacity currently being governed only by demand or by certain imposed green regulations; it is considered renewable as a resource, being a chemical compound resulting from the transesterification reaction between triglycerides (from vegetable oils, animal and vegetable fats, etc.) and methanol, in the presence of a catalyst [1-5]; it is not related to conflict areas and what makes it extremely valuable and useful is its complex of properties and characteristics similar (some even more advantageous) to those of diesel 2 [6,7]

Except for the non-catalytic, non-conventional processes, in the other processes the reaction between triglycerides and alcohol takes place in the presence of a catalyst. Without catalysts, the process is very, very slow [8].

Due to the high cost of refined raw materials and the difficulties associated with the use of homogeneous catalysts for the transesterification of low-quality raw materials for the purpose of biodiesel production, the need to develop heterogeneous catalysts has increased. The development of heterogeneous solid or enzyme-type catalysts could solve the problems associated with homogeneous catalysts.

Commercial biodiesel is obtained in homogeneous catalysis, a process that poses, among others, the problem of separating the reaction products and some of their washing steps. At present, most of the biodiesel is produced from edible oils and methanol in the presence of base catalysts in batch reactors [9-12].

We therefore aimed in this work to develop a solid catalyst, by a method which combines a certain type of catalytic support and a base catalyst, to heterogeneously catalyze transesterification reaction to alkyl esters. A new approach of material pretreatment was carried out, to ensure specific properties in terms of superficial surface of the material before functionalization. The developed catalyst was then tested in transesterification reaction of waste cooking oil to methyl esters (*ME*).

## 2. Experimental

### 2.1 Materials

Isopropyl alcohol 99% (Merck, Germany), methyl orange (Merck, Germany), phenolphthalein (Merck, Germany), potassium hydroxide pellets (Lach-Ner, Czech Republic), Bromophenol Blue (Merck, Germany), Methanol 99.99% (Merck, Germany), hydrochloric acid 1N, (Ingen Laboratory, Romania) were used for reaction and analysis. Cherry pits were the lignocellulosic residual biomass material used for the preparation of the catalytic support. To test the heterogeneous catalyst, domestic waste cooking oil was used for conversion to *ME*.

### 2.2 Experimental set-up and procedure

#### 2.2.1 Catalytic support preparation

The processing of vegetable matter as catalyst and then its use in methanol transesterification of degraded vegetable oils is the subject of our following subsections. Firstly, the cherry pits, as selected material for catalytic support, undergo to a series of thermal and mechanical pretreatments as shown in figure 1. After this, they go to chemical preparation phase to have our heterogeneous transesterification catalyst.

##### 2.2.1.1 Thermal treatment of cherry pits

According with Fig.1 the Drying I operation was carried out at a temperature of 70°C, using Ohaus MB23 Moisture Balance thermo balance.

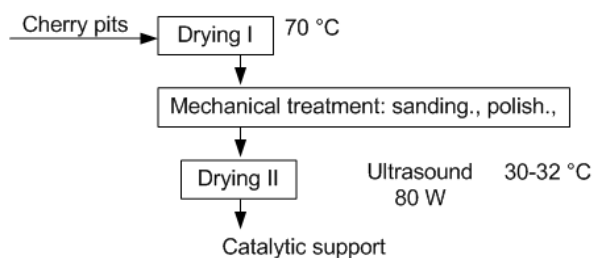


**Fig. 1.** Simplified operation scheme for pretreatment of cherry pits

The treatment of the material was correlated with the experimental catalyst testing matrix, considering that catalyst mass was one of the factor involved (Tabel 1). After mechanical treatment a secondary drying operation, with dry air

as drying agent, was carried out with a device with solid in ultrasonic field and completely dried air as drying agent (figure 2). Table 2 shows the catalytic support mass state after operation from figure 1 for some several catalyst preparation batches

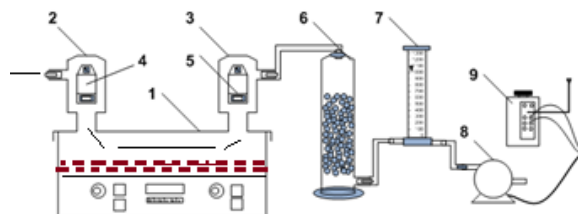


**Fig. 2.** Uniform vacuum squeeze: (1) ultrasonic bath; (2) exit enclosure; (3) entrance area; (4) data logger gas out; (5) data logger gas in; (6) silica gel column; (7) air rotameter; (8) air fan; (9) autotransformer.

Table 1

**Cherry pits mass following thermal treatment**

Crt no	Raw mat. mass [g]	Mass after D I [g]	Mass after sanding [g]	Mass after polishing [g]	Mass after D II [g]
1	46.62	43.57	41.69	40.87	39.47
2	46.35	43.40	41.37	40.56	39.00
3	48.58	45.28	43.08	42.15	40.73
4	47.54	44.27	42.36	41.33	39.72
5	91.81	86.21	82.34	80.72	78.93
6	92.77	86.94	82.57	80.40	78.60
7	94.26	87.93	84.14	82.49	79.09
8	92.56	86.51	82.08	80.55	78.20

### 2.2.1.2 Chemical treatment of cherry pits

Functionalization of the catalytic support involved specific operations, as it is shown in figure 3. The impregnation was carried out with 2M and 3M potassium hydroxide solutions.

Figure 4 shows the experimental set-up for functionalization stage. The impregnation procedure was initiated by dissolving the pre-calculated amounts of potassium hydroxide, by adding KOH in the flask (1) of  $V_i=1$  L volume over which methanol and distilled water were added until the mass of the solution reached 150 g. The mixture was kept at a temperature of 40°C with the help of a magnetic stirrer with heating (2) for 10 minutes, after which the catalytic support was added.

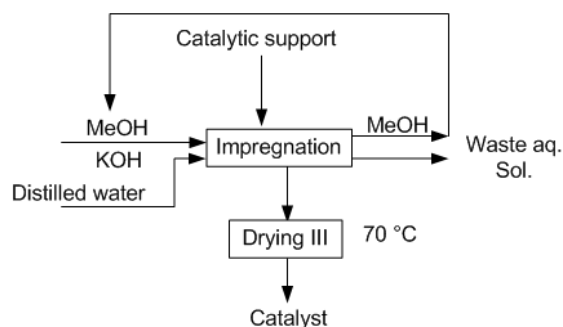


Fig. 3. Simplified operation scheme for chemical treatment of cherry pits

We opted for impregnation through a distillation process, which resulted in the recovery of methanol from the reaction mixture.

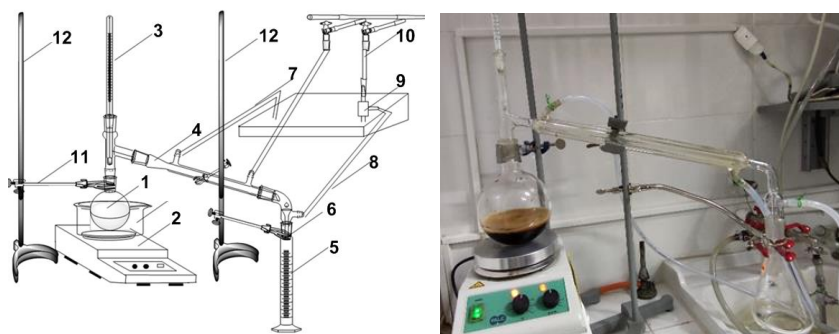


Fig. 4. Diagram of the catalytic support impregnation installation: 1) glass flask; 2) magnetic stirrer with heating; 3) thermometer; 4) refrigerant; 5) methanol collection vessel; 6) refrigerant connection; 7) evacuation; 8) water supply; 9) pump vacuum; 10) water source; 11) stand clamps; 12) stand

Thus, a reducer and refrigerant (4) and a vessel (5) for collecting the distillate (methanol) were added to the flask. The operating time was for impregnation/distillation was  $\tau_{ich} = 6$  hours, composed of  $\tau_{recMeOH} = 40-45$  min and the actual impregnation time  $\tau_{impr} = 320$  minutes.

### 2.2.1.3 Determination of the basic compound content in the heterogeneous catalyst

Different methods are used to determine the base or acid content of a solid, and in this paper, for this determination, the titration method was chosen. The determination method consisted in the titration with hydrochloric acid of pre-calculated amounts of the catalyst, using the set-up in figure 3.17:

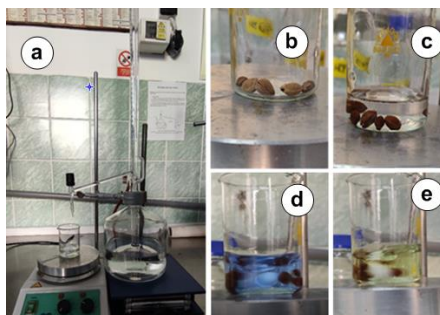


Fig. 5. Simplified operation scheme for chemical treatment of cherry pits

Determination of the basic compound content involved immersing a selected sample of the catalyst in isopropyl alcohol and kept at room temperature, under stirring, for the saturation of the solution with the compound basic. The saturation time of the solution with the base deposited on the catalytic support was approximately  $\tau_{sat} = 24$  hours. The solid sample mass was then added to a Berzelius glass, over which a volume of isopropyl alcohol of  $V_{iso} = 20.90-25.49$  mL was poured. After saturating the solution, 0.4 g of bromophenol blue indicator was added, and subsequently they were subjected to agitation until homogenization. At the end of homogenization, the titration with 0.01N HCl was initiated, noting the titration volume.

Table 2

Sample to determine basic concentration on solids				
Crt.no	Conc after impregn.	Solvent mass [g]	Sample mass [g]	HCl conc
1	2M	20	0.62	0.01 N
2	3M	20.14	0.91	0.01 N

The mass of potassium hydroxide in the catalyst was determined using Eq. (1):

$$x = \frac{V * C * m_{KOH}}{m_{HCl}} \quad (1)$$

where  $x$  - mass fraction of potassium hydroxide;  $V$  - solvent alcohol volume, l;  $C$  - titrant concentration, g/L;  $m_{KOH}$  - molecular mass of potassium hydroxide;  $m_{HCl}$  - molecular mass of hydrochloric acid.

The concentration of the solid was determined using Eq. (2):

$$c_{solid} = \frac{x}{m_{sample}} \quad (2)$$

where:  $c_{solid}$  - solid concentration;  $m_{sample}$  - mass of the analyzed catalyst sample;

#### 2.2.1.4 Catalyst testing in transesterification reaction to alkyl esters

Used cooking oil was used for conversion to *ME*, while for the study of the process parameters and the performance of the process we used a  $2^3$  design factorial plan.

A refrigerant (2) was attached to the top of the reactor for condensation and countercurrent circulation of methanol. The reaction temperature in the jacket was maintained with the help of a thermostatic bath (3) of  $75^\circ\text{C}$  temperature, equipped with a thermometer (4) and a thermometer with a thermostat (5). The methanol, in a molar ratio of 1:6 to the oil, was fed into the mixing vessel (6) of Vv.am.=500 mL volume, to which the refrigerant (7) was attached for the reflux condensation of methanol and recirculated for 15 minutes to activate the catalyst, directed from the mixing vessel using the pump (8) powered by the voltage transformer (9), powered itself at 220V. The temperature in the mixing vessel was ensured using a magnetic stirrer with thermostat heating (10).

The transesterification process started with the feeding of the waste cooking oil, preheated to  $60^\circ\text{C}$ , and continued with the recirculation of the reaction mixture by contacting the catalytic layer in the reactor, directed through the separation funnel (11), where the settling of glycerin took place with the formation of its reaction product and recirculated through the overflow connection throughout the process. The selected duration of the process was  $t_{FB}=90$  min, comparable to that of the commercial biodiesel production process in homogeneous liquid catalysis. At the end of the process, the reaction products, *ME* and glycerin, were removed and stored in optimal conditions, until the collection of samples for analysis. After the collection of samples, the reaction products were subjected to successive stages of purification, by washing and distillation, in the case of biodiesel and distillation, in the case of glycerin.

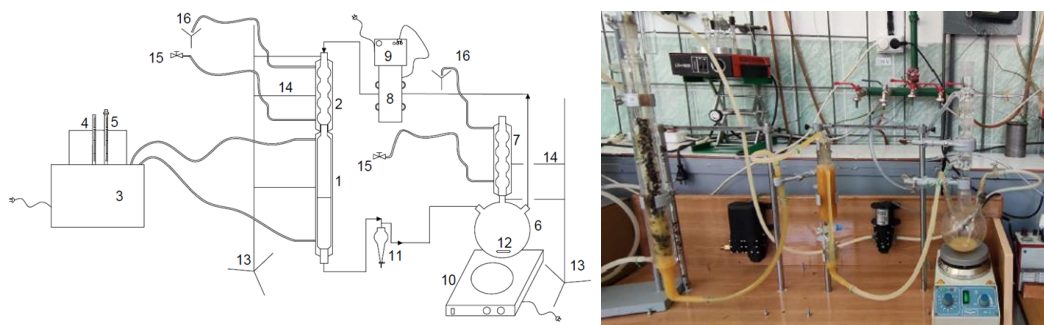


**Fig. 6.** Experimental set-up for obtaining biodiesel in a fixed-bed catalyst reactor: 1) reactor; 2) refrigerant; 3) thermostatic bath; 4) thermometer; 5) thermometer with thermostat; 6) mixing vessel; 7) refrigerant; 8) pump; 9) voltage transformer; 10) magnetic stirrer with heating; 11) glycerin decanter; 12) magnet; 13) stand; 14) clamps; 15) cold water feed; 16) water out



Characteristic factors of transesterification process carried out in the catalytic reactor were selected as follows: particle diameter ( $d_p=0.6, 1.2$  mm), KOH concentration ( $c_{KOH}=1, 2$  M), and reactant superficial velocity ( $w=1.49, 2.71$  cm/s). According to a  $2^3$  factorial plan (3 factors and 2 levels of each factors), 8 experimental runs were conducted.

Table 3

**Levels of process factors.**

Exp. no.	$d_p$ [mm]	KOH conc [mol/L]	$w$ [cm/s]	$x_1$	$x_2$	$x_3$
1	1.2	2M	2.71	+1	+1	+1
2	1.2	2M	1.49	+1	+1	-1
3	1.2	1M	2.71	+1	-1	+1
4	1.2	1M	1.49	+1	-1	-1
5	0.6	2M	2.71	-1	+1	+1
6	0.6	2M	1.49	-1	+1	-1
7	0.6	1M	2.71	-1	-1	+1
8	0.6	1M	1.49	-1	-1	-1

### 2.2.1.5 Purification of reaction main product

At the end of the process, biodiesel contained methanol and traces of monoglycerides, diglycerides or soap, so further washing and distillation were performed (Figure 7). In a separating funnel of volume  $V_{sfpurif} = 2$  L ME and glycerin from the mixture of reaction products were added, over which distilled water was slowly poured in a mass ratio of approximately water/ME of 1:2, thus opting for a static drying after which the obtained mixture was kept for  $\tau_{wash} = 48$  h in the funnel (Figure 8).

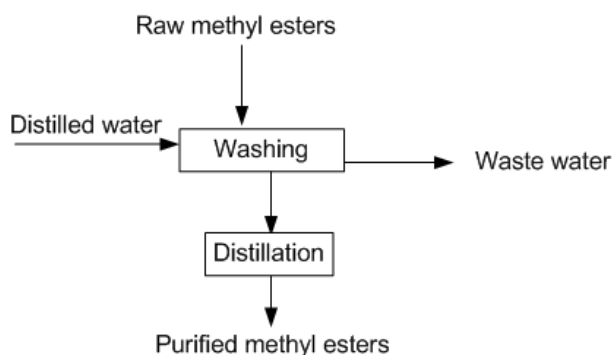
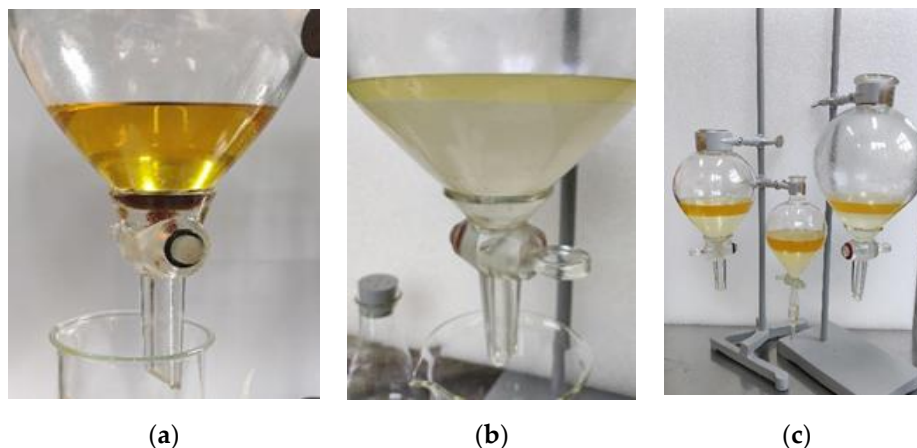


Fig. 7. Simplified process flow diagram of ME purification



(a) (b) (c)  
**Fig.8.** Post-transesterification operations: (a) glycerin removing; (b) washing;  
 (c) 48 h of static *ME* washing

For further purification volumes of biodiesel subjected to distillation were added to the distillation flask (1) of volume  $V_{dist} = 500$  mL. The process temperatures were maintained with the help of the magnetic stirrer with heating (5) and had the values  $t_{ama} = 89-151^{\circ}\text{C}$  and  $t_{vapa} = 33-63^{\circ}\text{C}$ , for the atmospheric distilled biodiesel, respectively  $t_{amv} = 89-192^{\circ}\text{C}$  and  $t_{vapv} = 49-67^{\circ}\text{C}$ , for vacuum-distilled biodiesel.

#### 2.2.1.6 Soap content in reaction main product

Determination of the soap content of the *ME* phase was performed immediately at the end of the process, as well as after the *ME* purification operation. The procedure was identical and was carried out using the titration station shown in Figure 5. Thus, from the *ME* phase a sample was taken with mass value in the range of  $m_{samB} = 0.76-1.22$  g, diluted then in isopropyl alcohol having mass values in the range of  $m_{solv} = 14.64-16.3$  g. The indicator used was bromophenol blue, and the titration was carried out using 0,01N hydrochloric acid.

#### 2.2.1.7 Reuse and reactivation of the catalyst

The reuse of the catalyst, *i.e.* its participation in several transesterification reactions, was studied. The reuse procedure involved the transfer of the product mixture at the end of the process to the separation zone while maintaining the catalyst in the reactor.

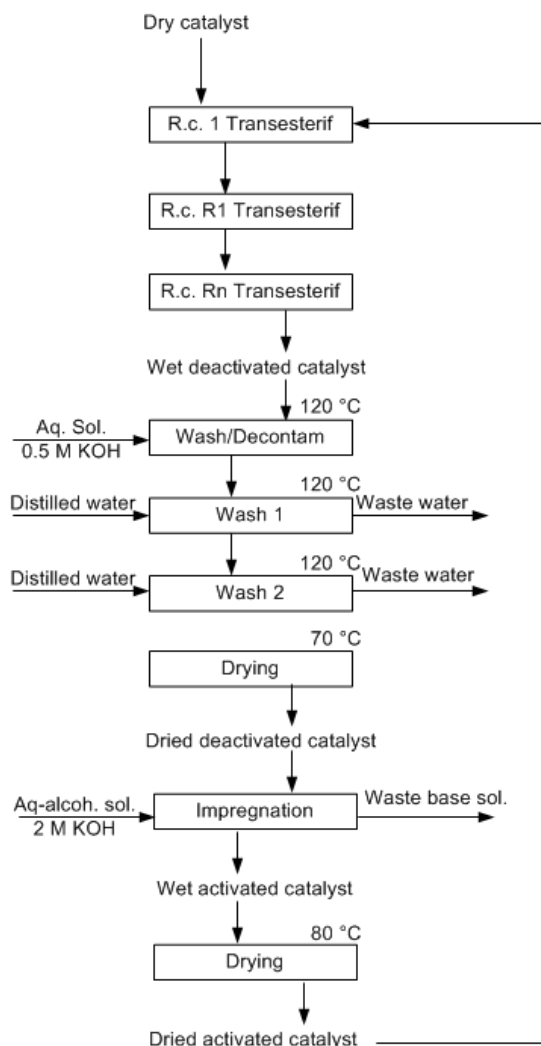


**Fig.9.** Process flow diagram of catalyst reusability and reactivation: *Rc1* –initial reaction; *RcR1* – the first reuse reaction; *Rcn* – *n* reuse reactions

The new reaction cycle was thus resumed under the conditions mentioned in the description of the working method: the methanol stream was fed at the temperature of  $t_{activ} = 50^{\circ}\text{C}$  for  $\tau_{activ} = 15$  min, after which the preheated oil at  $60^{\circ}\text{C}$  was added and left at temperature  $t_{reusR1} = 60^{\circ}\text{C}$  time of  $\tau_{reusR1} = 90$  min. In a similar procedure the reuse of the catalyst in the R2 reaction (and further in the Rn reactions) were carried out, while maintaining the catalyst in the reactor.

### 3. Results and discussions

#### 3.1 Thermal treatment of cherry pits

Drying of lignocellulosic material (Figure 7) as part of thermal treatment shows significant differences between pre-functionalization state (Figure 8) and after functionalization (Figure 9), with drying rate influenced by impregnation, consisting in different pore network response to thermal activity.



Fig. 10. Cherry pits: (a) functionalized; (b) functionalized and dried

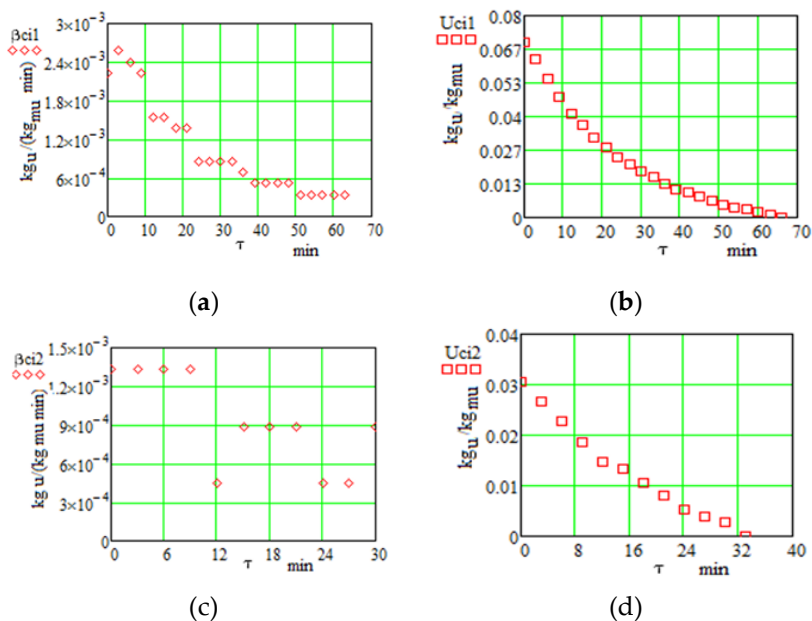
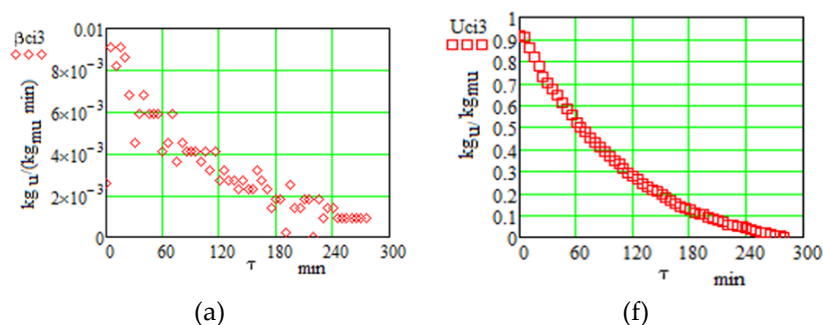


Fig. 11. Dynamics of Drying I: (a), (c) drying rate and (b), (d) moisture, before functionalization



**Fig. 12.** Dynamics of Drying III: (a) drying rate and (b) moisture, after functionalization

The drying curves in Figure 11 characterize the complete removal of residual water, drying being necessary for the functionalization of the material by impregnation to be achieved without the presence of water. In Figure 12, though, the drying curves after impregnation show that the water saturation reached  $0.95 \text{ kg}_{\text{moist}}/\text{kg}_{\text{dry}}$ , which denotes the characteristic of a rather porous material. The drying dynamics follows the drying curve in which the water diffusion process from the pores is predominant. The drying speed from the experimental data points is much tighter compared to the drying speed obtained during the initial drying of the cherry pit.

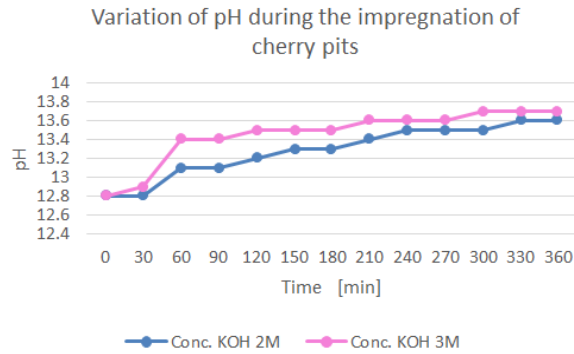
### 3.2 Determination of the base compound content in the heterogeneous catalyst

Table 3 shows the values for the solid concentration obtained in the impregnation stage, respectively 1.57-2.29% in the case of catalysts from cherry pits.

Table 4

Base concentration on solid catalyst					
Crt.no	Conc after impregn.	Solvent mass [g]	Sample mass [g]	HCl conc	Base conc. in catalyst [%]
1	2M	20	0.62	0.01 N	2.29
2	3M	20.14	0.91	0.01 N	1.57

Regarding the concentration of the base compound (potassium hydroxide) deposited on the support, concentrations of 2-3M were selected in the case of the catalytic support of cherry pits, for which it was monitored pH variation during impregnation (Figure 13).



**Fig. 13.** pH variation on functionalization of catalytic support

### 3.3 Catalyst testing in transesterification reaction to alkyl esters

Table 5 shows the process performances in terms of  $ME$  yield ( $Y_{ME}=81.5$ - $96.1\%$ ), glycerol yield ( $Y_G=7.8$ - $11.6\%$ ) under different operating conditions, while in Table 6 details the process factor interaction.

A statistical model based on a  $2^3$  factorial plan was used to predict the process performances depending on its factors particle diameter ( $d_p=0.6, 1.2$  mm), KOH concentration ( $c_{KOH}=1, 2$  M), and reactant superficial velocity ( $w=1.49, 2.71$  cm/s).

Table 5

**Experimental matrix for  $2^3$  factorial experiment**

Exp. no.	$d_p$ [mm]	KOH conc [mol/L]	$w$ [cm/s]	$x_1$	$x_2$	$x_3$	$Y_{ME}$ (%)	$Y_G$ (%)
1	1.2	2M	2.71	+1	+1	+1	87.6	10.6
2	1.2	2M	1.49	+1	+1	-1	94.3	10.2
3	1.2	1M	2.71	+1	-1	+1	95.7	9.4
4	1.2	1M	1.49	+1	-1	-1	93.3	9.8
5	0.6	2M	2.71	-1	+1	+1	96.1	11.6
6	0.6	2M	1.49	-1	+1	-1	89.5	8.9
7	0.6	1M	2.71	-1	-1	+1	81.5	7.8
8	0.6	1M	1.49	-1	-1	-1	90.1	7.8

Methyl ester yield  $Y_{ME}$  and glycerol yield  $Y_G$  are given by the Eqs.(3)-(4):

$$y_{ME} = 91.01 - 2.638 x_1 x_2 - 3.037 x_1 x_2 x_3 \quad (3)$$

$$y_G = 76.636 + 3.239 x_1 + 2.029 x_2 + 9.031 x_3 - 2.324 x_1 x_2 - 2.846 x_1 x_3 - 1.799 x_1 x_2 x_3 \quad (4)$$

Table 6

Experimental matrix for 2<sup>3</sup> factorial experiment

Exp.no.	Factori dimensionali			Dimensionless factors			Process factor interaction			
	Cat.layer height [cm]	Superficial velocity [cm/s]	KOH conc.[mol/L]	x <sub>1</sub>	x <sub>2</sub>	x <sub>3</sub>	x <sub>1</sub> x <sub>2</sub>	x <sub>1</sub> x <sub>3</sub>	x <sub>2</sub> x <sub>3</sub>	x <sub>1</sub> x <sub>2</sub> x <sub>3</sub>
1	15	1.49	2	-1	-1	-1	1	1	1	-1
2	15	1.49	3	-1	-1	1	-1	-1	-1	1
3	15	2.71	2	-1	1	-1	1	-1	-1	1
4	15	2.71	3	-1	1	1	-1	1	1	-1
5	30	1.49	2	1	-1	-1	-1	1	1	1
6	30	1.49	3	1	-1	1	1	-1	-1	-1
7	30	2.71	2	1	1	-1	-1	-1	-1	-1
8	30	2.71	3	1	1	1	1	1	1	1

Figure 11(a) shows the statistical model represented by points and the experimental data represented by line. In this case (also shown in Table 5), we observe that the yield is influenced by the height of the catalytic layer, the feed flow and the interaction between the height of the catalytic layer and the concentration of potassium hydroxide deposited on the catalytic support. Figure 11(b) shows the statistical model represented similar, by points and the experimental data represented by line. In this case, as also shown in Table 5, we observe that the yield is influenced by the height of the catalytic layer, the feed flow and the concentration of potassium hydroxide deposited on the catalytic support, but also by the interaction between the height of the catalytic layer and the feed flow, that between the height of the catalytic layer and the concentration of potassium hydroxide deposited on the catalytic support.

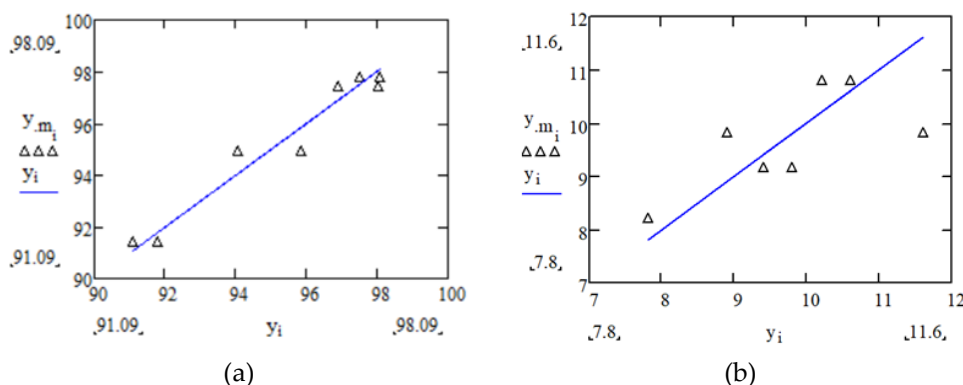
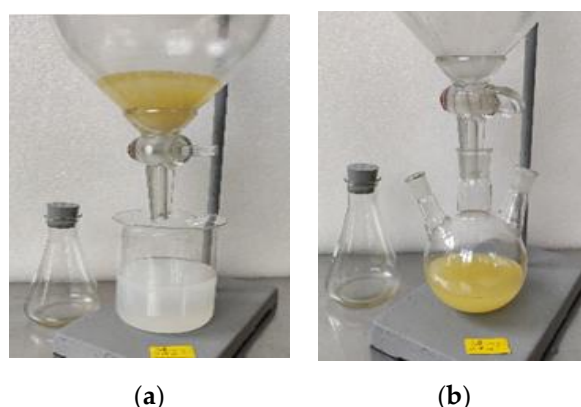


Fig. 14. Diagrams for ME and glycerine yield

### 3.4 Purification and soap content of ME

After the 48 hours from the initiation of the washing step and simultaneously with the clarification of the aqueous phase, suspended particles resulting from the affinity between the hydrophilic particles and water were observed, while the initial clear distilled water turned into soap content washing water (Figure 15.a).



**Fig. 15.** Diagrams for ME and glycerine yield

For ME and distilled wash water, the material balance is presented in Table 7, for B4, B5 and B6 of the corresponding experimental tests no. 4, 5 and 6.

The results obtained following the titration operations for the soap content are presented in Table 8, with samples B4, B5 and B6 from the corresponding experimental tests no. 4, 5 and 6, and show high soap content values, specific to a product before washing purification.

Table 7

**Material balance in ME soap content determination, from exp. 4, 5 and 6**

Exp. no.	ME in [g]	Distilled water in [g]	ME out [g]	Waste water out [g]
B4	142.51	145	136.38	151.13
B5	139.29	140	132.89	146.4
B6	142.58	145	133.71	153.87

Table 8

**ME post-transesterification soap content of exp. 4, 5 and 6**

Exp. no.	Isopropyl alc. [g]	ME sample [g]	HCl vol. [mL]	Soap content [ppm]
B4	15.47	0.94	0.70	2387.15
B5	16.13	1.70	12.9	24324.85
B6	15.87	1.08	6.00	17808.89



After the washing operation, the *ME* was subjected to an additional purification through the distillation process, as it was collected into distillation flask (Figure15.b). Dynamics of distillation temperature process can be seen in Figure 16.

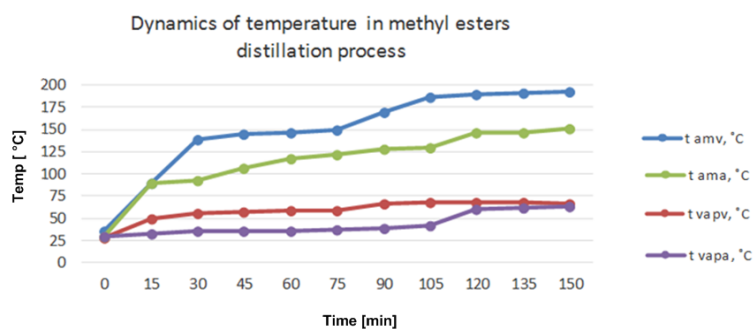


**Fig. 16.** Diagrams of temperature in *ME* distillation process: vacuum distillation: blue line – reaction mixture temperature and red line – vapor temperature; atmospheric distillation: green line – reaction mixture temperature and purple line - vapor temperature

Table 9

***ME* post-distillation soap content of esp. 4, 5 and 6**

Exp. no.	Isopropyl alc. [g]	<i>ME</i> sample [g]	HCl vol. [mL]	Soap content [ppm]
B4	14.64	0.90	0.50	1780.89
B5	14.82	0.95	3.50	11810.11
B6	16.30	1.40	4.30	9845.77

It can be observed that, post-process, the soap content was higher, with values in the range of 2387.15 - 24324.85 parts per million, while after purification by washing and distillation it was significantly reduced, to values in the range of 1265.37 - 11810.11 parts per million, after a single wash.

### 3.5 Reuse and reactivation of the catalyst

Both the initial pretreatment and chemical treatment operations of the catalyst, as well as those in the catalyst reactivation stage, allowed us to develop a catalyst whose properties were created and maintained in the two different stages (construction and reactivation). The catalysts obtained were able to catalyze both transesterification reactions of used vegetable oils with methanol *Rc. 1* with yield values of 96.10%, as well as those for reuse *Rn* with yield values in the range 88-80.5% *ME* content (Table 10)

Table 10

**Randamentele obținute la reutilizarea catalizatorului (BSF)**

Exp. No.	Rc. 1	Rc. R1	Rc. R2	Rc. R3
	$Y_{ME}$ [%]	$Y_{ME}$ [%]	$Y_{ME}$ [%]	$Y_{ME}$ [%]
B5	96.10	88.00	81.20	80.5

The catalyst retained residual biodiesel and glycerin on its surface. In general, the lack of potential inhibitors in a new reaction medium is preferred, but in the present case, biodiesel and glycerine residues did not have an inhibitory role, but on the contrary influenced the reaction from the inoculum position, starting faster, with the formation of a heterogeneous phase at the interface.

#### 4. Conclusions

A fixed –bed catalyst reactor carried out methanolysis reaction, for two hours operating time, at 70 °C process temperature, and yields values in the range of 88.97-95.01% were obtained.

The performance study of the processes carried out highlighted the importance of the height of the catalytic layer and the concentration of the catalyst, the interaction between them and the correlation with the feed rate of the reactants.

The solid concentration resulting from the impregnation of the catalytic support was in the range of 1.43-1.63 % in the case of catalysts from apricot kernels, respectively 1.57-2.29 % in the case of catalysts from cherry kernels, sufficient to catalyze reactions in which the oil mass could it varies between 100 and 200 g of used vegetable oil and between 200 and 400 g of fresh vegetable oil.

#### Acknowledgement

This work has been funded by the European Social Fund from the Sectoral Operational Program Human Capital 2014-2020, through the Financial Agreement with the title “Training of PhD students and postdoctoral researchers in order to acquire applied research skills—SMART”, Contract no. 13530/16.06.2022—SMIS code: 153734.

#### REFERENCES

- [1] Meher L. C., Vidya Sagar D., Naik S. N., Technical aspects of biodiesel production by transesterification—a review, *Renewable and Sustainable Energy Reviews*, 10 (2006), 248–268

- [2] Ejikeme P. M., Anyaogu., I. D., Ejikeme C. L., Nwafor N. P., Egbonu C. A. C., Ukogu K., J. A. Ibemesi, Catalysis in Biodiesel Production by Transesterification Processes-An Insight, *Journal of Chemistry*, 7(4) 2010, 1120-1132
- [3] Rathore V., Newalkar B. L., Badoni R. P., Processing of vegetable oil for biofuel production through conventional and non-conventional routes, *Energy for Sustainable Development*, 31 (2016), 24–49
- [4] Curto J. W., Giambone M. D., MacGrogan A. S., Williamson IV G. H., A Comparative Analysis of Biodiesel and Diesel Emissions - A Major Qualifying Project Report , Worcester Polytechnic Institute Digital WPI, 2015
- [5] Refaat A. A., El Sheltawy S. T., Sadek K. U., Optimum reaction time, performance and exhaust emissions of produced by microwave irradiation biodiesel, *Int. J. Environ. Sci. Tech.*, 5 (3) (2008), 315-322.
- [6] Graille J., Lozano P., Pioch D., Geneste P., Essais d'Alcoolise d'Huiles Végétales avec des Catalyseurs Naturels pour la Production de Carburants Diesels, *Oleagineux*, 40 (1985), 271-276
- [7] Hirano et al., Methods of Producing Fatty Acid and Lower Alkyl Ester from Fats and Oils, *United States Patent No. 6090959* July, 2000, 18
- [8] Demirbas A, Current advances in alternative motor fuels. *Energy Explor Exploit* 2003;21:475–87
- [9] Miao X., Li R., Yao H., Effective acid-catalyzed transesterification for biodiesel production, *Energy Convers Manag* 50 (2009), 2680–2684
- [10] Farag H.A., El-Maghraby A., Taha N.A., Optimization of factors affecting esterification of mixed oil with high percentage of free fatty acid, *Fuel Process Technol* 92 (2011), 507–510
- [11] Freedman B., Butterfield R. O., Pryde E. H., *J Am Oil Chem Soc.*, 63 (1986), 1375;
- [12] Peter S.K.F., Ganswindt R., Neuner H.P., Weidner E., Alcoholysis of triacylglycerols by heterogeneous catalysis, *European Journal of Lipid Science and Technology*, 104 (6) 2002, 324–330